



ENVIRONMENTAL
MONITORING

M-694 | 2016

Monitoring of greenhouse gases and aerosols at Svalbard and Birkenes in 2015

Annual report



COLOPHON

Executive institution

NILU - Norsk institutt for luftforskning
P.O. Box 100, 2027 Kjeller

ISBN: 978-82-425-2862-9 (electronic)
ISSN: 2464-3327

Project manager for the contractor

Cathrine Lund Myhre

Contact person in the Norwegian Environment Agency

Camilla Fossum Pettersen

M-no

694

Year

2016

Pages

125

Contract number

15078041

Publisher

NILU - Norsk institutt for luftforskning
NILU report 31/2016
NILU project no. O-99093/O-105020/O-113007

The project is funded by

Norwegian Environment Agency and
NILU - Norwegian Institute for Air Research.

Author(s)

C.L. Myhre, O. Hermansen, M. Fiebig, C. Lunder, A.M. Fjæraa, T. M. Svendby, S. M. Platt, G. Hansen, N. Schmidbauer, T. Krognes

Title - Norwegian and English

Monitoring of greenhouse gases and aerosols at Svalbard and Birkenes in 2015 - Annual report
Overvåking av klimagasser og partikler på Svalbard og Birkenes i 2015: Årsrapport

Summary - sammendrag

The report summaries the activities and results of the greenhouse gas monitoring at the Zeppelin Observatory situated on Svalbard in Arctic Norway during the period 2001-2015, and the greenhouse gas monitoring and aerosol observations from Birkenes for 2009-2015.

Rapporten presenterer aktiviteter og måleresultater fra klimagassovertvåkingen ved Zeppelin observatoriet på Svalbard for årene 2001-2015 og klimagassmålinger og klimarelevante partikkelmålinger fra Birkenes for 2009-2015.

4 emneord

Drivhusgasser, partikler, Arktis, halokarboner

4 subject words

Greenhouse gases, aerosols, Arctic, halocarbons

Front page photo

Ny-Ålesund, Svalbard. Photo: Kjetil Tørseth, NILU.

Preface

This report presents results from the national monitoring of greenhouse gases and aerosol properties in 2015. The observations are done at two atmospheric supersites; one regional background site in southern Norway and one Arctic site. The observations made are part of the national monitoring programme conducted by NILU on behalf of The Norwegian Environment Agency.

The monitoring programme includes measurements of 41 greenhouse gases at the Zeppelin Observatory in the Arctic; and this includes a long list of halocarbons, which are not only greenhouse gases but also ozone depleting substances. The number of measured species has increased by 16 since the report in 2014. In 2009, NILU upgraded and extended the observational activity at the Birkenes Observatory in Aust-Agder and from 2010, the national monitoring programme was extended to also include greenhouse gas observations and selected aerosol observations particularly relevant for understanding the interactions between aerosols and radiation.

The present report is the fourth of a series of annual reports for 2015, which cover the national monitoring of atmospheric composition in the Norwegian rural background environment. The other three reports are focuses on the atmospheric composition and deposition of air pollution of particulate and gas phase of inorganic constituents, particulate carbonaceous matter, ground level ozone and particulate matter, the second on persistent organic pollutants and heavy metals, and the third presents the monitoring of the ozone layer and UV.

Data and results from the national monitoring programme are also included in various international programmes, including: EMEP (European Monitoring and Evaluation Programme) under the CLTRAP (Convention on Long-range Transboundary Air Pollution), AGAGE (Advanced Global Atmospheric Gases Experiment), CAMP (Comprehensive Atmospheric Monitoring Programme) under OSPAR (the Convention for the Protection of the marine Environment of the North-East Atlantic) and AMAP (Arctic Monitoring and Assessment Programme). Data from this report are also contributing to European Research Infrastructure network ACTRIS (Aerosols, Clouds, and Trace gases Research InfraStructure Network) and implementation in ICOS (*Integrated Carbon Observation System*) is in progress.

All measurement data presented in the current report are public and can be received by contacting NILU, or they can be downloaded directly from the database: <http://ebas.nilu.no>.

A large number of persons at NILU have contributed to the current report, including those responsible for sampling, technical maintenance, chemical analysis and quality control and data management. In particular Cathrine Lund Myhre (coordinating the program), Ove Hermansen, Chris Lunder, Terje Krognnes, Stephen M. Platt, Norbert Schmidbauer, Ann Mari Fjæraa, Kerstin Stebel, Markus Fiebig, and Tove Svendby.

NILU, Kjeller, 23 November 2016

Cathrine Lund Myhre
Senior Scientist, Dep. Atmospheric and Climate Research

Content

Preface	1
Sammendrag (Norwegian)	4
Summary.....	6
1. Introduction to monitoring of greenhouse gases and aerosols.....	9
1.1 The monitoring programme in 2015	9
1.2 Central frameworks and relevant protocols	9
1.3 The ongoing monitoring programme and the link to networks and research infrastructures	11
1.4 Greenhouse gases, aerosols and their climate effects.....	15
2. Observations of climate gases at the Birkenes and Zeppelin Observatories	19
2.1 Climate gases with natural and anthropogenic sources	22
2.1.1 Carbon dioxide at the Birkenes and Zeppelin Observatories	22
2.1.2 Methane at the Birkenes and Zeppelin Observatories	25
2.1.3 Non-methane hydrocarbons (NMHC) at the Zeppelin Observatory	33
2.1.4 Other Volatile Organic Compounds (VOC) at the Zeppelin Observatory	35
2.1.5 Nitrous Oxide at the Zeppelin Observatory	37
2.1.6 Methyl Chloride at the Zeppelin Observatory	38
2.1.7 Methyl bromide - CH ₃ Br at the Zeppelin Observatory.....	40
2.1.8 Carbon monoxide at the Zeppelin Observatory	42
2.2 Greenhouse gases with solely anthropogenic sources	46
2.2.1 Chlorofluorocarbons (CFCs) at Zeppelin Observatory	46
2.2.2 Hydrochlorofluorocarbons (HCFCs) at Zeppelin Observatory	49
2.2.3 Hydrofluorocarbons (HFCs) at Zeppelin Observatory	52

2.2.4	Halons measured at Zeppelin Observatory.....	56
2.2.5	Other chlorinated hydrocarbons at Zeppelin Observatory	57
2.2.6	Perfluorinated (PFCs) compounds at Zeppelin Observatory	61
3.	Aerosols and climate: Observations from Zeppelin and Birkenes Observatories	65
3.1	Physical and optical aerosol properties at Birkenes Observatory.....	70
3.1.1	Optical Aerosol Properties Measured In Situ at the Surface	70
3.1.2	Physical Aerosol Properties Measured In Situ at the Surface	74
3.1.3	Birkenes Aerosol Properties Measured In Situ at the Surface: Summary	77
3.1.4	Column-Integrated Optical In Situ Aerosol Properties Measured by Ground-Based Remote Sensing.....	78
3.2	Physical and optical aerosol properties at Zeppelin Observatory	82
3.2.1	Aerosol Properties Measured In Situ at the Surface at Zeppelin Observatory ...	82
3.2.2	Column-Integrated Optical In Situ Aerosol Properties Measured by Ground-Based Remote Sensing at Ny-Ålesund.....	83
4.	References	88
	APPENDIX I: Data Tables.....	93
	APPENDIX II Description of instruments and methodologies	107
	APPENDIX III: Abbreviations.....	121

Sammendrag (Norwegian)

Denne årsrapporten beskriver aktivitetene i og hovedresultatene fra programmet "Overvåking av klimagasser og aerosoler på Zeppelin-observatoriet på Svalbard og Birkenes-observatoriet i Aust-Agder, Norge". Rapporten omfatter målinger av 41 klimagasser fram til år 2015; inkludert de viktigste naturlige forekommende drivhusgassene, syntetiske klimagasser og ulike partikkelegenskaper som har høy relevans for stråling og klimaet. Mange av gassene har også sterke ozonreducerende effekter. For de fleste klimagassene er utvikling og trender for perioden 2001-2015 rapportert, i tillegg til daglig og årlige gjennomsnittsmålinger. Programmet er utvidet med 16 nye gasser i 2015, med målinger analysert tilbake til 2010. Utviklingen av alle gassene som inngår i programmet er vist i tabell 1 på side 7. Ytterligere detaljer presenteres i kapittel 2 av rapporten.

Målingene på Zeppelin-observatoriet følger utviklingen i bakgrunnsnivåkonsentrasjonene av klimagasser i Arktis. Birkenes-observatoriet ligger i det området i Sør-Norge som er mest berørt av langtransportert luftforurensning, og et omfattende program for målinger av aerosoler utføres der. Observasjoner av CO₂ og metan (CH₄) foretas på begge steder. Påvirkning fra lokal vegetasjon er også særlig viktig for Birkenes.

Observasjonene fra 2015 viser nye rekordhøye nivåer for de fleste av de målte klimagassene. Spesielt er det viktig å være oppmerksom på de nye rekordnivåene av CO₂ og CH₄. CO₂ har passert 400 ppm (parts per million) på Zeppelin, Birkenes og globalt i 2015. Totalt har den atmosfæriske konsentrasjonen av alle de viktigste klimagassene vært økende siden 2001. Unntakene er ozonnedbrytende KFK-er og noen få halogenerte gasser, som reguleres gjennom den vellykkede Montrealprotokollen.

CO₂-konsentrasjonen har gått opp alle år siden starten av målingene på Zeppelin, i samsvar med økningen av menneskeskapte utslipp. De nye rekordnivåene for 2015 er 401,2 ppm på Zeppelin og 405,1 ppm på Birkenes. Økningen fra 2014 er på henholdsvis 1,6 ppm (parts per million) og 2,2 ppm, sammenlignet med den globale gjennomsnittøkningen på 2,3 ppm.

I 2015 nådde konsentrasjonen av metan et nytt rekordnivå, med en økning fra 2015 på så mye som 10 ppb (0.48 %) (parts per billion) og 8,5 ppb (0.44 %) på henholdsvis Zeppelin og Birkenes. Endringene i løpet av de siste 10 årene er store i forhold til utviklingen av metannivået i perioden 1998-2005, da var endringen nær null både på Zeppelin og globalt. Dog var økningen fra 2014 til 2015 på Birkenes lavere enn økningen for 2013-2014, som var på 15 ppb.

Også N₂O nådde nytt rekordnivå i 2015, og fortsatte stigningen som tidligere.

De syntetiske menneskeskapte klimagassene som inngår i overvåkingsprogrammet på Zeppelin er 4 klorfluorkarboner (KFK-er), 3 hydroklorfluorkarboner (HKFK-er), og 8 hydrofluorkarboner (HFK-er), de to sistnevnte gruppene er KFK-erstatninger. I tillegg inngår 2 haloner, og en gruppe med 9 andre halogenerte gasser. For første gang rapporteres også 4 perfluorerte karboner (PFK) med svært høyt potensiale for global oppvarming. I sin helhet gir utviklingen for KFK-gassene grunn til optimisme, og konsentrasjonen for de fleste observerte KFK-ene er synkende. Men KFK-erstatningsstoffene HKFK og HFK økte i perioden 2001-2015 - for HKFK dog med en liten demping i utviklingen det siste året. HFK-gassene øker kraftig fra 2001, og det gjelder også for 2015. Konsentrasjonene av HFK er fortsatt svært lave, noe som betyr at disse

menneskeskapt gassenes bidrag til den globale oppvarmingen per i dag er liten. Men, gitt den ekstremt raske økningen i bruk og atmosfæriske konsentrasjoner vi har observert, er det viktig å følge utviklingen nøye i fremtiden. PFK- og SF₆-konsentrasjonene er fortsatt lave, men konsentrasjonen av SF₆ har økt så mye som 70% siden 2001. PFK-ene er nye i overvåkningsprogrammet og rapporteres for første gang i år. De viser en svak til ingen endring siden 2014.

Aerosoler er små partikler i atmosfæren. Aerosolnivåene og egenskaper til partiklene ved Birkenes bestemmes i hovedsak av den langtransporterte luftforurensningen fra det kontinentale Europa og luft fra Arktis, i tillegg til regionale kilder - så som biogen partikkeldannelse og regionale forurensningshendelser. Den viktigste observasjonen er at partiklenes egenskaper blir mindre absorberende for hvert år i måleperioden. Observasjoner av den totale mengden av aerosolpartikler i atmosfæren over Ny-Ålesund (aerosol optisk dybde) viser økte konsentrasjonsnivåer i løpet av våren sammenlignet med resten av året. Dette fenomenet, som kalles arktisk dis (Arctic haze), skyldes transport av forurensning fra lavere breddegrader, hovedsakelig Europa og Russland, i løpet av vinteren/våren.

Summary

This annual report describes the activities and main results of the program “*Monitoring of greenhouse gases and aerosols at the Zeppelin Observatory, Svalbard, and Birkenes Observatory, Aust-Agder, Norway*”. The report comprises the measurements of 41 climate gases up to the year 2015; including the most important naturally occurring well-mixed greenhouse gases, synthetic greenhouse gases, and various particle properties with high relevance to climate. Many of the gases also have strong ozone depleting effects. For the climate gases, the development and trends for the period 2001-2015 are reported for most gases, in addition to daily and annual mean observations. The program is extended in 2015 with 16 new gases, with measurements analysed back to 2010. The trends of all gases included in the programme are shown in Table 1, further details are presented in section 2 of the report.

The measurements at Zeppelin Observatory track the trend in background level concentrations of greenhouse gases in the Arctic. Birkenes Observatory is located in an area in southern Norway most affected by long-range transport of pollutants, and a comprehensive aerosol measurements program is undertaken there. Observations of CO₂ and methane (CH₄) are available at both sites. The influence of local vegetation/terrestrial interactions is also important at Birkenes.

The observations from 2015 show new record high levels for most of the greenhouse gases measured. In particular it is important to note the new record levels of CO₂ and CH₄. CO₂ passed 400 ppm (parts per million) at Zeppelin, Birkenes and globally in 2015. In total, the concentration of all the main greenhouse gases have been increasing since 2001, except for ozone-depleting CFCs and a few halogenated gases which are regulated through the successful Montreal protocol.

CO₂ concentration has increased all years since the start of the measurements at Zeppelin, in accordance due to the increase in anthropogenic emissions. The annual average for 2015 are 401.2 ppm at Zeppelin and 405.1 ppm at Birkenes. The increases from 2014 are 1.6 ppm and 2.2 ppm, respectively, compared to the increase in global mean which was 2.3 ppm.

The concentration of CH₄ reached a new record level with an increase since 2015 of as much as 10 ppb (0.48 %) and 8.5 ppb (0.45 %) at Zeppelin and Birkenes respectively. The changes over the last 10 years are large compared to the evolution of the methane levels in the period 1998-2005, when the change was close to zero both at Zeppelin and globally. The increase from 2014 to 2015 at Birkenes was lower than the increase for 2013-2014 which was as high as 15 ppb.

Also N₂O reached a new record level in 2015, as expected and following the last year's development.

The synthetic manmade greenhouse gases included in the monitoring programme at Zeppelin are 4 chlorofluorocarbons (CFCs), 3 hydrochlorofluorocarbons (HCFCs), and 8 hydrofluorocarbons (HFCs) which are both CFC substitutes, and 2 halons, and a group of 9 other halogenated gases. For the first time 4 perfluorinated carbons (PFCs) with very high global warming potentials are reported. In total the development of the CFC gases gives reason for optimism as the concentration of most observed CFCs are declining.

However, the CFC substitutes **HCFCs and HFCs** increased over the period 2001-2015. For the HCFCs a relaxation in the upward trend was observed last year. The **HFCs** have increase strongly since 2001, and this trend is continuing. The concentrations of the HFCs are still very low, thus contribution from these manmade gases to the global warming is small today, but given the extremely rapid increase in the use of these gases, it is crucial to follow the development in the future.

PFCs and SF₆ concentrations are still low, but the concentration of SF₆ has increased as much as 70% since 2001. The PFCs are new and reported for first time this year, and they show a weak or no change since 2014.

Aerosols are small particles in the atmosphere and anthropogenic sources include combustion of fossil fuel, coal and biomass including waste from agriculture and forest fires. Aerosol can have warming or cooling effects on climate, depending on their properties. Aerosol properties at Birkenes are mainly determined by long-range transport of air pollution from continental Europe, and Arctic air, as well as regional sources like biogenic particle formation and regional pollution events. The main observation is that the particles properties become less absorbing year by year over the period. Observations of the total amount of aerosol particles in the atmosphere above Ny-Ålesund (aerosol optical depth) show increased concentration levels during springtime compared to the rest of the year. This phenomenon, called Arctic haze, is due to transport of pollution from lower latitudes (mainly Europe and Russia) during winter/spring.

Table 1: Key findings; Greenhouse gases measured at Zeppelin, Ny-Ålesund; lifetimes in years¹, global warming potential (GWP over 100 years), annual mean for 2015 and their trends per year over the period 2001-2015. The compounds marked in green are new, and implemented this year with measurements back to 2010 All concentrations are mixing ratios in ppm (parts per million) for CH₄, ppb for CH₄ and ppt for the other gases.

Component		Life-time	GWP	Annual mean 2015	Trend /yr
Main greenhouse gases with natural and anthropogenic sources					
Carbon dioxide - Zeppelin	CO ₂	-	1	401.0	2.1
Carbon dioxide - Birkenes				403.9	Too few years
Methane - Zeppelin	CH ₄	12.4	28	1920.2	5.2
Methane - Birkenes				1925.9	Too few years
Carbon monoxide	CO	few months	-	113.6	-1.3
Nitrous oxide	N ₂ O	121	265	327.1	-
Chlorofluorocarbons					
CFC-11*	CCl ₃ F	45	4 660	234.1	0.0
CFC-12*	CF ₂ Cl ₂	640	10 200	523.4	-2.1
CFC-113*	CF ₂ ClCFCl ₂	85	13 900	72.9	-0.7
CFC-115*	CF ₃ CF ₂ Cl	1 020	7 670	8.5	0.0

*The measurements of these components have higher uncertainty. See Appendix I for more details.

¹ From Scientific Assessment of Ozone Depletion: 2010 (WMO, 2011b) and the 4th Assessment Report of the IPCC

Component		Life-time	GWP	Annual mean 2015	Trend /yr
Hydrochlorofluorocarbons					
HCFC-22	CHClF ₂	11.9	1 760	244.73	6.5
HCFC-141b	C ₂ H ₃ FC1 ₂	9.2	782	26.08	0.6
HCFC-142b*	CH ₃ CF ₂ Cl	17.2	1 980	23.18	0.7
Hydrofluorocarbons					
HFC-125	CHF ₂ CF ₃	28.2	3 170	20.27	0.1
HFC-134a	CH ₂ FCF ₃	13.4	1 300	89.88	4.8
HFC-152a	CH ₃ CHF ₂	1.5	506	9.79	0.6
HFC-23	CHF ₃	228	12 400	28.89	1.0
HFC-365mfc	CH ₃ CF ₂ CH ₂ CF ₃	8.7	804	1.09	0.1
HFC-227ea	CF ₃ CHFCF ₃	38.9	3 350	1.10	0.1
HFC-236fa	CF ₃ CH ₂ CF ₃	242	8 060	0.14	0.0
HFC-245fa	CHF ₂ CH ₂ CF ₃	7.7	858	2.54	0.2
Perfluorinated compounds					
PFC-14	CF ₄	50 000	6 630	80.06	-
PFC-116	C ₂ F ₆	10 000	11 100	4.54	0.1
PFC-218	C ₃ F ₈	2600	8 900	0.56	0.0
PFC-318	C ₄ F ₈	3200	9 540	1.52	0.0
Nitrogen trifluoride	NF ₃	500	16 100		
Sulphurhexafluoride*	SF ₆	3 200	23 500	8.74	0.27
Halons					
H-1211*	CBrClF ₂	16	1 750	3.8	0.0
H-1301	CBrF ₃	65	7 800	3.8	0.0
Halogenated compounds					
Methylchloride	CH ₃ Cl	1	12	512.8	-0.3
Methylbromide	CH ₃ Br	0.8	2	6.9	-0.2
Dichloromethane	CH ₂ Cl ₂	0.4	9	54.1	1.8
Chloroform	CHCl ₃	0.4	16	13.7	0.2
Carbon tetrachloride	CCl ₄	26	1730	81.0	-0.9
Methylchloroform	CH ₃ CCl ₃	5	160	3.2	-0.3
Trichloroethylene	CHClCCl ₂	-	-	0.3	0.0
Perchloroethylene	CCl ₂ CCl ₂	-	-	2.4	-0.1
Volatile Organic Compounds (VOC)					
Ethane	C ₂ H ₆	Ca 78 days*		1651.4	38.7
Propane	C ₃ H ₈	Ca 18 days*		566.0	7.7
Butane	C ₄ H ₁₀	Ca 8 days*		184.4	0.97
Pentane	C ₅ H ₁₂	Ca 5 days*		60.4	-0.38
Benzene	C ₆ H ₆	Ca 17 days*		69.76	-3.7
Toluene	C ₆ H ₅ CH ₃	Ca 2 days*		25.75	-2.3

1. Introduction to monitoring of greenhouse gases and aerosols

1.1 The monitoring programme in 2015

The atmospheric monitoring programme presented in this report focuses on the concentrations of greenhouse gases and aerosols physical and optical properties in the Norwegian background air and in the Arctic. The main objectives are to quantify the levels of greenhouse gases including ozone depleting substances, describe the relevant optical and physical properties of aerosols, and document the development over time. Measurements of the greenhouse gas concentrations and aerosol properties are core data for studies and assessments of climate change, and also crucial in order to evaluate mitigation strategies and if they work as expected. The Norwegian monitoring sites are located in areas where the influence of local sources are minimal, hence the sites are representative for a wider region and for the detection of long-term atmospheric compositional changes.



Figure 1: Location of NILU's atmospheric supersites measuring greenhouse gases and aerosol properties.

1.2 Central frameworks and relevant protocols

The Norwegian greenhouse gas and aerosol monitoring programme is set up to meet national and international needs for greenhouse gas and aerosol measurement data, both for the scientific community, environmental authorities and other stakeholders. The targets set by the Kyoto protocol first and second commitment periods is to reduce the total emissions of greenhouse gases from the industrialized countries. To follow up on this, the Paris Agreement was negotiated and adopted by consensus at the 21st Conference of the Parties of the UNFCCC in Paris on 12 December 2015. Today 81 Parties have ratified to the Convention, and on 4 November 2016 the Agreement will enter into force. The central aim is to keep the increase in the global average temperature well below 2 °C above pre-industrial levels and to pursue efforts to limit the temperature increase to 1.5 °C. The EU Heads of State and Governments

agreed in October 2014 on the headline targets and the architecture for the EU framework on climate and energy for 2030. The agreed targets include a cut in greenhouse gas emissions by at least 40% by 2030 compared to 1990 levels².

In 1987 the Montreal Protocol was signed and entered into force in 1989 in order to reduce the production, use and eventually emission of the ozone-depleting substances (ODS). The amount of most ODS in the troposphere is now declining slowly and is expected to be back to pre-1980 levels around year 2050. It is central to follow the development of the concentration of these ozone depleting gases in order to verify that the Montreal Protocol and its amendments work as expected. The development of the ozone layer above Norway is monitored closely, and the results of the national monitoring of ozone and UV is presented in “*Monitoring of the atmospheric ozone layer and natural ultraviolet radiation: Annual report 2015*” (Svendby et al, 2016). The ozone depleting gases and their replacement gases are strong greenhouse gases making it even more important to follow the development of their concentrations.

To control the new replacement gases, a historical agreement was signed on 15 October 2016 when negotiators from 197 countries agreed on a deal reducing emissions of hydrofluorocarbons (HFCs). The agreement was finalized at the United Nations meeting in Kigali, Rwanda, aiming to reduce the projected emissions of HFCs by more than 80% over the course of the twenty-first century. The agreement in Kigali represents an expansion of the 1987 Montreal Protocol. The HFCs can be up to 10000 times as effective at trapping heat as carbon dioxide. Today HFCs account for a small fraction of the greenhouse-gas emissions and have had limited influence on the global warming up to know. However, the use of HFCs is growing rapidly and the projected HFC emission could contribute up to 0.5°C of global warming by the end of this century if not regulated (Xu et al., 2013). Because the agreement in Kigali is an expansion of the Montreal Protocol, which was ratified back in the 1990s, this new deal is legally binding.

As a response to the need for monitoring of greenhouse gases and ozone depleting substances, the *Norwegian Environment Agency* and *NILU - Norwegian Institute for Air Research* signed a contract commissioning NILU to run a programme for monitoring greenhouse gases at the Zeppelin Observatory, close to Ny-Ålesund in Svalbard in 1999. This national programme includes now monitoring of 43 greenhouse gases and trace gases at the Zeppelin Observatory in the Arctic, many of them also ozone depleting substances. In 2009, NILU upgraded and extended the observational activity at the Birkenes Observatory in Aust-Agder. From 2010, the Norwegian Environment Agency/NILU monitoring programme was extended to also include the new observations from Birkenes of the greenhouse gases CO₂ and CH₄ and selected aerosol observations particularly relevant for the understanding of climate change. Relevant components are also reported in “*Monitoring of long-range transported air pollutants in Norway, annual report 2015*” (Aas et al, 2016), this includes particulate and gaseous inorganic constituents, particulate carbonaceous matter, ground level ozone and particulate matter for 2015. This report also includes a description of the weather in Norway in 2016 in Chap. 2, which is relevant for the observed concentrations of greenhouse gases and aerosols.

² Details here: <http://ec.europa.eu/clima/policies/strategies/2030/> and here http://www.consilium.europa.eu/uedocs/cms_data/docs/pressdata/en/ec/145397.pdf

1.3 The ongoing monitoring programme and the link to networks and research infrastructures

The location of both sites are shown in Figure 1, and pictures of the sites are shown in Figure 2. The unique location of the Zeppelin Observatory at Svalbard, together with the infrastructure of the scientific research community in Ny-Ålesund, makes it ideal for monitoring the global changes of concentrations of greenhouse gases and aerosols in the atmosphere. There are few local sources of emissions, and the Arctic location is also important as the Arctic is a particularly vulnerable region. The observations at the Birkenes Observatory complement the Arctic site. Birkenes Observatory is located in a forest area with few local sources. However, the Observatory often receives long-range transported pollution from Europe and the site is ideal to analyse the contribution of long range transported greenhouse gases and aerosol properties.



Figure 2: The two atmospheric supersites included in this programme, Zeppelin above and Birkenes to the left

Data and results from the national monitoring programme are also included in various international programmes. Both sites are contributing to EMEP (European Monitoring and Evaluation Programme) under the CLTRAP (Convention on Long-range Transboundary Air Pollution). Data from the sites are also reported to CAMP (Comprehensive Atmospheric Monitoring Programme) under OSPAR (the Convention for the Protection of the marine Environment of the North-East Atlantic, <http://www.ospar.org>); AMAP (Arctic Monitoring and Assessment Programme <http://www.amap.no>), WMO/GAW (The World Meteorological

Organization, Global Atmosphere Watch programme, <http://www.wmo.int>) and AGAGE (Advanced Global Atmospheric Gases Experiment)

Zeppelin and Birkenes are both included into two central EU research infrastructures (RI) focusing on climate forcers. This ensure high quality data with harmonised methods and measurements across Europe and also with a global link through GAW, to have comparable data and results. This is essential to reduce the uncertainty on trends and in the observed levels of the wide range of climate forcers. International collaboration and harmonisation of these types of observations are crucial for improved processes understanding and satisfactory quality to assess trends.

The two central RIs are ICOS (Integrated Carbon Observation System) focusing on the understanding of carbon cycle, and ACTRIS (Aerosols, Clouds, and Trace gases Research InfraStructure Network, www.actris.net) focusing on short-lived aerosol climate forcers and related reactive gases, and clouds. NILU host the data centres of the European Monitoring and Evaluation Programme (EMEP), ACTRIS (Aerosols, Clouds, and Trace gases Research InfraStructure Network) and the WMO Global Atmosphere Watch (GAW) World Data Centre for Aerosol (WDCA) and GAW- World Data Centre for Reactive Gases (WDCRG) (from 2015), and numerous other projects and programs (e.g. AMAP, HELCOM) and all data reported are accessible in the EBAS data base: <http://ebas.nilu.no>. All data from these frameworks are reported to this data base.

Compiled key information on the national monitoring programme at the sites are listed in Table 2. From 2015 the programme was extend with 16 new greenhouse gases and trace gases, mainly HFCs and non-methane hydrocarbons. More detailed information on the monitoring program and measurement frequencies are provided in Appendix II. For the measurements of aerosol properties more details are also presented in chapter 4.

Table 2: Summary of the ongoing relevant measurement program run under NILU responsibility at Birkenes and Zeppelin Observatory 2015. The components marked in green are implemented in the programme in 2015 and reported for the first time.

Component	Birkenes Start	Zeppelin Start	International network and QA program	Comment
Trace gases				
CO ₂	2009	2012	ICOS	Measured at Zeppelin since 1988 by Univ. Stockholm. By NILU at Zeppelin since 2009, now included in the programme. Qualified as ICOS class 1 site, and passed first step in September, 2016. ICOS labelling scheduled in 2017 for Birkenes
CH ₄	2009	2001	ICOS, EMEP	ICOS labelling and implementation scheduled in 2016 for Zeppelin, 2017 for Birkenes
N ₂ O	-	2009	ICOS	ICOS labelling and implementation scheduled in 2017 for Zeppelin
CO	-	2001	ICOS	ICOS labelling and implementation scheduled in 2017 for Zeppelin
Ozone (surface)	1985	1989	EMEP	Reported in M-562/2016, Aas et al, 2016.
CFCs				
CFC-11*				
CFC-12*				
CFC-113*				
CFC-115*				
HCFCs				
HCFC-22		2001/ 2010 and later	AGAGE	*The measurements of “*” these components are not within the required precision of AGAGE, but a part of the AGAGE quality assurance program. Other components are also measured (like new replacements). New compounds marked in blue are included in the national monitoring program from 2015, with harmonised time series and measurements back to 2010 when the Medusa instrument was installed at Zeppelin.
HCFC-141b				
HCFC-142b				
HFC-125				
HFC-134a				
HFC-152a				
HFCs				
HFC-125				
HFC-134a				
HFC-152a				
HFC-23				
HFC-227ea				
HFC-236fa				
HFC-245fa				
HFC-365mfc				
PFCs				
PFC-14				
PFC-116				
PFC-218				
PFC-318				
Halons				
H-1211				
H-1301				
Other chlorinated				
CH ₃ Cl				
CH ₃ Br				
CH ₂ Cl ₂				
CHCl ₃				
CCl ₄				
CH ₃ CCl ₃				
CHClCCl ₂				
CCl ₂ CCl ₂				
Other fluorinated				
SF ₆				
NF ₃		2016	AGAGE	
VOCs				
C ₂ H ₆ - ethane				NMHC and VOCs are included in the national monitoring program from 2015, but the measurements are harmonised back to 2010.
C ₃ H ₈ - propane		2010	ACTRIS, EMEP	
C ₄ H ₁₀ - butane				
C ₅ H ₁₂ - pentane				
C ₆ H ₆ - benzene				
C ₆ H ₅ CH ₃ - toluene				

Component	Birkenes Start	Zeppelin Start	International network and QA program	Comment
Aerosol measurements				
Absorption properties	2009	2015	ACTRIS, EMEP	Measured by Univ. of Stockholm at Zeppelin, New from late 2015
Scattering properties	2009	-	ACTRIS, EMEP	Measured by Univ. of Stockholm at Zeppelin
Number Size Distribution	2009	2010	ACTRIS, EMEP	Reported in M-562/2016, Aas et al, 2016.
Cloud Condensation Nuclei	2012	-	ACTRIS	Zeppelin: In collaboration with Korean Polar Research Institute
Aerosol Optical depth	2010	2007	Birkenes: AERONET, Ny-Ålesund: GAW-PFR	
PM ₁₀	2001		EMEP	Reported in M-562/2016, Aas et al, 2016.
PM _{2.5}	2001		EMEP	
Chemical composition -inorganic	1978	1979	EMEP	
Chemical composition - carbonaceous matter	2001		EMEP	

1.4 Greenhouse gases, aerosols and their climate effects

The IPCC's Fifth Assessment Report (IPCC AR5) and the contribution from Working Group I “*Climate Change 2013: The Physical Science Basis*” was published in September 2013. This substantial climate assessment report presents new evidence of past and projected future climate change from numerous independent scientific studies ranging from observations of the climate system, paleoclimate archives, theoretical studies on climate processes and simulations using climate models. Their main conclusion is that:

“Warming of the climate system is unequivocal, and since the 1950s, many of the observed changes are unprecedented over decades to millennia. The atmosphere and ocean have warmed, the amounts of snow and ice have diminished, sea level has risen, and the concentrations of greenhouse gases have increased”

(IPCC, Summary for policy makers, WG I, 2013)

Their conclusions are based on a variety of independent indicators, some of them are observations of atmospheric compositional change. The overall conclusion with respect to the development of the concentrations of the main greenhouse gases is:

“The atmospheric concentrations of carbon dioxide, methane, and nitrous oxide have increased to levels unprecedented in at least the last 800,000 years. Carbon dioxide concentrations have increased by 40% since pre-industrial times, primarily from fossil fuel emissions and secondarily from net land use change emissions. The ocean has absorbed about 30% of the emitted anthropogenic carbon dioxide, causing ocean acidification”

(IPCC, Summary for policy makers, 2013)

In particular chapter 2, “*Observations: Atmosphere and Surface*”, presents all types of atmospheric and surface observations, including observations of greenhouse gases since the start of the observations in mid-1950s and changes in aerosols since the 1980s. In the IPCC AR5 report was the first time long term changes of aerosols were included in the report, based on global and regional measurement networks and satellite observations. The main conclusion with respect to development of the aerosol levels is that “*It is very likely that aerosol column amounts have declined over Europe and the eastern USA since the mid-1990s and increased over eastern and southern Asia since 2000*” (Hartmann et al, 2013). This is important since the total effect of aerosols is atmospheric cooling, counteracting the effect of greenhouse gases. The changes in Europe and USA is mainly due to mitigation strategies of e.g. sulphur, while the emissions are increasing rapidly in Asia, including increasing emissions of the warming component black carbon.

The basic metric to compare the effect of the various climate change drivers is radiative forcing (RF). RF is the net change in the energy balance of the Earth system due to some imposed change. RF provides a quantitative basis for comparing potential climate response to different changes. Forcing is often presented as the radiative change from one time-period to another, such as pre-industrial to present-day. For many forcing agents the RF is an appropriate way to compare the relative importance of their potential climate effect. However, rapid adjustments in the troposphere can either enhance or reduce the perturbations, leading to large differences in the forcing driving the long-term climate change. In the last IPCC report it was also introduced a new concept, the effective radiative forcing (ERF). The ERF concept aims to take rapid adjustments into account, and is the change in net TOA (Top Of Atmosphere) downward radiative flux after allowing for atmospheric temperatures, water vapour and clouds to adjust, but with surface temperature or a portion of surface conditions unchanged (Myhre et al, 2013b). Figure 3 shows the RF and ERF of the main components referring to a change in the atmospheric level since 1750, pre-industrial time.

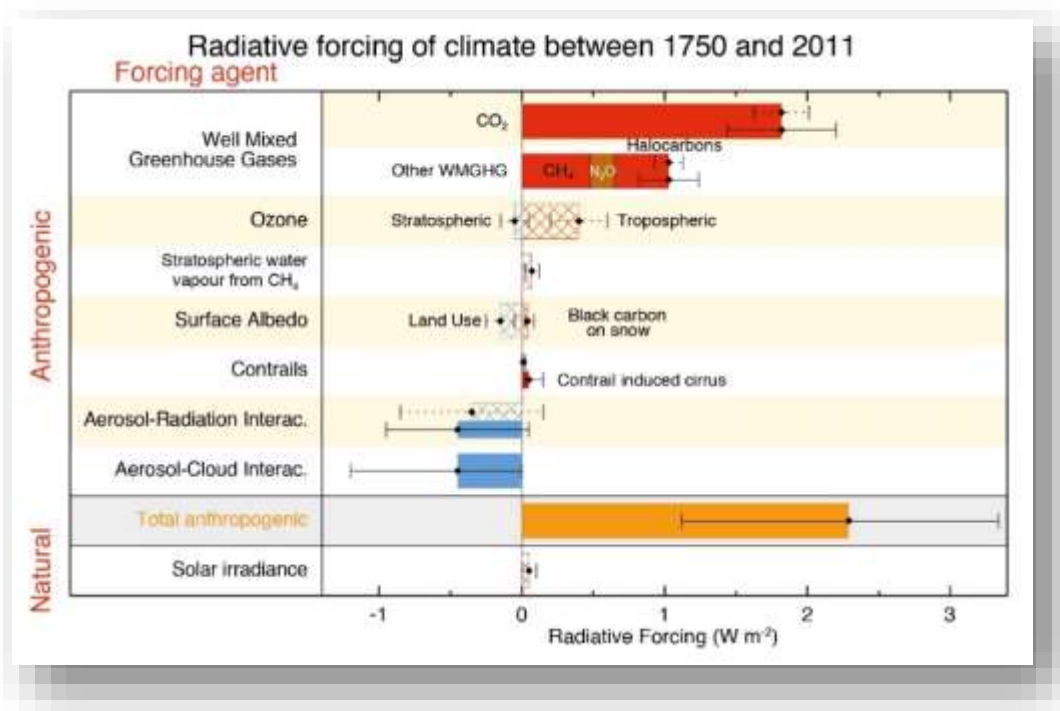


Figure 3: Bar chart for RF (hatched) and ERF (solid) for the period 1750-2011. Uncertainties (5 to 95% confidence range) are given for RF (dotted lines) and ERF (solid lines). (Taken from Myhre et al, 2013b).

Total adjusted anthropogenic forcing is 2.29 W m^{-2} , [1.13 to 3.33], and the main anthropogenic component driving this is CO₂ with a total RF of 1.82 W m^{-2} . The direct and indirect effect of aerosols are cooling and calculated to -0.9 W m^{-2} . The diagram in Figure 4 shows a comparison in percent % of the various contribution from the long-lived greenhouse gases to the total forcing of the well-mixed greenhouse gases, based on 2011 levels.

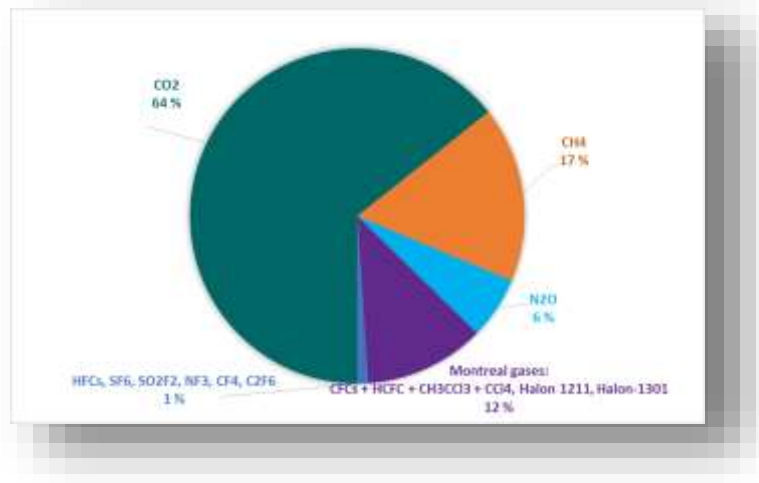


Figure 4: The contribution in % of the well-mixed greenhouse gases to the total forcing of the well-mixed greenhouse gases for the period 1750-2011 based on estimates in Table 8.2 in Chap 8, of IPCC (Myhre et al, 2013b).

An interesting and more detailed picture of the influence of various emissions on the RF is illustrated in Figure 5. This Figure shows the forcing since 1750 by emitted compounds, to better illustrate the effects of emissions and potential impact of mitigations.

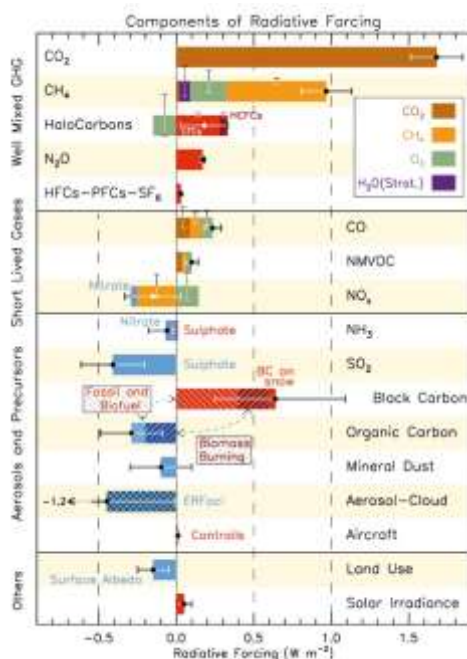


Figure 5: RF bar chart for the period 1750-2011 based on emitted compounds (gases, aerosols or aerosol precursors) or other changes. Red (positive RF) and blue (negative forcing) are used for emitted components which affect few forcing agents, whereas for emitted components affecting many compounds several colours are used as indicated in the inset at the upper part the figure. The vertical bars indicate the relative uncertainty of the RF induced by each component. Their length is proportional to the thickness of the bar, that is, the full length is equal to the bar thickness for a $\pm 50\%$ uncertainty. The net impact of the individual contributions is shown by a diamond symbol and its uncertainty (5 to 95% confidence range) is given by the horizontal error bar. ERFaci is ERF due to aerosol-cloud interaction. BC and OC are co-emitted, especially for biomass burning emissions (given as Biomass Burning in the figure) and to a large extent also for fossil and biofuel emissions (given as Fossil and Biofuel in the figure where biofuel refers to solid biomass fuels) (The Figure is taken from Myhre et al, 2013b).

As seen, the number of emitted compounds and changes leading to RF is larger than the number of compounds causing RF directly. This is due to indirect effects, in particular components involved in atmospheric chemistry that affects e.g. CH_4 and ozone. Emissions of CH_4 , CO, and NMVOC all lead to excess CO_2 as one end product if the carbon is of fossil origin, and this is the reason why the RF of direct CO_2 emissions is slightly lower than the RF of abundance change of CO_2 in Figure 3. Note also that for CH_4 , the contribution from emission is estimated to be almost twice as large as that from the CH_4 concentration change, 0.97 W m^{-2} versus 0.48 W m^{-2} shown in Figure 3 and Figure 5 respectively. This is because emission of CH_4 leads to ozone production (shown in green colour in the CH_4 bar in Figure 5), stratospheric water vapour, CO_2 (as mentioned above), and importantly affects its own lifetime. As seen from the Figure, there is also a particularly complex picture of the effects of aerosols. Black carbon heats the atmosphere, originating from both fossil fuel, biofuel and biomass burning. The direct effect of black carbon from fossil and biofuel is $+0.4 \text{ W m}^{-2}$, while black carbon from biomass burning is 0 in total due to co-emitted effects of organic carbon, cooling the atmosphere and cancelling out the heating effect.

In addition there is a small heating effect of black carbon on snow (0.04 W m^{-2} since 1750). The effect of black carbon on snow since 1750 is currently in the order of one year increase of CO_2 concentration in the atmosphere (around 2 ppm).

2. Observations of climate gases at the Birkenes and Zeppelin Observatories

NILU measures 41 climate gases at the Zeppelin Observatory at Svalbard and 2 at Birkenes, in addition to surface ozone reported in Aas et al. (2016). The results from these measurements, and analysis are presented in this chapter. Also observations of CO₂ since 1989 at Zeppelin performed by the Stockholm University - Department of Applied Environmental Science (ITM), are included in the report.

Table 3 summarize the main results for 2015 and the trends over the period 2001-2015. Also a comparison of the main greenhouse gas concentrations at Zeppelin and Birkenes compared to annual mean values given in the 5th Assessment Report of the IPCC (Myhre et al. 2013b) is included.

Table 3: Greenhouse gases measured at Zeppelin and Birkenes; lifetimes in years, global warming potential (GWP) for 100 year horizon, and global mean for 2011 is taken from 5th Assessment Report of the IPCC, Chapter 8 (Myhre et al, 2013b). Global mean is compared to annual mean values at Zeppelin and Birkenes for 2011. Annual mean for 2015, change last year, the trends per year over the period 2001-2015 is included. All concentrations are mixing ratios in ppt, except for methane, nitrous oxide and carbon monoxide (ppb) and carbon dioxide (ppm). The components marked in green are implemented in the programme in 2015, with measurements back to 2010, and reported for the first time.

Component		Life-time	GWP	Global mean 2011	Annual mean 2011	Annual mean 2015	Absolute change last year	Trend /yr
Carbon dioxide - Zeppelin	CO ₂	-	1	391 ± 0.2	392.5	401.0	1.6	2.1
Carbon dioxide - Birkenes					397.4	403.9	2.2	-
Methane - Zeppelin	CH ₄	12.4	28	1803 ± 2	1879.5	1920.2	10.2	5.2
Methane - Birkenes					1895.5	1925.9	8.5	-
Carbon monoxide	CO	few months	-	-	115.2	113.6	0.4	-1.3
Nitrous oxide	N ₂ O	121	265	324 ± 0.1	324.2	328.1	1.1	-
Chlorofluorocarbons								
CFC-11*	CCl ₃ F	45	4 660	238 ± 0.8	238.3	234.1	-0.9	0.0
CFC-12*	CF ₂ Cl ₂	640	10 200	528 ± 1	531.5	523.4	-2.0	-2.1
CFC-113*	CF ₂ ClCFCl ₂	85	13 900	74.3 ± 0.1	74.6	72.9	-0.6	-0.7
CFC-115*	CF ₃ CF ₂ Cl	1 020	7 670	8.37	8.42	8.5	0.0	0.0

Component		Life-time	GWP	Global mean 2011	Annual mean 2011	Annual mean 2015	Absolute change last year	Trend /yr
Hydrochlorofluorocarbons								
HCFC-22	CHClF ₂	11.9	1 760	213 ± 0.1	226	244.73	4.7	6.5
HCFC-141b	C ₂ H ₃ FCl ₂	9.2	782	21.4 ± 0.1	23	26.08	0.7	0.6
HCFC-142b*	CH ₃ CF ₂ Cl	17.2	1 980	21.2 ± 0.2	22.7	23.18	0.0	0.7
Hydrofluorocarbons								
HFC-125	CHF ₂ CF ₃	28.2	3 170	9.58 ± 0.04	10.9	20.27	2.4	0.1
HFC-134a	CH ₂ FCF ₃	13.4	1 300	62.7 ± 0.3	68.4	89.88	5.5	4.8
HFC-152a	CH ₃ CHF ₂	1.5	506	6.4 ± 0.1	10.1	9.79	-0.3	0.6
HFC-23	CHF ₃	228	12 400	-	-	28.89	1.1	1.0
HFC-365mfc	CH ₃ CF ₂ CH ₂ CF ₃	8.7	804	-	-	1.09	0.1	0.1
HFC-227ea	CF ₃ CHFCF ₃	38.9	3 350	-	-	1.10	0.1	0.1
HFC-236fa	CF ₃ CH ₂ CF ₃	242	8 060	-	-	0.14	0.0	0.0
HFC-245fa	CHF ₂ CH ₂ CF ₃	7.7	858	-	-	2.54	0.20	0.2
Perfluorinated compounds								
PFC-14	CF ₄	50 000	6 630	-	-	80.06	-	-
PFC-116	C ₂ F ₆	10 000	11 100	-	-	4.54	0.1	0.1
PFC-218	C ₃ F ₈	2600	8 900	-	-	0.56	0.0	0.0
PFC-318	C ₄ F ₈	3200	9 540	-	-	1.52	0.0	0.0
Nitrogen trifluoride	NF ₃	500	16 100				From 2016	
Sulphurhexafluoride*	SF ₆	3 200	23 500	7.28 ± 0.03	7.49	8.74	0.3	0.27
Halons								
H-1211*	CBrClF ₂	16	1 750		4.2	3.8	-0.1	0.0
H-1301	CBrF ₃	65	7 800		3.3	3.8	-0.1	0.0
Halogenated compounds								
Methylchloride	CH ₃ Cl	1	12	-	508.2	512.8	-1.4	-0.3
Methylbromide	CH ₃ Br	0.8	2	-	7.02	6.9	0.0	-0.2
Dichloromethane	CH ₂ Cl ₂	0.4	9	-	41.2	54.1	-0.5	1.8
Chloroform	CHCl ₃	0.4	16	-	11.9	13.7	0.3	0.2
Carbon tetrachloride	CCl ₄	26	1730			81.0	-1.6	-0.9
Methylchloroform	CH ₃ CCl ₃	5	160	6.32 ± 0.07	6.48	3.2	-0.6	-0.3

Component		Life-time	GWP	Global mean 2011	Annual mean 2011	Annual mean 2015	Absolute change last year	Trend /yr
Trichloroethylene	CHClCCl ₂	-	-	-	0.549	0.3	-0.2	0.0
Perchloroethylene	CCl ₂ CCl ₂	-	-	-	2.8	2.4	-0.1	-0.1
Volatile Organic Compounds (VOC)								
Ethane	C ₂ H ₆	Ca 78 days*	-	-	1625.5	34.9	38.7	
Propane	C ₃ H ₈	Ca 18 days*	-	-	503.2	-1.2	7.7	
Butane	C ₄ H ₁₀	Ca 8 days*	-	-	184.4	-5.6	0.97	
Pentane	C ₅ H ₁₂	Ca 5 days*	-	-	60.4	-2.8	-0.38	
Benzene	C ₆ H ₆	Ca 17 days*	-	-	68.3	2.5	-3.7	
Toluene	C ₆ H ₅ CH ₃	Ca 2 days*	-	-	24.6	3.6	-2.3	

*The lifetimes of VOC and NMHC are strongly dependant on season, sunlight, other components etc. The estimates are global averages given in C. Nicholas Hewitt (ed.): *Reactive Hydrocarbons in the Atmosphere*, Academic Press, 1999, p. 313. The times series for these are short and the trend is very uncertain.

Greenhouse gases and other climate gases have numerous sources, both anthropogenic and natural. Trends and future changes in concentrations are determined by their sources and the sinks, and in section 2.1 are observations and trends of the monitored greenhouse gases with both natural and anthropogenic sources presented in more detail. In section 2.2 are the detailed results of the ozone depleting substances with purely anthropogenic sources presented.

We have used the method described in Appendix II in the calculation of the annual trends, and also include a description of the measurements at Zeppelin at Svalbard and Birkenes Observatory in southern Norway in more details. Generally, Zeppelin Observatory is a unique site for observations of changes in the background level of atmospheric components. All peak concentrations of the measured gases are significantly lower here than at other sites at the Northern hemisphere, due to the station's remote location. Birkenes is closer to the main source areas. Further, the regional vegetation is important for regulating the carbon cycle, resulting in much larger variability in the concentration level compared to the Arctic region.

2.1 Climate gases with natural and anthropogenic sources

The annual mean concentrations for all gases included in the program for all years are given in Appendix I, Table A 1 at page 95. All the trends, uncertainties and regression coefficients are found in Table A 2 at page 95. Section 2.1 focuses on the measured greenhouse gases that have both natural and anthropogenic sources.

2.1.1 Carbon dioxide at the Birkenes and Zeppelin Observatories

Carbon dioxide (CO₂) is the most important anthropogenic greenhouse gas with a radiative forcing of 1.82 W m⁻² since the year 1750, and an increase since the previous IPCC report (AR4, 2007) of 0.16 Wm⁻² (Myhre et al., 2013b). The increase in forcing is due to the increase in concentrations over these last years. CO₂ is the end product in the atmosphere of the oxidation of all main organic compounds, and it has shown an increase of as much as 40 % since the pre industrial time (Hartmann et al, 2013). This is mainly due to emissions from combustion of fossil fuels and land use change. CO₂ emissions from fossil fuel burning and cement production increased by 2.3% in 2013 since 2012, with a total of 9.9±0.5 GtC (billion tonnes of carbon) equal to 36 GtCO₂ emitted to the atmosphere, 61% above 1990 emissions (the Kyoto Protocol reference year). Emissions are projected to decrease slightly (-0.6%) in 2015 according to Global Carbon Project estimates <http://www.globalcarbonproject.org>.

NILU started CO₂ measurements at the Zeppelin Observatory in 2012 and the results are presented in Figure 6, together with the time series provided by ITM, University of Stockholm, back to 1988. ITM provides all data up till 2012 and we acknowledge the effort they have been doing in monitoring CO₂ at the site. Until 2009 the only Norwegian site measuring well-mixed greenhouse gases (LLGHG) greenhouse gases was Zeppelin, but after upgrading Birkenes there are continuous measurements of CO₂ and CH₄ from mid May 2009 also at this site.

The atmospheric daily mean CO₂ concentration measured at Zeppelin Observatory for the period mid 1988-2015 is presented in Figure 6 upper panel, together with the shorter time series for Birkenes in the lower panel.

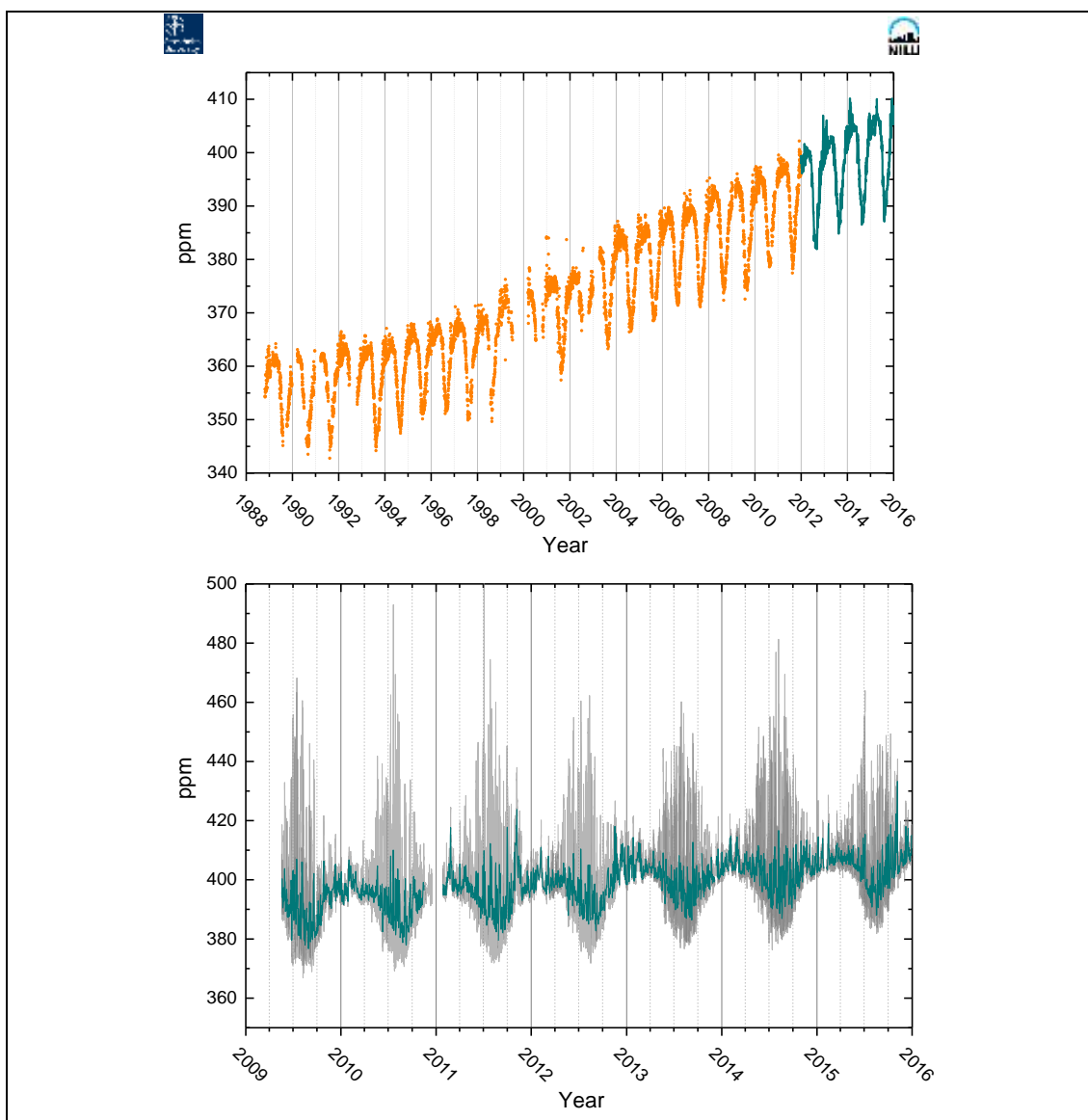


Figure 6: The atmospheric daily mean CO₂ concentration measured at Zeppelin Observatory for the period mid 1988-2015 is presented in the upper panel. Prior to 2012, ITM University of Stockholm provides all data, shown as orange dots and the green solid line is from the Picarro instrument installed by NILU in 2012. The measurements for Birkenes are shown in the lower panel, the green line is the daily mean and the hourly mean is shown as the grey line.

The results show continuous increase since the start of the observations at both sites. As can be seen there are much stronger variability at Birkenes than Zeppelin. At Zeppelin the largest variability is during winter/spring. For Birkenes hourly mean, (lower panel, grey) it is clear that the variations are largest during the summer months. In this period, there is a clear diurnal variation with high values during the night and lower values during daytime. This is mainly due to changes between plant photosynthesis and respiration, but also the general larger meteorological variability and diurnal change in planetary boundary layer, particularly during summer contributes to larger variations in the concentrations. In addition to the diurnal variations, there are also episodes with higher levels at both sites due to transport of pollution from various regions. In general, there are high levels when the meteorological situation results in transport from Central Europe or United Kingdom at Birkenes, and central Europe or Russia at Zeppelin. The maximum daily mean value for CO₂ in 2015 was 433.2 ppm

at Birkenes 6th November, and at Zeppelin the highest daily mean value was 410.2 ppm at 6th December 2015.

Figure 7 shows the development of the annual mean concentrations of CO₂ measured at Zeppelin Observatory for the period 1988-2015 in orange together with the values from Birkenes in green since 2010. The global mean values as given by WMO in black. The yearly annual change is shown in the lower panel.

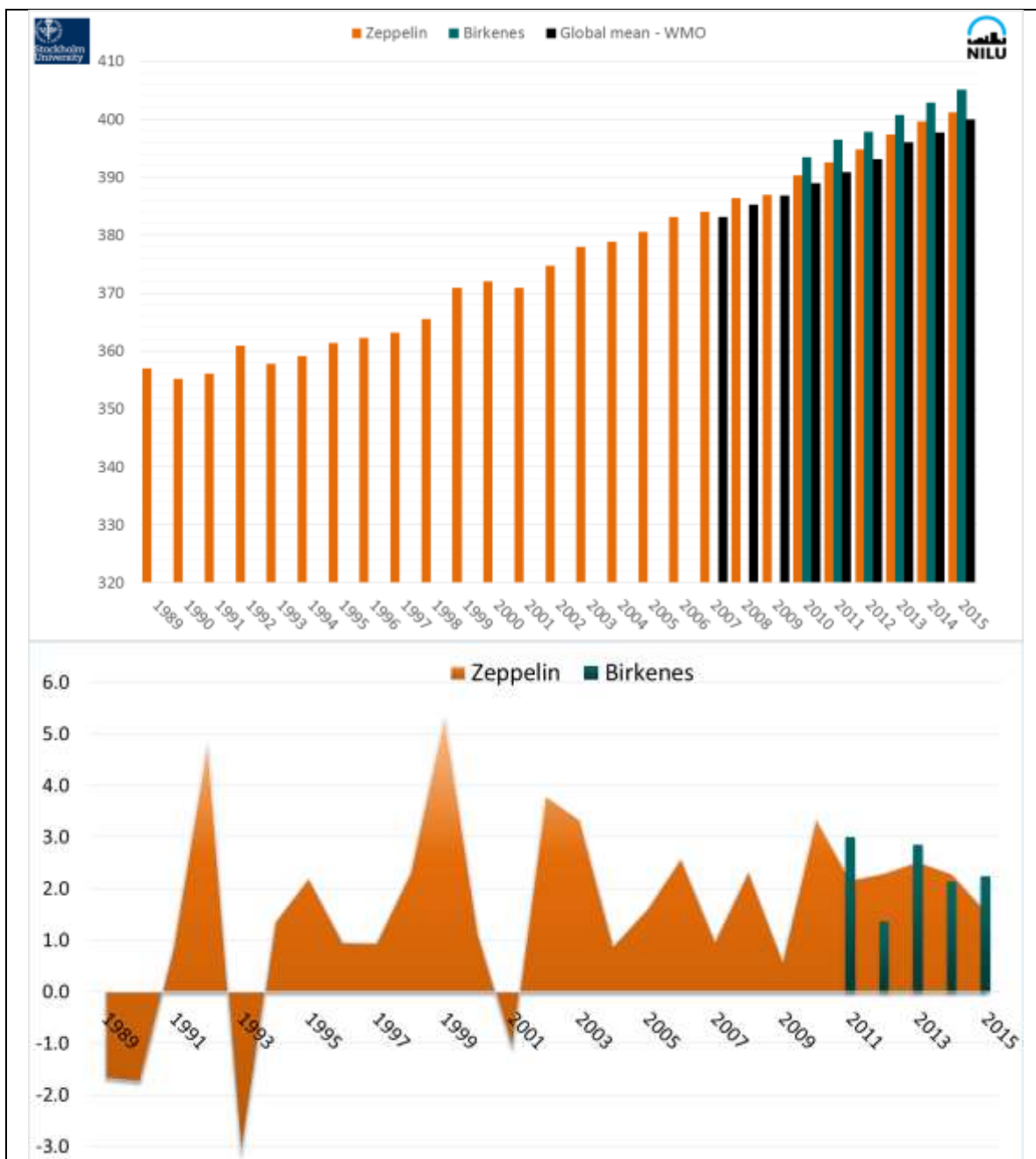


Figure 7: Upper panel: the annual mean concentrations of CO₂ measured at Zeppelin Observatory for the period 1988-2015 shown in orange. Prior to 2012, ITM University of Stockholm provides all data. The annual mean values from Birkenes are shown as green bars. The global mean values as given by WMO are included in black. The yearly annual change is shown in the lower panel, orange for Zeppelin, green for Birkenes.

The global mean increase for 2014 to 2015 was 2.3 (WMO, 2016). The annual mean values for Birkenes and Zeppelin are higher than the global mean as, there are more anthropogenic sources and pollution at the Northern hemisphere. The mixing to the southern hemisphere takes time, ca 2-3 years. The annual change shown in the lower panel shows an increase of only 1.6 ppm at Zeppelin since 2014, which is remarkably low compared to global mean increase and the reason for this would need a thorough study. At Birkenes, the increase since 2014 was 2.2 ppm, in line with the last year's development and the expectations. The time series for CO₂ at Birkenes is too short to be used in trend calculations.

Key findings for CO₂: CO₂ concentration has increased all years subsequently, in accordance with the global mean development and increase of anthropogenic emissions. **The new record levels in 2015 are 401.2 ppm at Zeppelin and 405.1 ppm at Birkenes.** The increase from 2014 to 2015 is 1.6 ppm and 2.2 ppm, respectively, compared to global mean which was 2.3 ppm increase. The increase at Zeppelin is lower than expected, and currently there is no clear explanation for this.

2.1.2 Methane at the Birkenes and Zeppelin Observatories

Our measurements from 2015 reveal a pronounced new record in the observed CH₄ level, both at Zeppelin and Birkenes. Methane (CH₄) is the second most important greenhouse gas from human activity after CO₂. The radiative forcing is 0.48 W m⁻² since 1750 and up to 2011 (Myhre et al., 2013b), but as high as 0.97 W m⁻² for the emission based radiative forcing (Figure 5, page 18) due to complex atmospheric effects. In addition to being a dominant greenhouse gas, methane also plays central role in the atmospheric chemistry. The atmospheric lifetime of methane is approx. 12 years, when indirect effects are included, as explained in section 1.4.

The main sources of methane include boreal and tropical wetlands, rice paddies, emission from ruminant animals, biomass burning, and extraction and combustion of fossil fuels. Further, methane is the principal component of natural gas and e.g. leakage from pipelines; off-shore and on-shore installations are a known source of atmospheric methane. The distribution between natural and anthropogenic sources is approximately 40% natural sources, and 60% of the sources are direct result of anthropogenic emissions. Of natural sources there is a large unknown potential methane source under the ocean floor, so called methane hydrates and seeps. Further, a large unknown amount of carbon is bounded in the permafrost layer in Siberia and North America and this might be released as methane if the permafrost layer melts as a feedback to climate change.

The average CH₄ concentration in the atmosphere is determined by a balance between emission from the various sources and reaction and removal by free hydroxyl radicals (OH) to produce water and CO₂. A small fraction is also removed by surface deposition. Since the reaction with OH also represents a significant loss path for the oxidant OH, additional CH₄ emission will consume additional OH and thereby increasing the CH₄ lifetime, implying further increases in atmospheric CH₄ concentrations (Isaksen and Hov, 1987; Prather et al., 2001). The OH radical has a crucial role in the tropospheric chemistry by reactions with many emitted components and is responsible for the cleaning of the atmosphere (e.g. removal of

CO, hydrocarbons, HFCs, and others). A stratospheric impact of CH₄ is due to the fact that CH₄ contributes to water vapour build up in this part of the atmosphere, influencing and reducing stratospheric ozone.

The atmospheric mixing ratio of CH₄ was, after a strong increase during the 20th century, relatively stable over the period 1998-2006. The global average change was close to zero for this period, also at Zeppelin. Recently an increase in the CH₄ levels is evident from our observations both at Zeppelin and Birkenes as well as observations at other sites, and in the global mean (see e.g. section 2.2.1.1.2 in Hartmann et al, 2013, WMO, 2014).

Figure 8 depicts the daily mean observations of CH₄ at Zeppelin since the start in 2001 in the upper panel and Birkenes since start in 2009 in the lower panel.

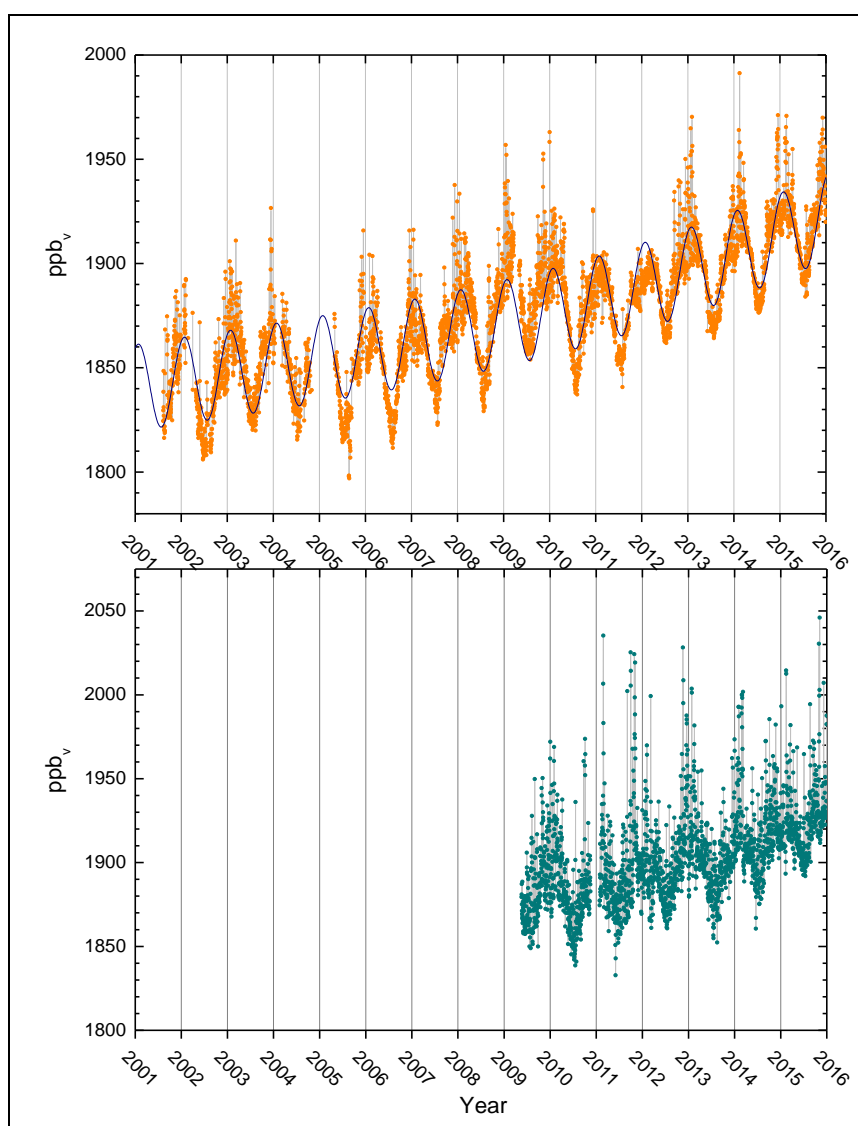


Figure 8: Observations of daily averaged methane mixing ratio for the period 2001-2015 at the Zeppelin Observatory in the upper panel. Grey: all data, orange dots: daily concentrations, black solid line: empirical modelled background methane mixing ratio (fit does not include transport episodes). The right panel show the transport of air to Zeppelin the 15th February, where maximum CH₄ is observed (see the green circle). Daily mean observations for Birkenes are shown in the lower panel as green dots.

As can be seen from the Figure there has been an increase in the concentrations of CH₄ observed at both sites the last years, and in general the concentrations are much higher at Birkenes than at Zeppelin. The highest ever ambient background CH₄ concentration detected at Zeppelin was on the 15th February 2014. This was 1991.3 ppb, and the transport pattern of that day shows strong influence from Russian industrial pollution. Fugitive emission from Russian gas installations is a possible source of this CH₄ however, on this particular day, both CO and CO₂ levels were also very high, indicative of an industrial and urban pollution episode. This year there were several strong episodes, but not with the high value as observed in 2014. As a part of a research project, we could investigate these in more detail this year, and this is included in see section 2.1.2.1 at page 30.

For both Zeppelin and Birkenes, the seasonal variations are clearly visible, although stronger at Birkenes than Zeppelin. This is due longer distance to the sources at Zeppelin, and thus the sink through reaction with OH dominates the variation. The larger variations at Birkenes are explained by both the regional sources in Norway, as well as a stronger impact of pollution episodes from long range transport of pollution from Europe. For the daily mean in Figure 8, the measurements show very special characteristics in 2010 and 2011 at Zeppelin. As shown, there is remarkably lower variability in the daily mean in 2011 with fewer episodes than the typical situation in previous and subsequent e.g. summer/autumn 2012. The reason for this has been intensively investigated as part of various national and international research programmes, also at NILU (e.g. Thompson *et al*, 2016).

At Zeppelin there are now almost 15 years of data, for which the trend has been calculated. To retrieve the annual trend in the methane for the entire period, the observations have been fitted by an empirical equation. The fit to the observed methane values are shown as the black solid line in Figure 8. Only the observations during periods with clean air arriving at Zeppelin are used in the model, thus the model represents the background level of methane at the site (see Appendix I for details). This corresponds to an average increase of 5.2 ppb per year, or ca 0.4% per year, the last years. The pronounced increase started in November/December 2005 and continued throughout the years 2007 - 2009, and is particularly evident in the late summer-winter 2007, and summer-autumn 2009. For Birkenes shown in the lower panel, the time series is too short for trend calculations, but a yearly increase is evident since the start 2009. There are also episodes with higher levels due to transport of pollution from various regions. In general, there are high levels when the meteorological situation results in transport from Central Europe.

The year 2015 showed 1845 ppb CH₄ as the new record in global annual mean values (WMO, 2016), and Zeppelin and Birkenes revealed new record levels at both sites. The annual mean increase in the CH₄ levels the last years is visualised in Figure 9 showing the CH₄ annual mean mixing ratio for the period 2001-2015 from Zeppelin (orange) and for Birkenes (green) from 2010-2015. The global mean value given by WMO (WMO, 2016) is included for comparison, together with the published IPCC global mean value for 2011 (IPCC, 2013).

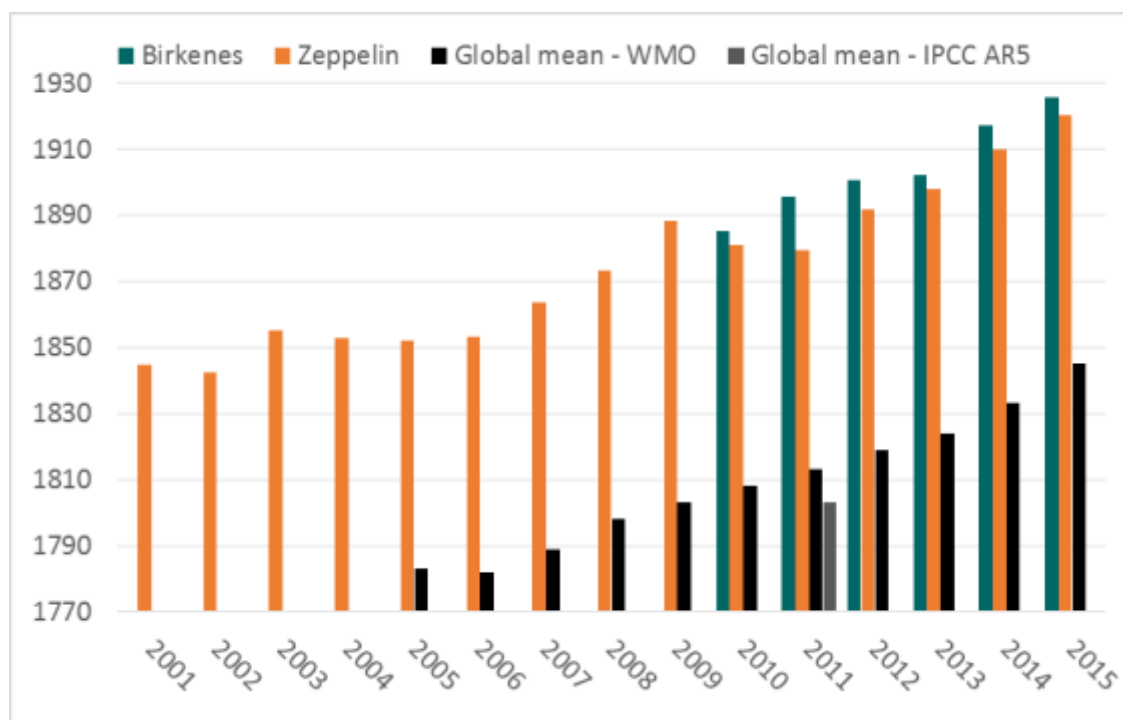


Figure 9: Development of the annual mean mixing ratio of methane in ppb measured at the Zeppelin Observatory (orange bars) for the period 2001-2015, Birkenes for the period 2010-2015 in green bars, compared to global mean provided by WMO as black bars (WMO, 2016).

The annual means are based on the measured methane values. Modelled empirical background values are used, when data is lacking in the calculation of the annual mean. The diagram in Figure 9 clearly illustrates the increase in the concentrations of methane at Zeppelin since 2005 a small decrease from 2010 to 2011, and then a new record level in 2015. The annual mean mixing ratio for 2015 was 1920 ppb, an increase of 10 ppb, compared from 2014 to 2015. The annual mean value for 2015 confirms that there is still a strong increase from year to year in Arctic methane. The global mean for 2015 was 1945 ppb, with an increase of 11 ppb from the year before. The increase at Birkenes was slightly weaker for 2014-2015; 8.5 ppb. The increase since 2005 at Zeppelin is 68 ppb (approx. 3.7 %) which is high compared to the development of the methane mixing ratio in the period from 1999-2005 at Zeppelin, Svalbard and globally. It is also slightly higher than the global mean increase since 2005 which was 60 ppb, as published in the yearly bulletins by WMO (WMO, 2011, 2012, 2013, 2014, 2015, 2016). The global mean shows an increase since 2006, which over the years 2009-2013 was e.g. 5-6 ppb per year but as high as 9 ppb from 2013-2014 and 12 ppb from 2014-2015, close to what we detected at Zeppelin from 2013-2014.

Larger fluctuations are evident at Zeppelin. This is explained by the distribution of the sources; there are more sources in the northern hemisphere, and thus more inter-annual variations. The global mean is lower as this includes all areas of the globe, e.g. remote locations such as Antarctica and is therefore lower than the values at Zeppelin and Birkenes, located closer to the sources. Hence, there is a time lag in the development. For comparison, during the 1980s when the methane mixing ratio showed a strong increase, the annual global mean change was around 15 ppb per year.

Currently, the observed increase over the last years is not fully explained. The recent observed increase in the atmospheric methane concentrations has led to enhanced focus and

intensified research to improve the understanding of the methane sources and changes particularly in responses to global and regional climate change. Leaks from gas installations, world-wide, both onshore and offshore might be an increasing source. Hence, it is essential to find out if the increase since 2005 is due to high emissions from point sources, or if it is caused by newly initiated processes releasing methane to the atmosphere e.g. the thawing of the permafrost layer or processes in the ocean, both related to permafrost and others. Recent and ongoing scientific discussions point in the direction of increased emissions from wetlands located both in the tropical region and in the Arctic region. This is also investigated in a collaboration between NILU and Cicero (Dalsøren et al., 2016). Gas hydrates at the sea floor are widespread in thick sediments in this area between Spitsbergen and Greenland. If the sea bottom warms, this might initiate further emissions from this source. This is the core of the large polar research project *MOCA - Methane Emissions from the Arctic Ocean to the Atmosphere: Present and Future Climate Effects*³, which started at NILU in October 2013, and is expected to be finalized by spring 2017 (see <http://moca.nilu.no>). A few results from this is included in next the section.

Key findings for Methane - CH₄: In 2015 the mixing ratios of methane increased to a **new record level both at Zeppelin, Birkenes and globally**. At Zeppelin the annual mean value reached 1920 ppb with an increase of as much as 10 ppb since 2014. The changes in the last 10 years are large compared to the evolution of the methane levels in the period 1998-2005, when the change was close to zero both at Zeppelin and globally, after a strong increase during the mid 20th Century. The methane increase at the Zeppelin observatory from 2005 to 2015, (69 ppb, or around 3.7%) was larger than the global increase in the same period (approx. 62 ppb, or 3.5 %). The measurements of CH₄ at Birkenes showed an annual mean value for 2015 of 1925 ppb, which is higher than the annual values both for Zeppelin and the global mean. The increase from 2014 to 2015 at Birkenes was 8.5 ppb. This is lower than the increase for 2013-2014 which was as high as 15 ppb.

There is a combination of causes explaining the increase in methane the last years, and the dominating reason is not clear. A probable explanation is increased methane emissions from wetlands, both in the tropics as well as in the Arctic region, in addition to increases in emission from the fossil fuel industry. Melting permafrost, both in terrestrial regions and in marine region, might introduce new possible methane emission sources initiated by the temperature increase the last years in the Arctic region.

³ <http://moca.nilu.no/>

2.1.2.1 Methane from Arctic Ocean to the atmosphere?

There is an ongoing comprehensive research project at NILU “*MOCA - Methane Emissions from the Arctic Ocean to the Atmosphere: Present and Future Climate Effects*” focusing on methane from Arctic Ocean to the atmosphere. This is collaboration with CAGE (The Centre for Arctic Gas Hydrate, Environment and Climate, at UiT The Arctic University of Norway) and Cicero, but lead by NILU. The driving questions for MOCA are:

- I. What is the status and current release of methane from marine seep sites and methane hydrates in the Arctic Ocean, and specifically around Svalbard?
- II. How are these processes depending on trends in sea temperature and annual variations?
- III. Where are the most important areas in the Arctic Ocean which could constitute a possible source of atmospheric methane, now and in the future?
- IV. What is the present CH₄ emission from the seabed to the atmosphere?
- V. What is the most likely change in flux, the next 50 and 100 years under realistic climate scenarios? And what is the global effect of this?
- VI. What is the ocean temperature threshold for large changes in emission of methane from hydrates?

In this project we use integrated approaches to answer these questions. Figure 10 shows the exploratory platforms involved. Comprehensive measurement campaigns involving ship, aircrafts and Zeppelin have been performed. We have used additionally we use models both atmospheric chemistry, methane hydrates modelling at sea floor, and and climate models.

What are gas hydrates?

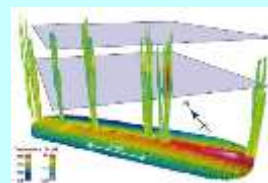
Large amounts of natural gas, mainly methane, are stored in the form of hydrates in continental margins worldwide, particularly, in the Arctic. Gas hydrate consists of ice-like crystalline solids of water molecules



encaging gas molecules, and is often referred to as ‘the ice that burns’.

What are seeps?

Cold seeps are locations where hydrocarbons are emitted from sub-seabed gas reservoirs into the ocean. This can be both from petroleum reservoirs and methane hydrates. The illustration is gas bubbles rising 800 m up from Vestnesa Ridge, offshore Svalbard (Smith et al. 2014). <http://cage.uit.no>



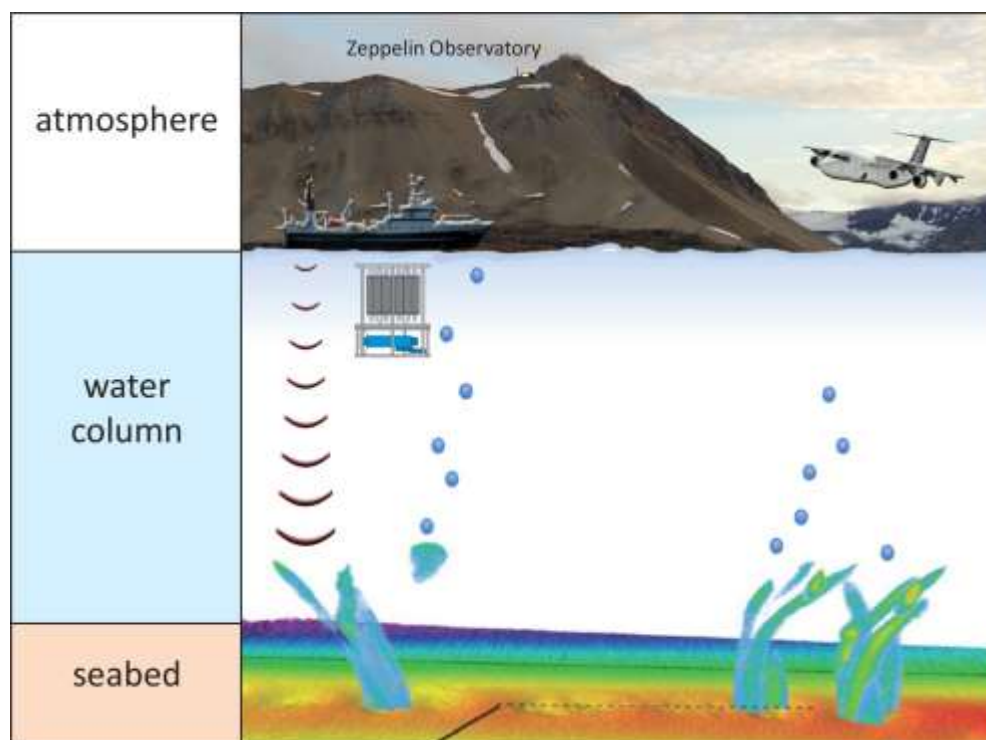


Figure 10: Field campaign and measurement platforms at the sea floor, in the water column, and in the atmosphere west of Svalbard in June-July 2014. Seeps on the seafloor, represented here by swath bathymetry, release gas bubbles that rise through the water column. The Research Vessel Helmer Hanssen detected gas bubbles and collected water samples at various depths, and provided online atmospheric CH₄, CO and CO₂ mixing ratios and discrete sampling of complementary trace gases and isotopic ratios. The Facility of Airborne Atmospheric Measurements (FAAM) aircraft measured numerous gases in the atmosphere, and an extended measurement program was performed at the Zeppelin Observatory close to Ny-Ålesund. Data from Zeppelin was used for comparison to detect possible oceanic sources.

We have used different state-of-the-art models to assess and understand the variation in Arctic methane, to investigate potential oceanic sources in various regions, in particular methane hydrates and cold seeps. First, results are presented in Myhre et al (2016), Pisso et al (2016), Thompson et al (2016), and some information can be found here: <http://forskning.no/havforskning-klima-arktis/2016/05/metan-slipper-ikke-ut-av-polhavet-om-sommeren>.

As a part of this, we included a detailed analysis of the 2015 methane time series at Zeppelin, using the FLEXPART model at NILU. Detail information about sources regions for 5 episodes are included in Figure 11.

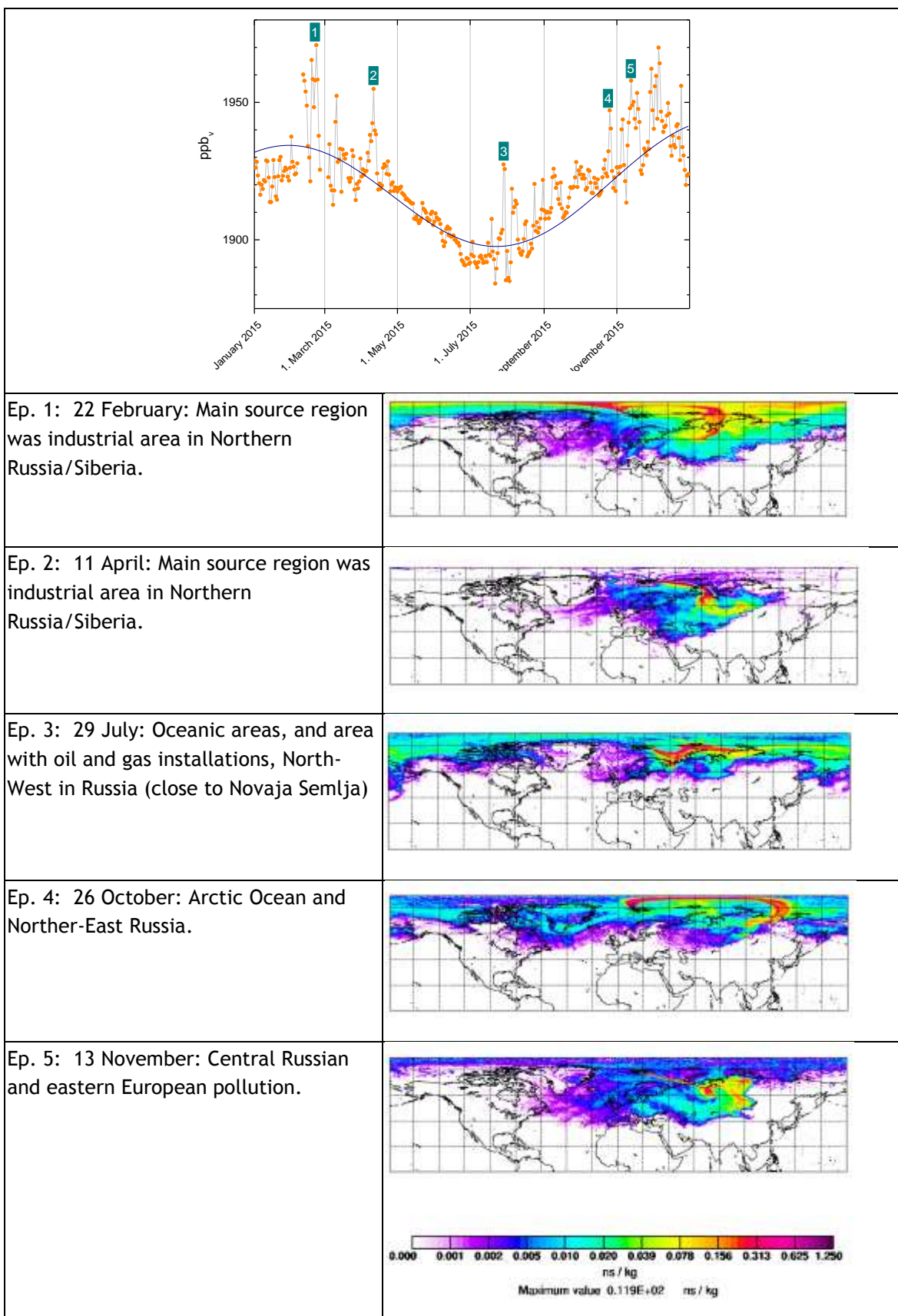


Figure 11: Illustration of impact on CH₄ at Zeppelin from different regions in the Arctic by use of FLEXPART (See also Pisso et al, 2016).

2.1.3 Non-methane hydrocarbons (NMHC) at the Zeppelin Observatory

Atmospheric NMHC oxidation contributes to the production of tropospheric ozone and influences photochemical processing, both impacting climate and air quality. Sources of NMHCs (here ethane, propane, butane, pentane) include natural (mostly geological but also from wild fires) and anthropogenic (fossil fuels) ones. CH_4 and NMHCs are co-emitted from oil and natural gas sources, for CH_4 to ethane the mass ratio varies from 7 to 14 (Helmig et al, 2016). The atmospheric ethane budget is not well understood and state-of-the-art atmospheric models underestimate ethane-mixing ratios, implying that current emission inventories require additional sources to balance the global atmospheric ethane budget.

Helmig et al (2016) showed, from long-term observations of ethane from a global network that concentrations are increasing (since circa 2010), and that there is a strong latitudinal gradient, with the highest abundances observed in the Arctic, and a steep decline towards the south. They concluded that emissions from North American oil and natural gas development are the primary cause of increasing concentrations in recent years. However, there might be other factors. A recent study by Nicewonger *et al* (2016) used analysis of polar ice cores to estimate the pre-industrial emissions and concluded that natural ethane emissions from geologic seeps contributed significantly to the preindustrial ethane budget. Etiope and Ciccioli (2009) suggested that a substantial part of the missing ethane source can be attributed to gas seepage, but they did not include the Arctic in their study.

Figure 12 shows the daily mean observations of the four NMHCs included in the programme, ethane, propane, butane and pentane, at Zeppelin since the start in September 2010.

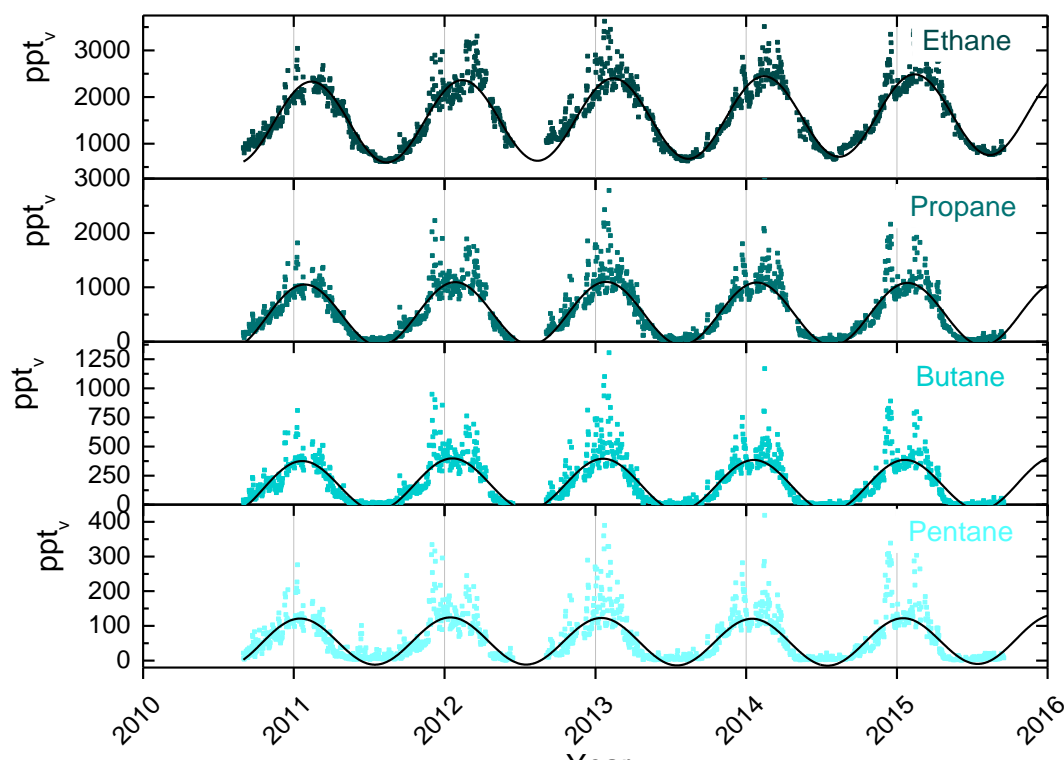


Figure 12: Observations of daily averaged mixing ratio of benzene (upper panel) and toluene (lower panel) for the period September 2010 - 2015 at the Zeppelin Observatory.

Due to the short lifetimes ranging from a few days for pentane to 2-3 months for ethane, the annual cycles are very strong. The time series are too short for calculation of trends, but annual mean development are given in Figure 13.

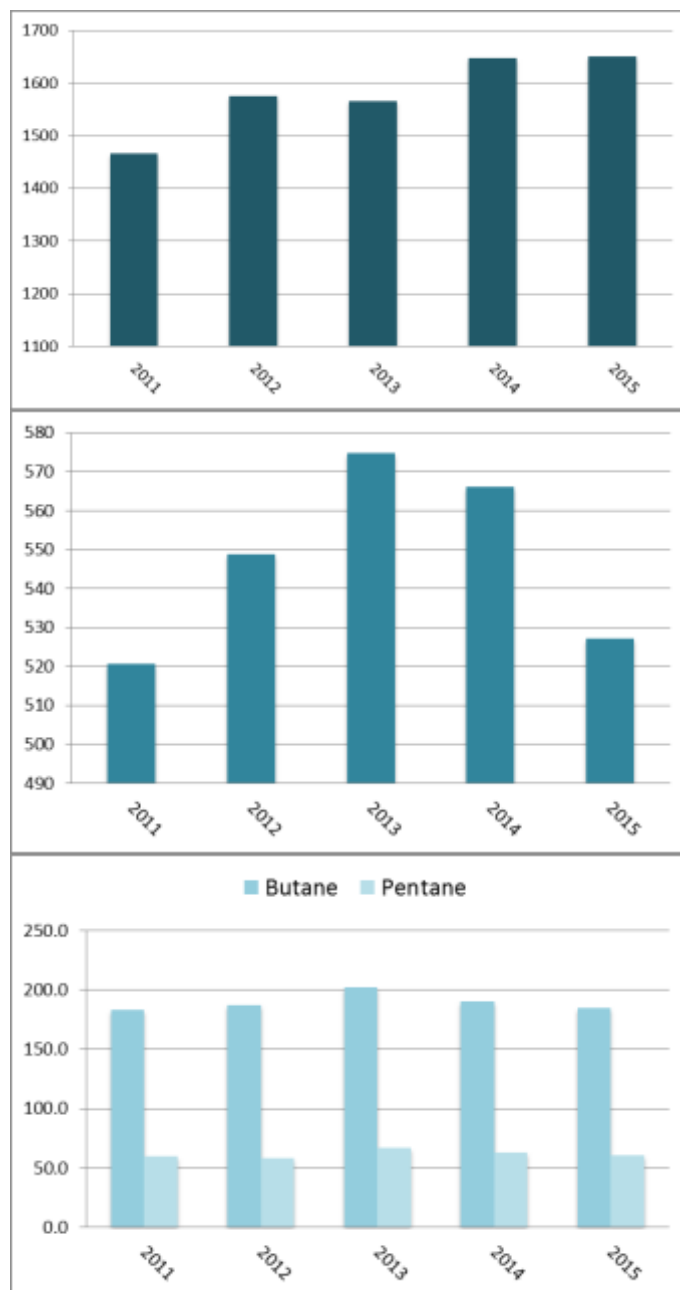


Figure 13: Development of the annual means of the measured non-methane hydrocarbons at the Zeppelin Observatory for the period 2011-2015. Upper panel in dark green: ethane, mid-panel propane, and lower panel Butane and Pentane.

The data coverage the compounds are relatively low over the period, hence the development is uncertain. Still, it seems that the development of the annual means since 2011

demonstrates that ethane has increased and have a different development than the more heavy NMHCs in the lower panels, although many of the sources are considered as the same. Hence, this can indicate that some of dominating ethane sources, with less content of the heavier NMHC is increasing, compared to the others.

Key findings - NMHC: The hydrocarbon **ethane**, often co-emitted with fossil fuel methane, is increasing at Zeppelin, but **toluene** and **benzene** (see next section), show stable values since 2014. These are short lived climate gases important for the levels of aerosols, ozone, CO and contribute to CO₂ and others, but with low direct greenhouse gas effects.

2.1.4 Other Volatile Organic Compounds (VOC) at the Zeppelin Observatory

Volatile Organic Compounds (VOCs) are a large group of carbon-based compounds that have a high vapor pressure and easily evaporate at room temperature. At Zeppelin two important VOCs are measured, benzene and toluene, which belong to a group of VOCs found in petroleum hydrocarbons, such as gasoline. The compounds have attracted much attention since they are considered a strong carcinogen (especially benzene), but they are also important for climate. The VOCs have relatively short atmospheric lifetimes and small direct impact on radiative forcing. However, anthropogenic secondary organic aerosols (SOA) are formed from photo oxidation of benzene and toluene (Ng et al., 2007), which indirectly impacts the climate. The SOA formation from these VOCs is most effective under low-NO_x conditions and when ambient concentration of organic aerosols is high. Thus, benzene and toluene influence climate through their production of secondary organic aerosols and their involvement in photochemistry, i.e., production of O₃ in the presence of light.

Figure 14 depicts the daily mean observations of benzene and toluene at Zeppelin since the start in September 2010.

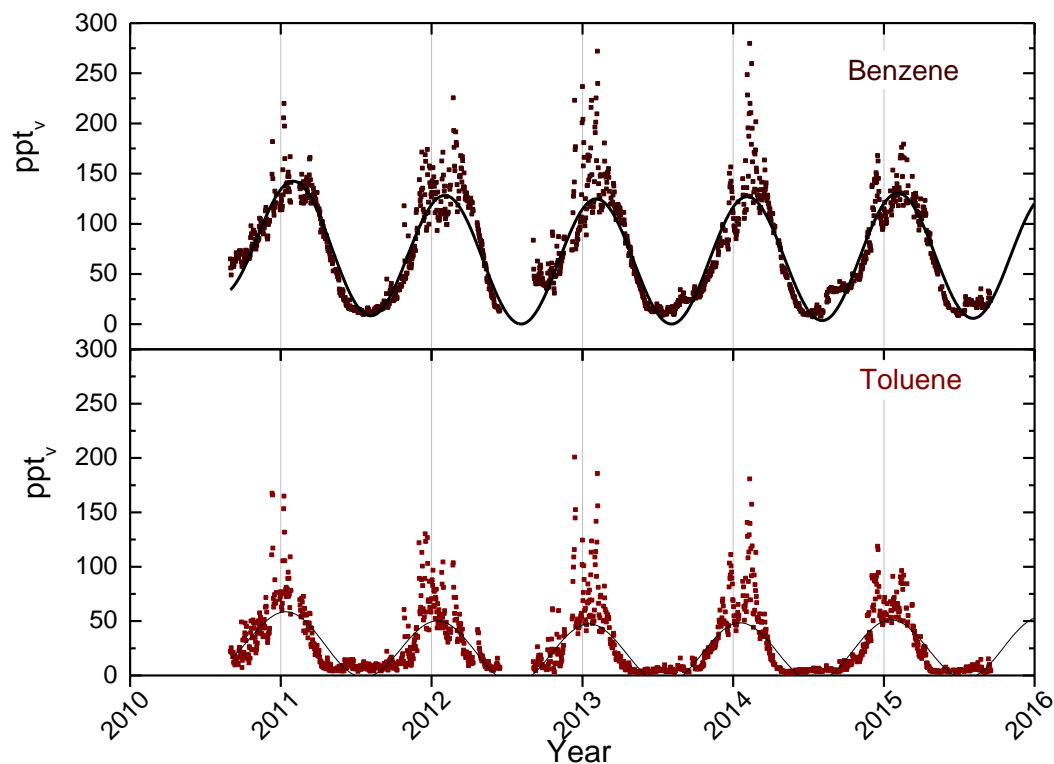


Figure 14: Observations of daily averaged mixing ratio of benzene (upper panel) and toluene (lower panel) for the period September 2010 - 2015 at the Zeppelin Observatory.

As can be seen from the Figure there is strong annual variations, mainly explained by the reactions induced by sunlight. For both component there seem to be a decreasing trend, but this is far too early to conclude, due to the short time series available.

The annual means of benzene and toluene for the period 2010-2015 is presented in Figure 15. The period 2010 to 2015 was relatively stable for both components, with strong episodes during wintertime due to transport of urban polluted air from lower latitudes.

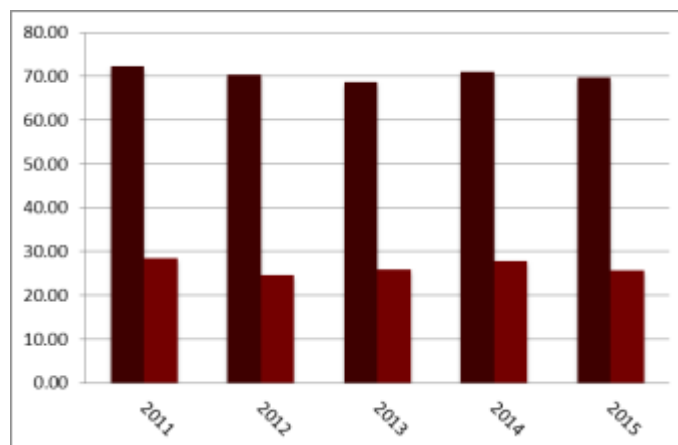


Figure 15: Development of the annual means of benzene (deep brown) and toluene (dark red) for the period September 2011 - 2015 at the Zeppelin Observatory.

2.1.5 Nitrous Oxide at the Zeppelin Observatory

Nitrous Oxide (N_2O) is a greenhouse gas with both natural and anthropogenic sources. The sources include oceans, tropical forests, soil, biomass burning, cultivated soil and use of particular synthetic fertilizer, and various industrial processes. There are high uncertainties in the major soil, agricultural, combustion and oceanic sources of N_2O . Also frozen peat soils in Arctic tundra is reported as a potential source (Repo et al., 2009), but recent studies lead by NILU identify tropical and sub-tropical regions as the largest source regions (Thompson et al, 2013). N_2O is an important greenhouse gas with a radiative forcing of 0.17 W m^{-2} since 1750 contributing around 6 % to the overall well-mixed greenhouse gas forcing over the industrial era. N_2O is also the major source of the ozone-depleting nitric oxide (NO) and nitrogen dioxide (NO_2) in the stratosphere, thus the component is also influencing the stratospheric ozone layer. The Assessment of the ozone depletion (WMO, 2011) suggests that current emissions of N_2O are presently the most significant substance that depletes ozone.

N_2O has increased from around 270 ppb prior to industrialization and up to an average global mean of 328.0 ppb in 2015 (WMO, 2016). In 2009, NILU installed a new instrument at Zeppelin measuring N_2O with high time resolution of 15 minutes. The instrument was in full operation in April 2010 and the results for 2010 -2015 are presented in Figure 16, with the global mean included as horizontal lines for each year.

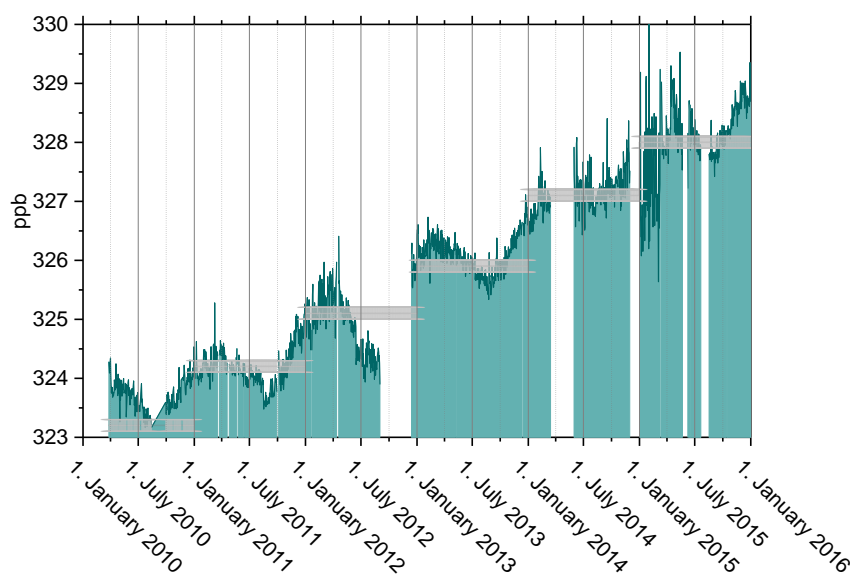


Figure 16: Measurements of N_2O at the Zeppelin Observatory for 2010-2015. The grey shaded areas are global annual mean, with the given uncertainty (WMO, 2011, 2012, 2013, 2014, 2015, 2016)

The time series is too short for trend calculations, but according to WMO (WMO, 2016) the global mean increase of 1 ppb since 2014. Annual mean for Zeppelin in 2015 was 328.1 with a standard deviation of 0.66 ppb. Due to instrumental problems there was a higher uncertainty this year, compared to earlier periods. As can be seen a high variability in 2015 is evident. As a part of ICOS-Norway a Norwegian infrastructure project funded by Norwegian Research Council, a new instrument is purchased and installed autumn 2016. The two instruments will run in parallel to ensure overlap and consistent long time series.

Key findings Nitrous Oxide - N_2O : The global mean level of N_2O has increased from around 270 ppb prior to industrialization and up to an average global mean of 328.1 ppb in 2015, which is new record level after an increase of 0.7 ppb since 2014

2.1.6 Methyl Chloride at the Zeppelin Observatory

Methyl chloride (CH_3Cl) is the most abundant chlorine containing organic gas in the atmosphere, and it contributes approx. 16% to the total chlorine from the well-mixed gases in the troposphere (WMO, 2011). The main sources of methyl chloride are natural, and dominating source is thought to be emissions from warm coastal land, particularly from tropical islands are shown to be a significant source but also algae in the ocean, and biomass burning. Due to the dominating natural sources, this compound is not regulated through any of the Montreal or Kyoto protocols, but is an important natural source of chlorine to the stratosphere. To reach the stratosphere, the lifetime in general needs to be in the order of 2-4 years to have significant chlorine contribution, but this is also dependant on the source strength and their regional distribution. Methyl chloride has relatively high mixing ratios, and contributes to the stratospheric chlorine burden.

The results of the measurements of this substance for the period 2001-2015 are shown in Figure 17.

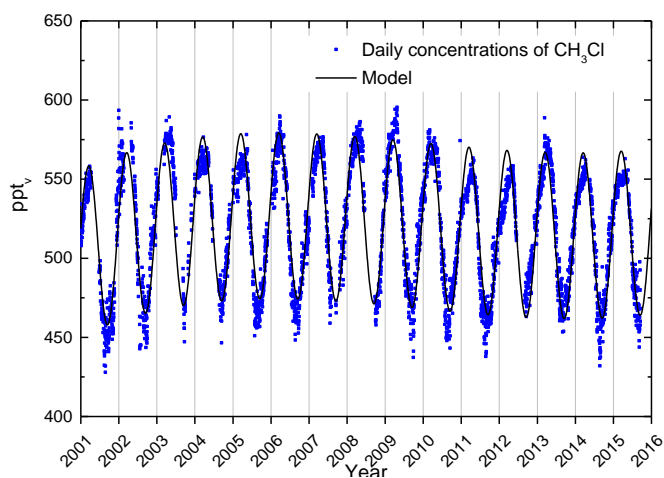


Figure 17: Observations of methyl chloride, CH_3Cl , for the period 2001-2015 at the Zeppelin Observatory. Dots: daily averaged concentrations from the observations, solid line: empirical modelled background mixing ratio.

The lifetime of the compound is only one year resulting in large seasonal fluctuations, as shown in the Figure, responds rapid to changes in emissions. There is a decrease the last years, but this seems to relax in 2011-2012, and a strong increase was detected in 2013. However, it is positive to note that in 2014, the levels were lower, back on the same concentration as in 2012, and a further decrease in 2015, see also Figure 18 with the annual means.

The trend over period 2001-2015 is -0.27 ppt/year. The annual means of methyl chloride for the period 2001-2015 is presented in Figure 18. The period 2002-2009 was relatively stable, but since 2009 there is larger variability. From 2009 to 2015 there was an increase of more than 30 ppt in our data corresponding to an increase of 20%. 2015 showed a reduction compared to 2014, and since 2009 a reduction of 13% is detected. The reasons to this are not clear, and sources resulting the rapid observed changed the last years will be investigated at NILU the coming year. A closer study of source variation for this compound is also recommended by WMO (WMO, 2011), as the sources are also related to atmospheric temperature change and ocean.

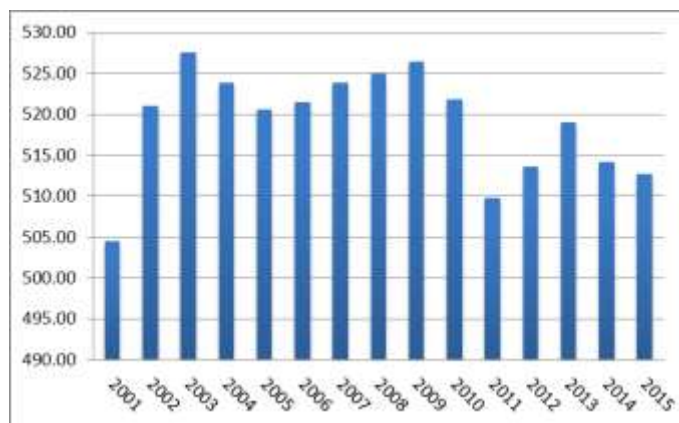


Figure 18: Development of the annual means methyl chloride measured at the Zeppelin Observatory for the period 2001-2015.

2.1.7 Methyl bromide - CH₃Br at the Zeppelin Observatory

The sources of methyl bromide (CH₃Br) are both from natural and anthropogenic activities. The natural sources such as the ocean, plants, and soil, can also be a sink for this substance. Additionally there are also significant anthropogenic sources; it is used in a broad spectrum of pesticides in the control of pest insects, nematodes, weeds, pathogens, and rodents. Biomass burning is also a source and it is used in agriculture primarily for soil fumigation, as well as for commodity and quarantine treatment, and structural fumigation. Even though methyl bromide is a natural substance, the additional methyl bromide added to the atmosphere by humans contributes to the man-made thinning of the ozone layer. Total organic bromine from halons and methyl bromide peaked in 1998 and has declined since. The tropospheric abundance of bromine is decreasing, and the stratospheric abundance is no longer increasing (WMO, 2011).

The results of the daily averaged observations of this compound for the period 2001-2015 are shown in Figure 19. A relatively large change is evident after the year 2007, a reduction of approx. 20% since the year 2005 at Zeppelin. Methyl bromide is a greenhouse gas with a lifetime of 0.8 years and it is 2 times stronger greenhouse gas than CO₂ (Myhre et al, 2013b) if the amount emitted of both gases were equal. The short lifetime explains the stronger annual and seasonal variations of this compound.

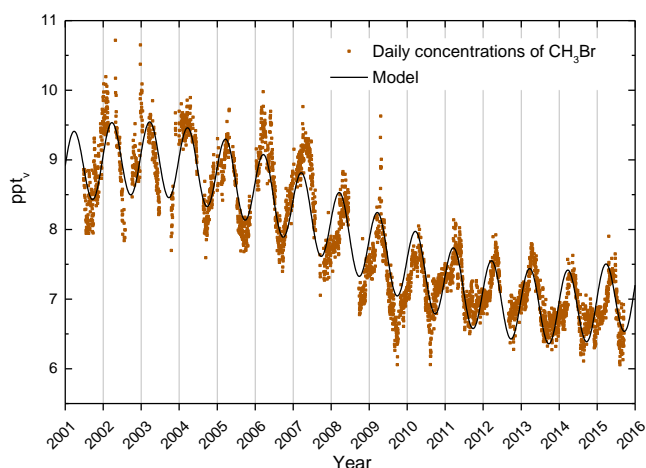


Figure 19: Observations of methyl bromide, CH_3Br , for the period 2001-2015 at the Zeppelin Observatory. Dots: daily averages mixing ratios from the observations, solid line: empirical modelled background mixing ratio.

For the period 2001-2015 there is a reduction in the mixing ratio of -0.18 ppt per year, with a relaxation in the trend the last years. However, note that the observed changes are small (approx. 1.7 ppt since 2005).

The development of the annual means for the period 2001-2015 is presented in Figure 20, clearly illustrating the decrease in the last years. In general atmospheric amounts of methyl bromide have declined since the beginning in 1999 when industrial production was reduced as a result of the Montreal protocol. The global mean mixing ratio was 7.3 - 7.5 ppt in 2011 (Myhre et al, 2013b), slightly lower than at Zeppelin. The differences are explained by slower inter hemispheric mixing. The recent reduction is explained by considerable reduction in the use of this compound; in 2008 the use was 73% lower than the peak year in late 1990s (WMO, 2011).

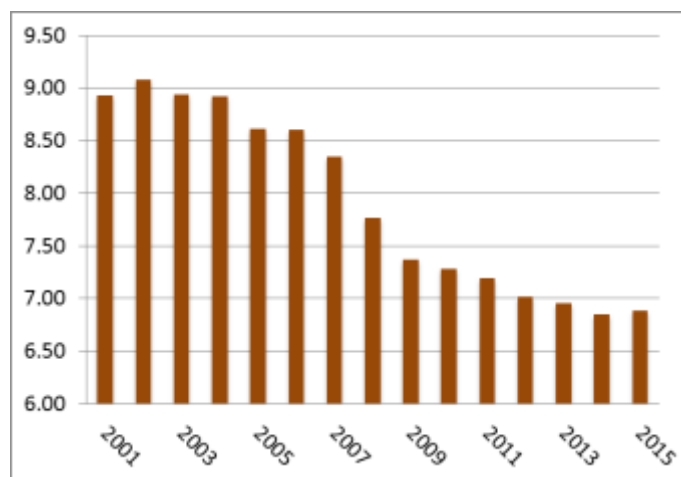


Figure 20: Development of the annual means of methyl bromide (in ppt) measured at the Zeppelin Observatory for the period 2001-2015.

2.1.8 Carbon monoxide at the Zeppelin Observatory

Atmospheric Carbon monoxide (CO) sources are the oxidation of various organic gases as volatile organic compounds (VOC) emitted from fossil fuel, biomass burning, and also oxidation of methane is important. Additionally, emissions from plants, fires and ocean are important sources. CO is not considered as a direct greenhouse gas, mostly because it does not absorb terrestrial thermal IR energy strongly enough. However, CO is able to modulate the level of methane and production of tropospheric ozone, which are both very important greenhouse gas and hence CO is considered as a relevant climate. CO is closely linked to the cycles of methane and ozone and, like methane; CO plays a key role in the control of the OH radical.

CO at Zeppelin is include in the national monitoring programme and the observed CO mixing ratios for the period September 2001-2015 are shown in Figure 21.

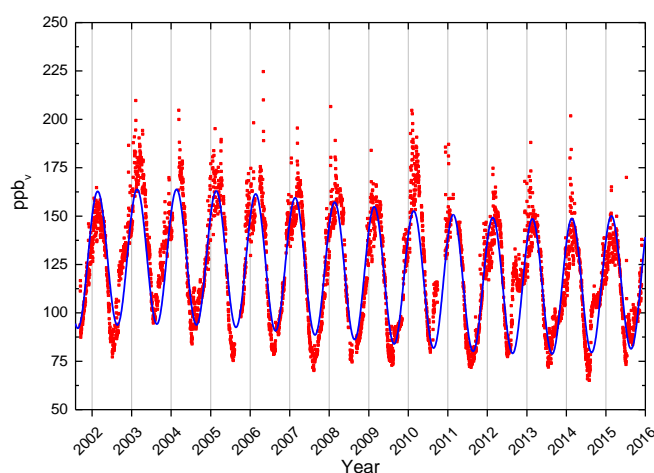


Figure 21: Observations of carbon monoxide (CO) from September 2001 to 31.12.2015 at the Zeppelin observatory. Red dots: daily averaged observed mixing ratios. The solid line is the modelled background mixing ratio.

The concentrations of CO show characteristic seasonal variations. This seasonal cycle is driven by variations in OH concentration as a sink, emission by industries and biomass burning, and transportation on a large scale. As seen from the Figure there are also peak values due to long-range transport of polluted air to Zeppelin and the Arctic. The highest mixing ratio of CO ever observed at Zeppelin; is 217.2 ppb on the 2nd of May 2006. These peak values are due to transport of polluted air from lower latitudes; urban pollution (e.g. combustion of fossil fuel) and in spring 2006 it was from agricultural fires in Eastern Europe. The maximum in 2015 was on 10th of April; 170.1 ppb. The maximum value is caused by transport of pollution from Central Russia, and also CH₄ and CO₂ had yearly maximum value this day, see Figure 8 and also section 2.1.2.1 for comments to this episode. We calculated a trend at Zeppelin of -1.3 ppb per year for the period 2001-2015.

CO has a clear annual cycle with a late winter (February/March) maximum and a late summer (August) minimum, but for the 2015 data the month of July differs slightly from the expected behaviour, a pattern recognized also for the 2014 data. Where in summer usually a decline in the CO concentration is expected, the measurements shows elevated values of CO for the air arriving at measured at Zeppelin Observatory in July.

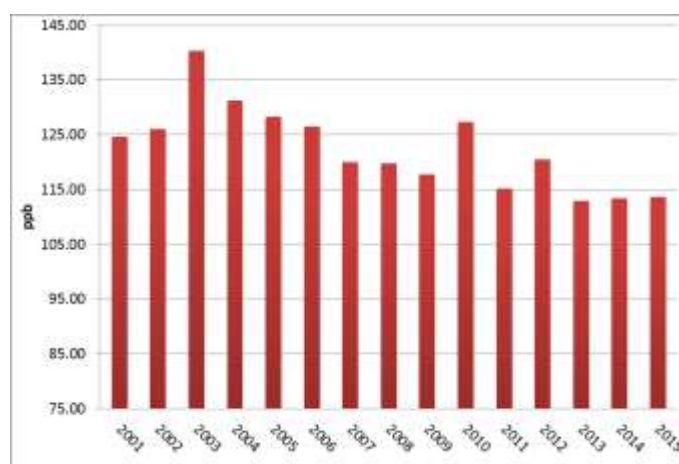


Figure 22: Development of the annual means of CO measured at the Zeppelin Observatory for the period 2001-2015.

CO is an excellent tracer for transport of smoke from fires (biomass burning, agricultural- or forest fires). The elevated concentrations in July 2015 are related to long-range transport of smoke and ash from wildfires in Canada and Alaska. An analyse of the meteorological situation in the first two weeks of July 2015 shows a synoptically high pressure area over Greenland and Canada, with easterly wind direction from Canada towards the northwest, and air masses further arriving in the Arctic via the polar area. 7-days backwards trajectories from the FLEXTRA model, Figure 23, illustrates the synoptical situation on July 10th.

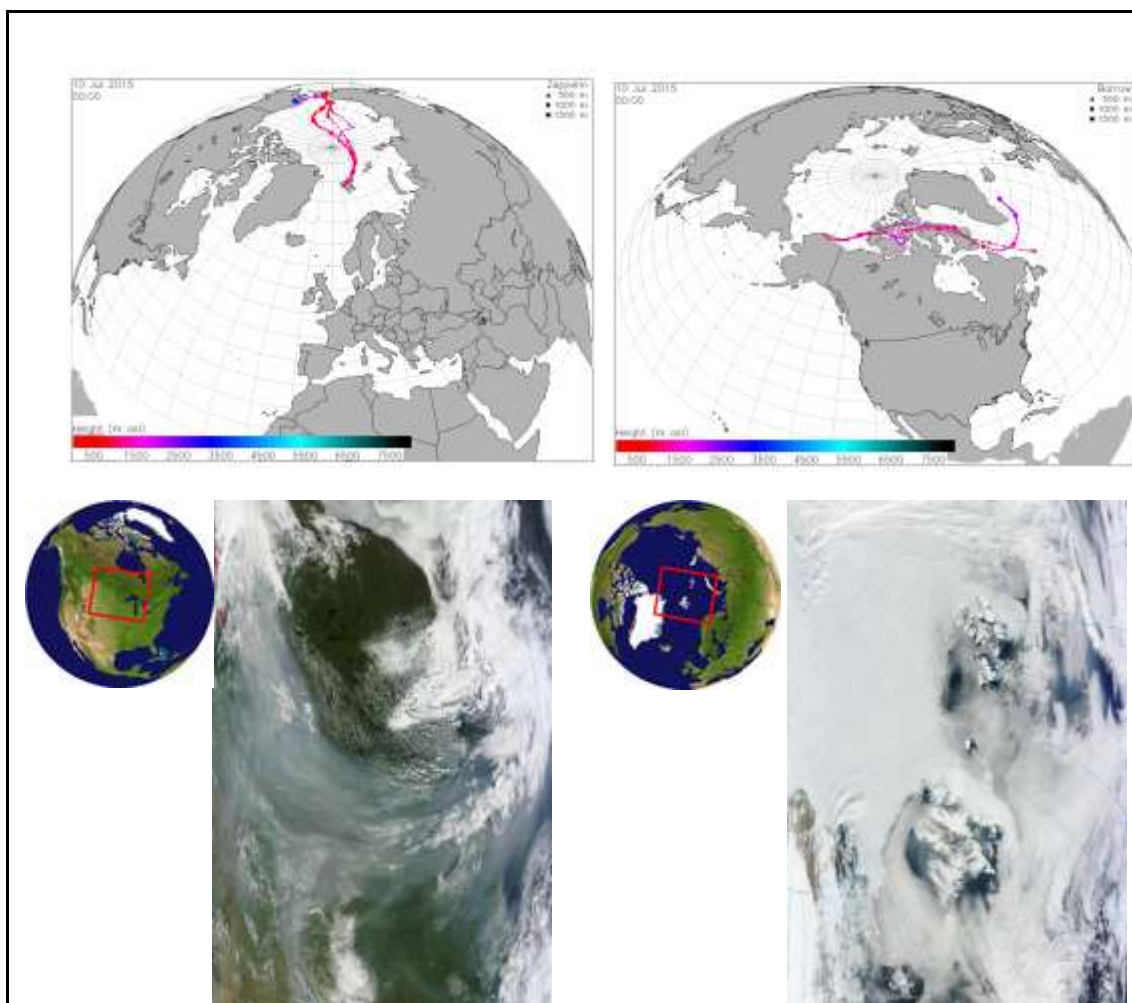


Figure 23: Upper panel: 7-days backwards trajectories from the FLEXTRA model and the synoptical situation on July 10th. Lower panel: the smoke as detected from the MODIS satellite instrument and spread out over North America on July 3rd 2015 (left) and visible above the Svalbard Islands on July 10th (right)

The increased CO concentrations arises as a result of air masses arriving at Zeppelin Observatory is polluted with smoke and particles from more than 200 individual forest fires across British Columbia, Saskatchewan, and Alberta in July 2015, centred in the northwest of the continent. In western Canada, more than three times the area that's normally burned was affected. (<http://www.npr.org/2015/07/11/421995880/wildfires-in-canada-and-alaska-drive-thousands-from-homes>). High record temperatures in most of Alaska also underpinned the situation. The figure also shows the smoke as detected from the MODIS satellite instrument and spread out over North America on July 3rd 2015 (left) and visible above the Svalbard Islands on July 10th (right). The situation lasted until August 8, when the wind in the Arctic shifted to a more southerly direction again bringing air masses with CO concentrations close to the expected average for the season to Zeppelin.

Both summer 2014 and 2015 have shown similar patterns in fluctuations in CO concentration, but it is currently not possible to conclude whether this is due to long term changes in synoptic and long-range transport situations, and/or changes in the frequency and magnitude of fires in the forest fire season. Smoke from wildfires is often injected in the stratosphere and can be transported around the globe with the prevailing jet streams. Soot can stay in the atmosphere for years. The Zeppelin Observatory is a unique station in the Arctic context and it

is thus very important to facilitate the provision of long time series from this observatory for monitoring the situation.

The development of the annual means for the period 2001-2015 are presented in *Figure 22*, clearly illustrating a maximum in the year of 2003. In general the CO concentrations measured at Zeppelin show a decrease during the period 2003 to 2009, and stable levels the last years with a small peak in 2010.

2.2 Greenhouse gases with solely anthropogenic sources

All the gases presented in this chapter have solely anthropogenic sources. These are purely man-made greenhouse gases and are CFCs, HCFCs, HFCs, SF₆ and halons, and most of these gases did not exist in the atmosphere before the 20th century. All these gases except for SF₆ are halogenated hydrocarbons. Although the gases have much lower concentration levels than most of the natural gases mentioned in the previous section, they are strong infrared absorbers, many of them with extremely long atmospheric lifetimes resulting in high global warming potentials; see Table 3. Together as a group, the gases contribute to around 12% to the overall global radiative forcing since 1750 (Myhre et al, 2013b). The annual mean concentrations for all the gases included in the monitoring program for all years are given in Appendix I, Table A 1 at page 95, while all trends, uncertainties and regression coefficients are found in Table A 2 at page 95.

Some of these gases are ozone depleting, and consequently regulated through the Montreal protocol. Additional chlorine and bromine from CFCs, HCFCs and halons added to the atmosphere contributes to the thinning of the ozone layer, allowing increased UV radiation to reach the earth's surface, with potential impact not only to human health and the environment, but to agricultural crops as well. In 1987 the Montreal Protocol was signed in order to reduce the production and use of these ozone-depleting substances (ODS) and the amount of ODS in the troposphere reached a maximum around 1995. The amount of most of the ODS in the troposphere is now declining slowly and one expects to be back to pre-1980 levels around year 2050. In the stratosphere the peak is reached somewhat later, around the year 2000, and observations until 2004 confirm that the level of stratospheric chlorine has not continued to increase (WMO, 2011).

The CFCs, consisting primarily of CFC-11, -12, and -113, accounted for ~62% of total tropospheric chlorine in 2004 and accounted for a decline of 9 ppt chlorine from 2003-2004 (or nearly half of the total chlorine decline in the troposphere over this period) (WMO, 2011).

There are two generations of substitutes for the CFCs, the main group of the ozone depleting substances. The first generation substitutes is now included in the Montreal protocol as they also deplete the ozone layer. This comprises the components called HCFCs listed in Table 3. The second-generation substitutes, the HFCs, are included in the Kyoto protocol. The general situation now is that the CFCs have started to decline, while their substitutes are increasing, and many of them have a steep increase.

2.2.1 Chlorofluorocarbons (CFCs) at Zeppelin Observatory

This section includes the results of the observations of the CFCs: CFC-11, CFC-12, CFC-113, and CFC-115. These are the main ozone depleting gases, and the anthropogenic emissions started around 1930s and were restricted in the first Montreal protocol. The main sources of these compounds were foam blowing, aerosol propellant, temperature control (refrigerators), solvent, and electronics industry. The highest production of the observed CFCs was around 1985 and maximum emissions were around 1987. The lifetimes of the compounds are long, as

given in Table 3, and combined with strong infrared absorption properties, the GWP is high. Figure 24 shows the daily averaged observed mixing ratios of these four CFCs.

The instrumentation employed at Zeppelin is not in accordance with recommendations and criteria of AGAGE for measurements of CFCs, and there are relatively high uncertainties in the observations of these compounds, see also Appendix I. As a result, the trends are connected with large uncertainties. From September 2010, new and improved instrumentation was installed at Zeppelin providing more accurate observations of these compounds. The higher precisions are clearly visualised in Figure 24, but due to several severe instrumental problems in 2015, there are few days with measurements of these compounds⁴.

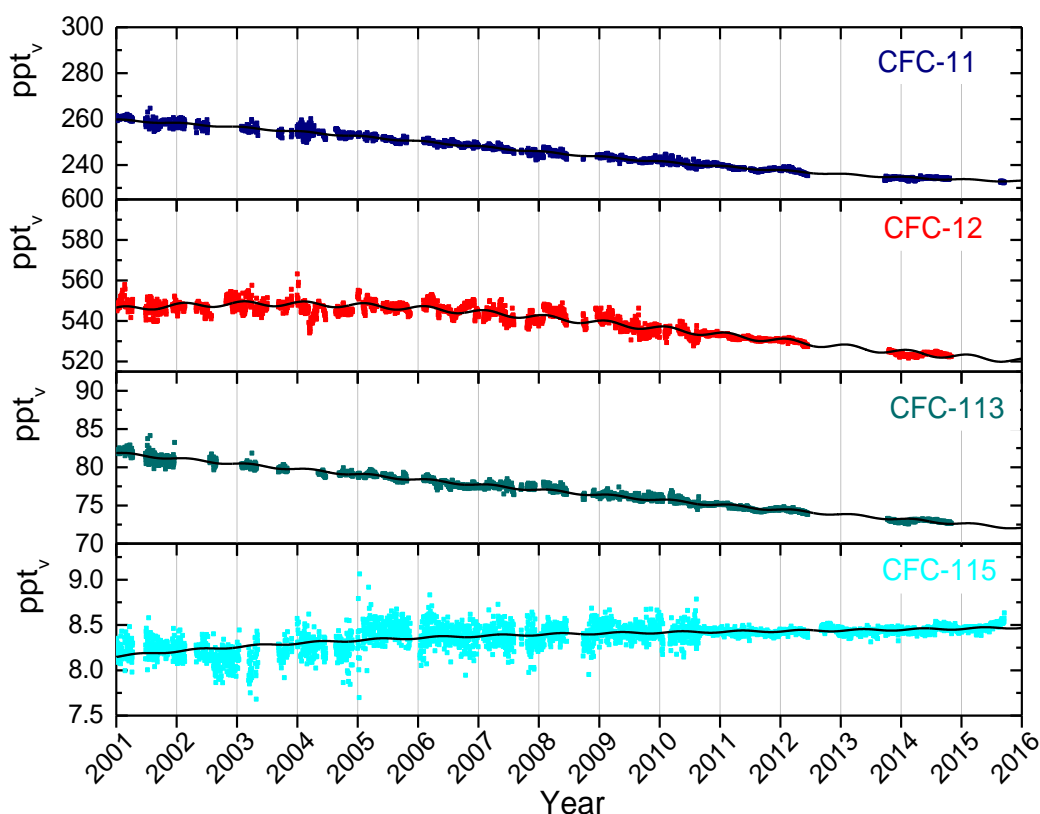


Figure 24: Daily averaged mixing ratios of the monitored CFCs: CFC-11 (dark blue), CFC-12 (red), CFC-113 (green) and CFC-115 (light blue) for the period 2001-2015 at the Zeppelin observatory. The solid lines are modelled background mixing ratio.

The trends per year for the substances CFC-11, CFC12 and CFC-113 given in Table 3 are all negative, and the changes in the trends are also negative, indicating acceleration in the decline⁴. For the compound CFC-115, the trend is still slightly positive, +0.02 ppt/year, and there is a new increase last years, after a stable period. However, it is important to note the low data coverage the last year, and hence a higher uncertainty. In total, the development of

⁴ The current instrumentation is not in accordance with recommendations and criteria of AGAGE for measurements of the CFCs and there are larger uncertainties in the observations of this compound, see also Appendix I. This is also why these compounds are very sensitive to instrumental problems.

the CFC levels at the global background site Zeppelin is very promising, and as expected in accordance with the compliance of the Montreal protocol.

The development of the annual means for all the observed CFCs is shown in Figure 25. The global annual mean of 2011 as given in IPCC (Chapter 8, Myhre et al, 2013b) is included as black bars for comparison. As can be seen, the concentrations at Zeppelin are very close to the global mean for these compounds, as the lifetimes are long and there are hardly any present-day emissions.

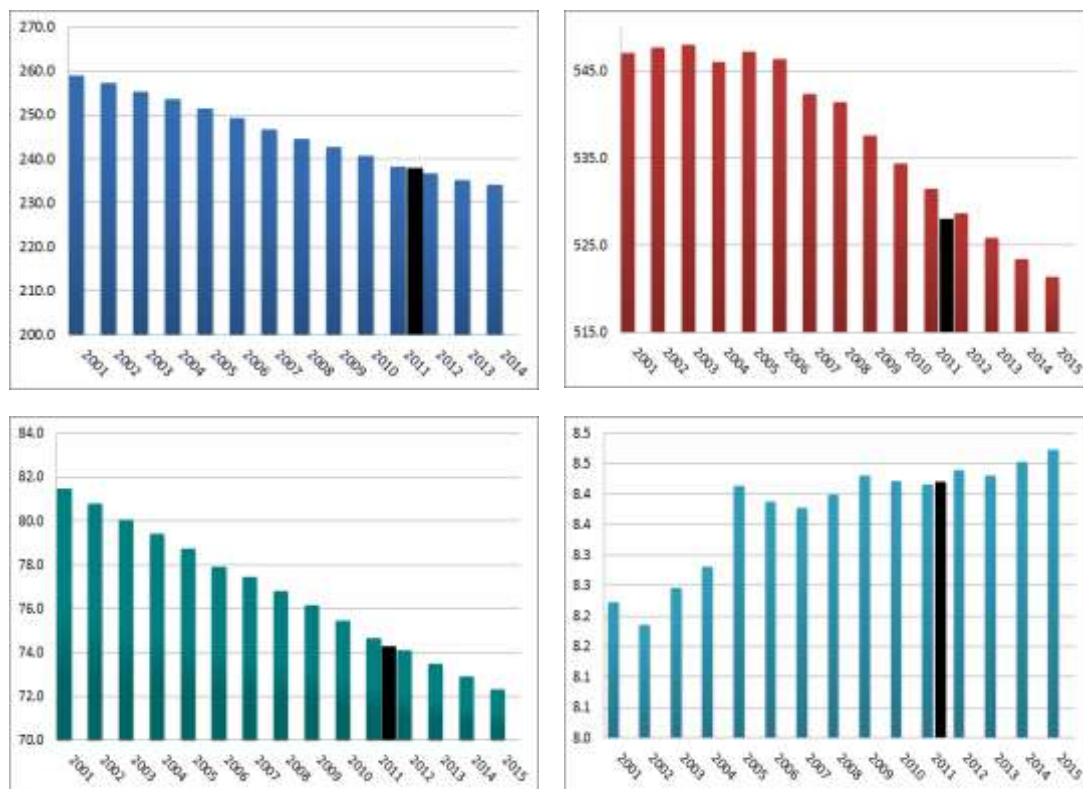


Figure 25: Development of the annual means all the observed CFCs at the Zeppelin Observatory for the period 2001-2015. Upper left panel: CFC-11, upper right panel: CFC-12, lower left panel: CFC-113, lower right panel: CFC-115. See Appendix I for data quality and uncertainty. The global annual mean as given in IPCC (Chapter 8, Myhre et al, 2013b) is included as grey bars. All units are ppt.

According to WMO (WMO, 2011) the global mean mixing ratios of CFC-11 are decreasing with approximately 2.0 ppt +/- 0.01 ppt. This is in accordance with our results at Zeppelin (2.1 ppt/year). CFC-12 (the red diagram) has high GWP, 10200, the third highest of all gases observed at Zeppelin. The global averaged atmospheric mixing ratio of CFC-12 has been decreasing at a rate of 0.5% over the year 2004-2008 (WMO, 2011). This fits well with our observations as CFC-12 has the maximum in 2003-2004. There is a clear reduction the last years of -23 ppt since the maximum year 2005.

Key findings - CFCs: In total the development of the CFC gases measured at the global background site Zeppelin give reason for optimism. The concentration of the observed CFCs, **CFC-11, CFC-12 and CFC-113 are declining**. The mixing ratios of these gases are now reduced with approx. 9.6%, 4.3% and 10.5% respectively since the start in 2001. **CFC-115**

seems to have stabilized but was in 2015 slightly higher than in 2014, and has a total increase of 2,8% over the whole period.

2.2.2 Hydrochlorofluorocarbons (HCFCs) at Zeppelin Observatory

This section includes the observations of the following components: HCFC-22, HCFC-141b and HCFC-142b. These are all first generation replacement gases for the CFCs and their lifetimes are rather long, see Table 3. The main sources of these gases are temperature control (refrigerants), foam blowing and solvents, as for the CFCs, which they are supposed to replace. All these gases are regulated through the Montreal protocol as they all contain chlorine. The use of the gases is now frozen, but they are not completely phased out. The gases they have potentially strong warming effects, depending on their concentrations and absorption properties; their GWPs are high (see Table 3). The compound HCFC-142b has the highest GWP of these, and the warming potential is 1980 times stronger than CO₂, per kg gas emitted. These gases also contain chlorine, and thus are contributing to the depletion of the ozone layer.

The daily averaged observations of these gases are shown in Figure 26 for the period 2001-2015.

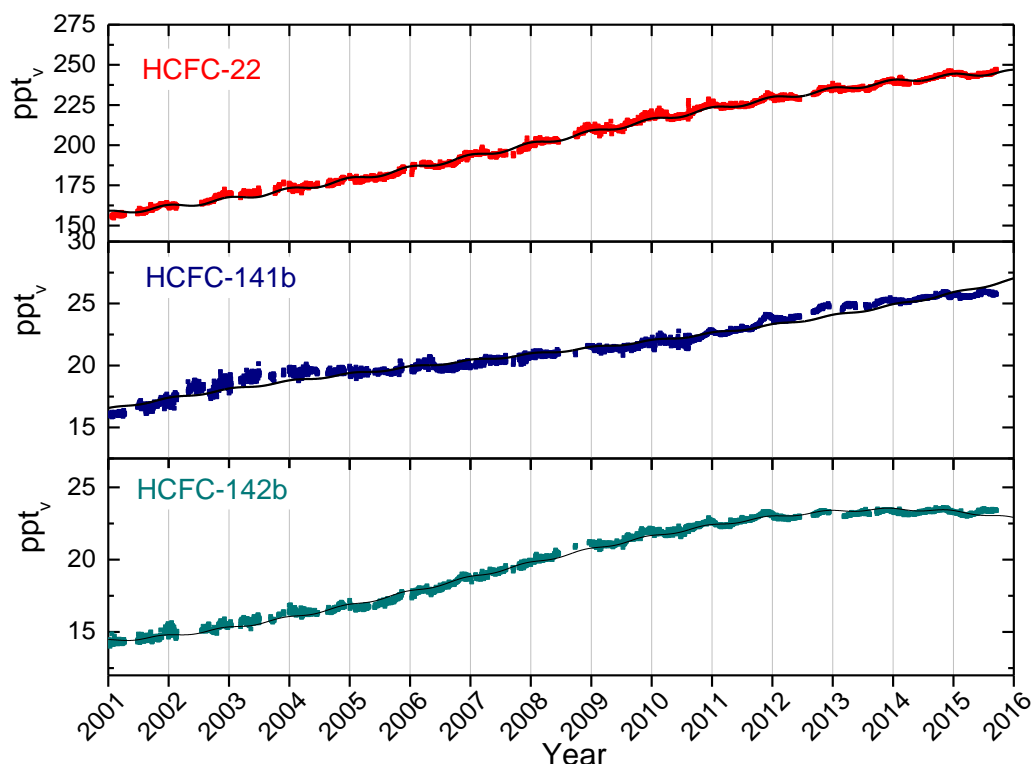


Figure 26: Daily average mixing ratios of the monitored HCFCs: HCFC-22 (red), HCFC-141b (dark blue) HCFC-142b (green) for the period 2001-2015 at the Zeppelin observatory. The solid lines are modelled background mixing ratios. All units are ppt.

The trends per year for the compounds HCFC-22, HCFC-141b and HCFC-142b are all positive over the period. HCFC-22 is the most abundant of the HCFCs and is currently increasing at a rate of 6.5 ppt/year over the period 2001-2015. The concentration of the two other HCFCs included are a factor of ten lower, and also the annual increase is about a factor ten lower; HCFC-141b and HCFC-142b have increased by 0.6 ppt/yr and 0.7 ppt/year, respectively over the same period. Last years' HCFC-142b show a very positive development, with no significant changes since 2011, and even slight decrease from 2014-2015. This is illustrated better in Figure 27, which shows the annual means for the full period for the three compounds, clearly illustrating the development; a considerable increase over the period, but for HCFC142b reveal a stabilisation over the last years. With lifetimes in the order of 10-20 years, it is central to continue monitoring the development of these compounds for many years to come as they have an influence both on the ozone layer and are strong climate gases. The global annual mean of 2011 as given in IPCC (Chapter 8, Myhre et al, 2013b) is included as black bars for comparison. As can be seen, the development and concentrations at Zeppelin are ca 2-3 ppt ahead of the global mean.

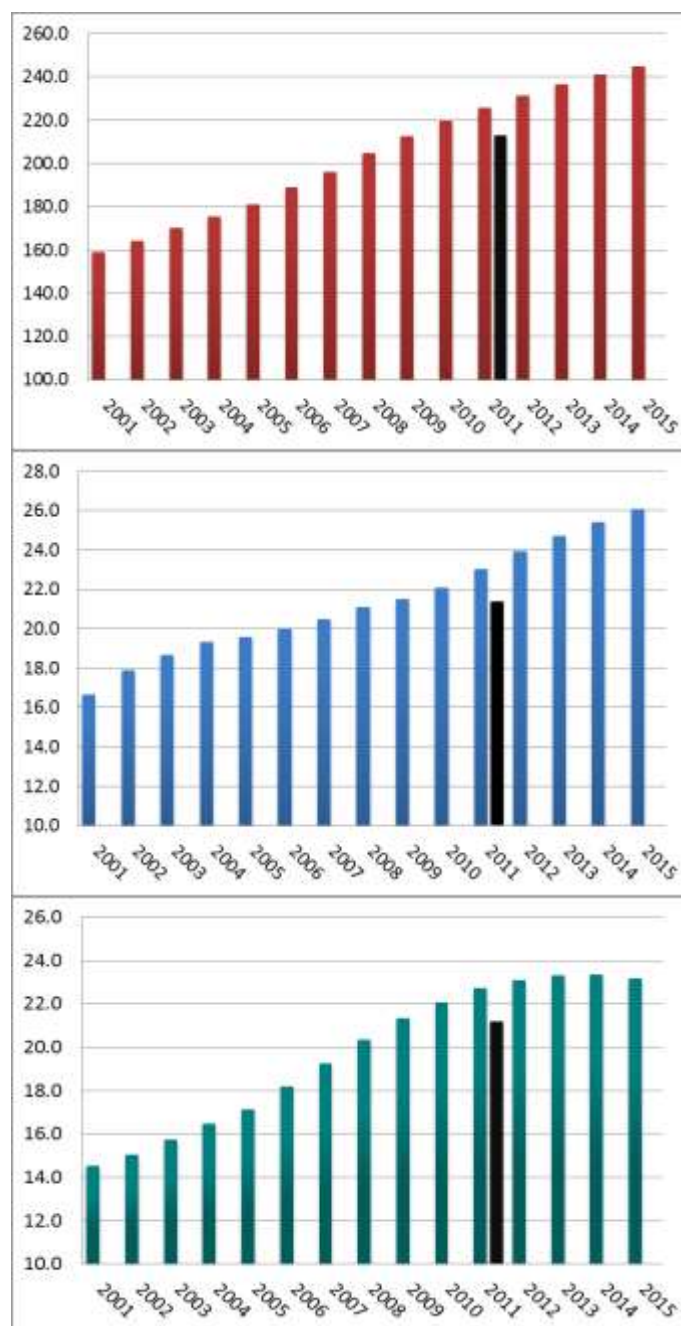


Figure 27: Development of the annual means the observed HCFCs at the Zeppelin Observatory for the period 2001-2015. Red: HCFC-22, Blue: HCFC-141b, and green: HCFC-142b. All units are ppt. The global annual mean in 2011 as given in IPCC, Chapter 8 (Myhre et al, 2013b) are included as black bars.

Key findings HCFCs: *HCFCs:* The CFC substitutes HCFC-22, HCFC-141b and HCFC-142b have a strong increase in the measured at Zeppelin from 2001-2015. HCFC-22, used for refrigeration equipment and foam blowing, had the largest growth rate. This is the most abundant of the HCFCs and its mixing ratio at Zeppelin increased by a rate of 6.5 ppt/year which is almost 4% per year, and the increase is as much as a 52% since 2001. HCFC-142b had the strongest relative increase with more than 61% since 2001, but the concentration is about a factor 10 lower than HCFC-22, and hence the climate effect is weaker as the GWP is circa the same.

2.2.3 Hydrofluorocarbons (HFCs) at Zeppelin Observatory

The substances called HFCs are the so called second generation replacements of CFCs, which means that they are considered as better alternatives to the CFCs with respect to the ozone layer than HCFCs. However, many of these are strong greenhouse gases. Even if these compounds are better alternatives for the protection of the ozone layer as they do not contain chlorine or bromine, they are still problematic as they are highly potent greenhouse gases. 1 kg of the gas HFC-125 is as much as 3170 times more powerful greenhouse gas than CO₂ (See Table 3). However, their mixing ratios are currently rather low, but the background mixing ratios are increasing rapidly, except for HFC-152a, see Figure 28. Last period there has been a great focus on these and expansion of the Montreal protocol to reduce these (see also section 1.2). This was agreed in Kigali, October 2016, and an important step to prevent further global warming. Presently, the contribution to global warming posed by these compounds are very limited. However, many of these compounds have a very strong increase, as documented in our measurements presented in this section. At the same time, the compounds are strong infrared absorbers, with high GWP (see Table 3 at page 19) hence it is crucial to reduce the use in the future, to prevent further warming by emissions of new greenhouse gases.

This sub-section includes measurements of the components: HFC-125, HFC-134a, and HFC-152a with lifetimes in the order of 1.5-29 years, over the period 2001-2015. Additionally, the program was extended with new compounds in 2015. These are HFC-23, HFC-365mfc, HFC-227ea, HFC-236fa, HFC-245fa. They have been measured at Zeppelin since 2010, but not analysed or reported to international data bases. This was included in 2015 as a part of the national program, and will be presented here.

Generally, the HFCs include substances used for refrigeration and air conditioning, foam blowing, and fire extinguishing. Both HFC-245fa and HFC-365mfc are substitutes for HCFC-141b in foam blowing applications. HFC-236fa is also a foaming agent, in addition to a fire suppression agent and a refrigerant. HFC-227ea is mainly used to suppress fire in data equipment and telecommunication facilities, and in protection of flammable liquids and gases. As an aerosol propellant, HFC-227ea is applied in pharmaceutical dose inhalers for e.g. asthma medication.

The three main HFCs are HFC-23 (part of the national monitoring program from 2010), HFC-134a and HFC-152a. HFC-134a is the most widely used refrigerant for temperature control, and also in air conditioners in cars. Since 1990, when it was almost undetectable in the atmosphere, concentrations of HFC-134a have risen massively, and it is the one with the highest concentration of these compounds.

The seasonal cycle in the observed mixing ratios of these substances is caused by the variation in the incoming solar radiation and is clearly visible in the time series shown in Figure 28 for HFC-152a. HFC-152a has the shortest lifetime and is mainly destroyed in the lowest part of the atmosphere by photolysis and reactions with OH. This is the first year we detected a reduction of the development of the concentration for one of these components. This is clearly illustrated in Figure 30 showing the development of the annual means.

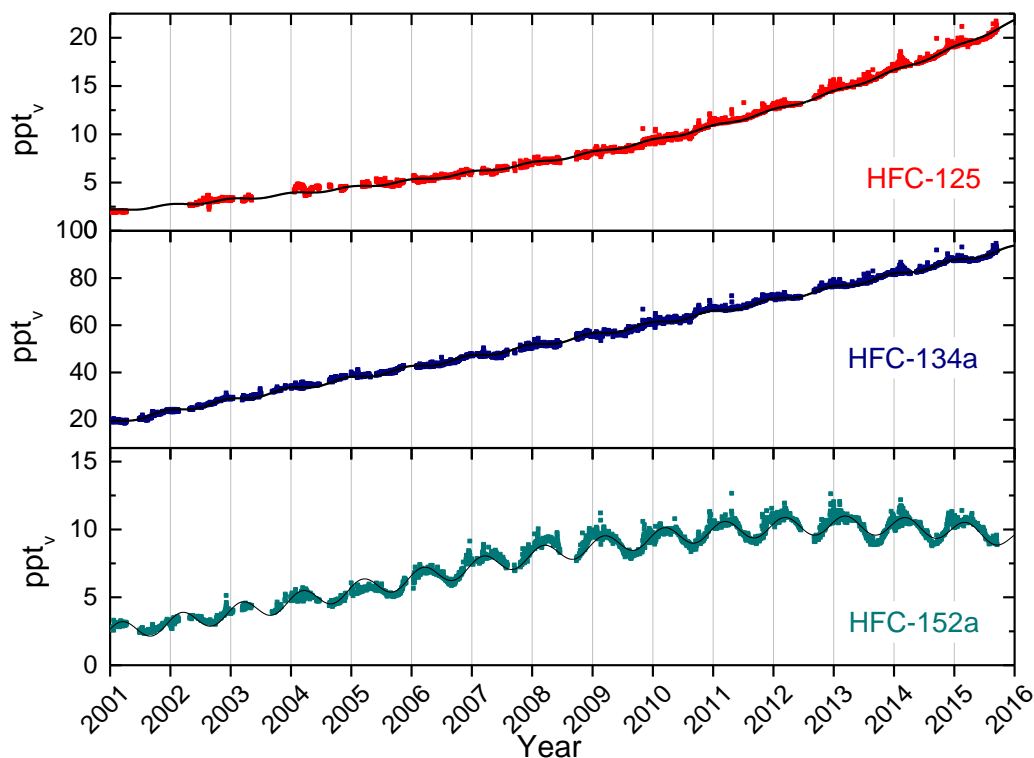


Figure 28: Daily average concentrations of the monitored HFCs: HFC-125 (red), HFC-134a (dark blue), and HFC-152a (green) for the period 2001-2015 at the Zeppelin observatory. The solid lines are empirical modelled background mixing ratio.

HFC-152a reveals a reduction since last years. For the period 2001-2015, we find an increasing trend of 4.8 ppt per year for HFC-134a which leaves this compound as the one with the second highest change per year of the all the halocarbons measured at Zeppelin, after HCFC-22. The mixing ratios of HFC-125, HFC-134a and HFC-152a have increased by as much as 670%, 305% and 265% respectively since 2001, and HFC-125 show even an acceleration on the development and trend.

The five new HFCs included in the programme in 2015 are shown in Figure 29.

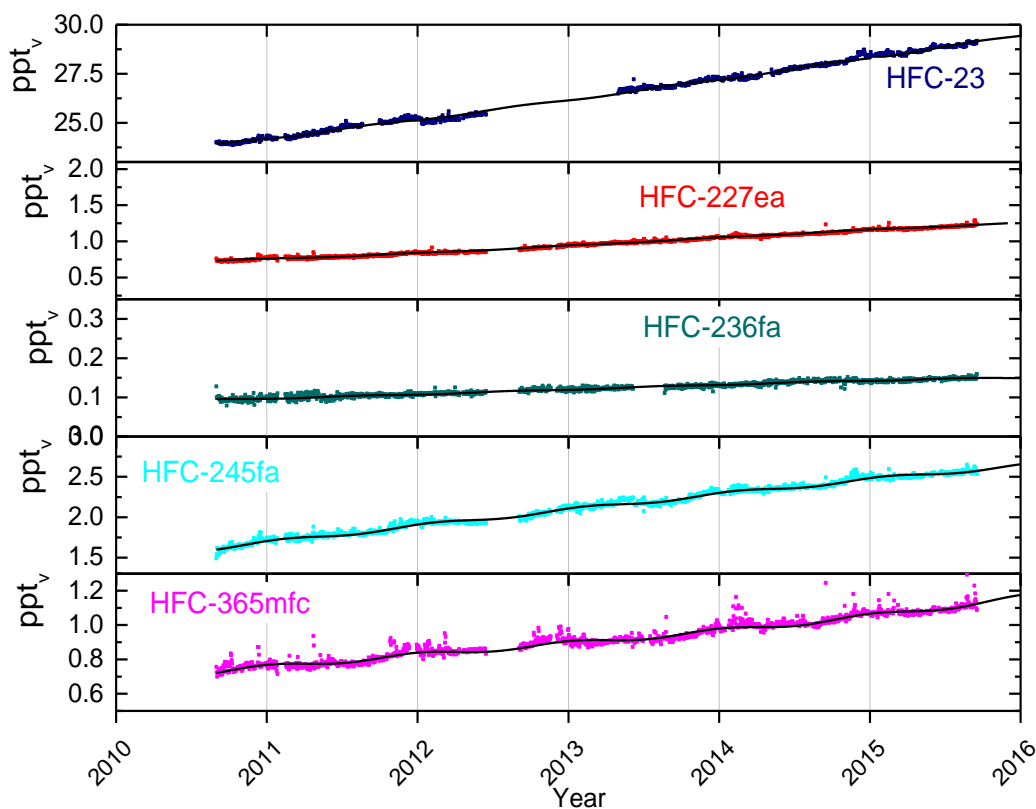


Figure 29: Daily average concentrations of the monitored HFCs: HFC-23 (blue), HFC-227ea (red), and HFC-236fa (green), HFC-245fa (light blue) and HFC-365mfc (pink) for the period 2010-2015 at the Zeppelin observatory. The solid lines are empirical modelled background mixing ratio.

The time series is too short for trend calculations, but all these compounds are showing increasing development, but relatively low concentrations except for HFC-23.

The development of the annual mean of all reported HFCs is shown in Figure 30. The global annual means of 2011 as given in IPCC (Chapter 8, Myhre et al, 2013b) are included as black bars for comparison. As for HCFCs the development and concentrations at Zeppelin is ca 2-3 years ahead of the global mean. As can be seen, the increasing tendency each year is very clear, but the concentrations are very low, particularly of the new HFC-365mfc, HFC-245fa, HFC-236fa, HFC-227ea, with 2.5 ppt as maximum for HFC-245fa.

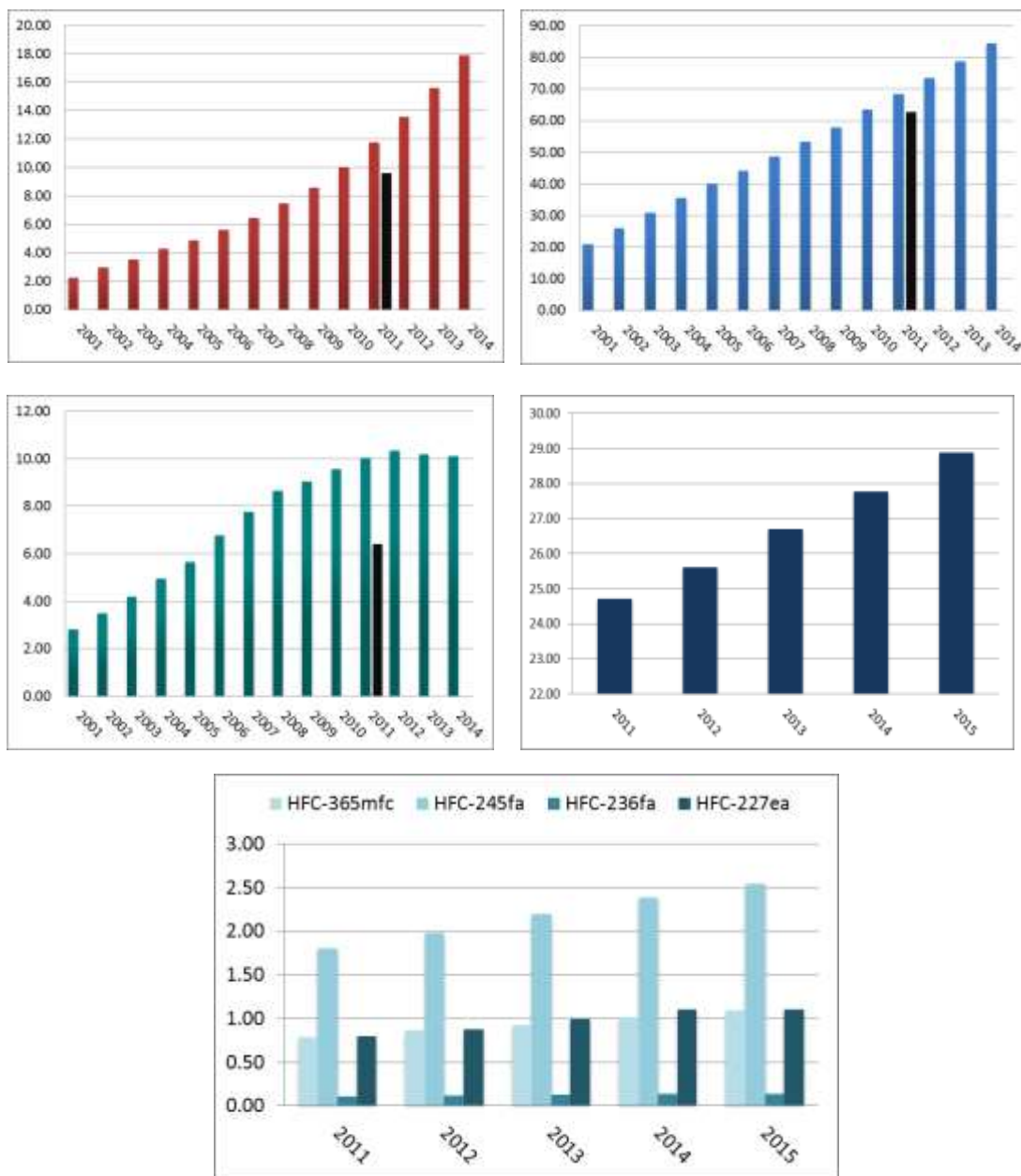


Figure 30: Development of the annual means of the observed HFCs at the Zeppelin Observatory for the period 2001-2015. Red: HFC-125, Blue: HFC-134a, and green: HFC-152a, dark blue: HFC-23, and light to dark cerise HFC-365mfc, HFC-245fa, HFC-236fa, HFC-227ea. The global annual mean in 2011 as given in IPCC, Chapter 8 (Myhre et al, 2013b) are included as black bars. All units are in ppt.

Key findings Hydrofluorocarbons - HFCs: These gases replace the strongly ozone depleting substances CFCs, and HCFCs and are relatively new gases emitted to the atmosphere. They are all of solely anthropogenic origin. The mixing ratios of HFC-125, HFC-134a, HFC-152a have increased by as much as 677%, 304% and 262% respectively since 2001 at the Zeppelin observatory. HFC-125 is increasing strongly. The compounds HFC-23, HFC-227ea, HFC-236fa, HFC-245fa, HFC-365mfc with measurements back to 2010 show a weak or no increase over this period, except for HFC-23. This is the one with highest concentration of these, and also the strongest increase last year. The concentrations of these gases are still very low, thus

the total radiative forcing of these gases since the start of their emissions around 1970 and up to 2011 is only about 0.016 W m^{-2} . For comparison: The forcing of a typical 2 ppm annual increase in CO_2 is ca. 0.03 W m^{-2} . Thus the contribution from these manmade gases to the global warming is small today, but given the observed extremely rapid increase in the use and atmospheric concentrations, it is crucial to follow the development of these gases in the future.

2.2.4 Halons measured at Zeppelin Observatory

Of the halons, H-1301 and H-1211 are measured at the Zeppelin Observatory. These greenhouse gases contain bromine, thus also contributing to the depletion of the ozone layer. Actually, bromine is even more effective in destroying ozone than chlorine. The halons are regulated through the Montreal protocol, and are now phased out. The main source of these substances were fire extinguishers. The ambient concentrations of these compounds are very low, both below 4 ppt. Figure 31 presents the daily average concentrations of the monitored halons at Zeppelin.

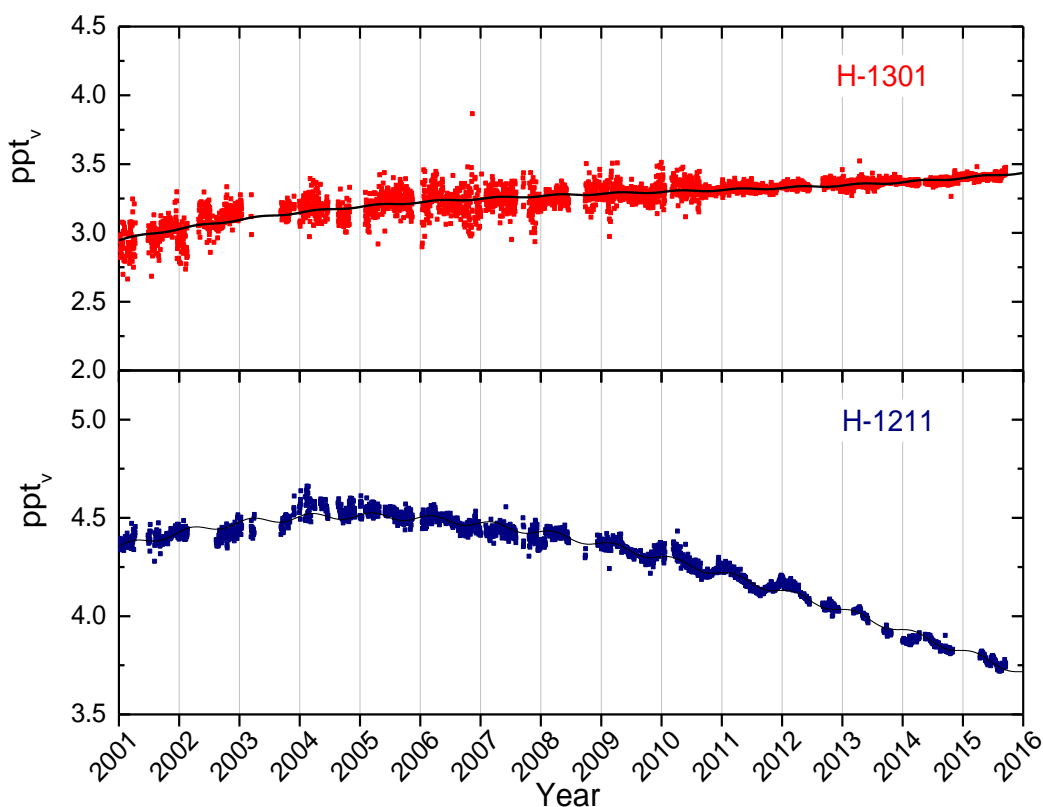


Figure 31: Daily average concentrations of the monitored halons: H-1301 (red in the upper panel) and H-1211 (blue in the lower panel) for the period 2001-2015 at the Zeppelin Observatory. The solid lines are empirical modelled background mixing ratio.

The trends of these compounds listed in Table 3 shows that for the period 2001-2015 there is an increase for H-1301, and a relaxation for H1211. The concentration of the compound H-1211 is lower now than when we started the measurements, ca 10% as also depicted in the development of the annual means in Figure 32.

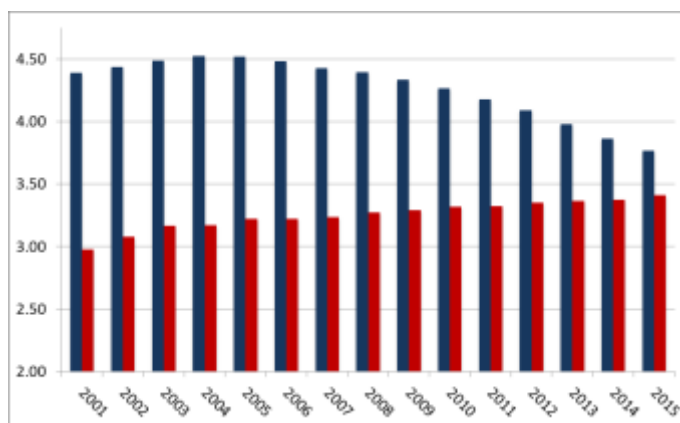


Figure 32: Development of the annual means of the observed Halons at the Zeppelin Observatory for the period 2001-2015. Red: Halon-1301, Blue: H-1211. All units are in ppt.

The development of the annual means are relatively stable over the measured period, explained by low emissions and relatively long lifetimes (11 years for H-1211 and 65 years for H-1301). However, a clear reduction is evident in Halon-1211, with the shortest lifetime. According to the last Ozone Assessment (WMO, 2011), the total stratospheric bromine concentration is no longer increasing, and bromine from halons stopped increasing during the period 2005-2008. H-1211 decreased for the first time in this period, while H-1301 continued to increase, but at a slower rate than previously.

Key findings Halons: For Halons are Bromine containing halocarbons the recent results indicate that there was a maximum in 2004 for halon-1211 at Zeppelin, and a small decline after that. Since 2001, this compound is reduced by ca. 14 %. At the same time, halon-1301 has increased since 2001 with 14.6%. According to the last Ozone Assessment (WMO, 2011) the total stratospheric Bromine concentration is no longer increasing and Bromine from halons stopped increasing during the period 2005-2008.

2.2.5 Other chlorinated hydrocarbons at Zeppelin Observatory

This section includes measurements of the components: trichloromethane (also called methyl chloroform, CH_3CCl_3), dichloromethane (CH_2Cl_2), chloroform (CHCl_3), trichloroethylen (CHClCCl_2), perchloroethylene (CCl_2CCl_2). Additionally, a new compound is added this year; CCl_4 . The main sources of all these substances are solvents. Chloroform do also has natural sources, and the largest single source being in offshore seawater. The daily averaged concentrations are shown in Figure 33.

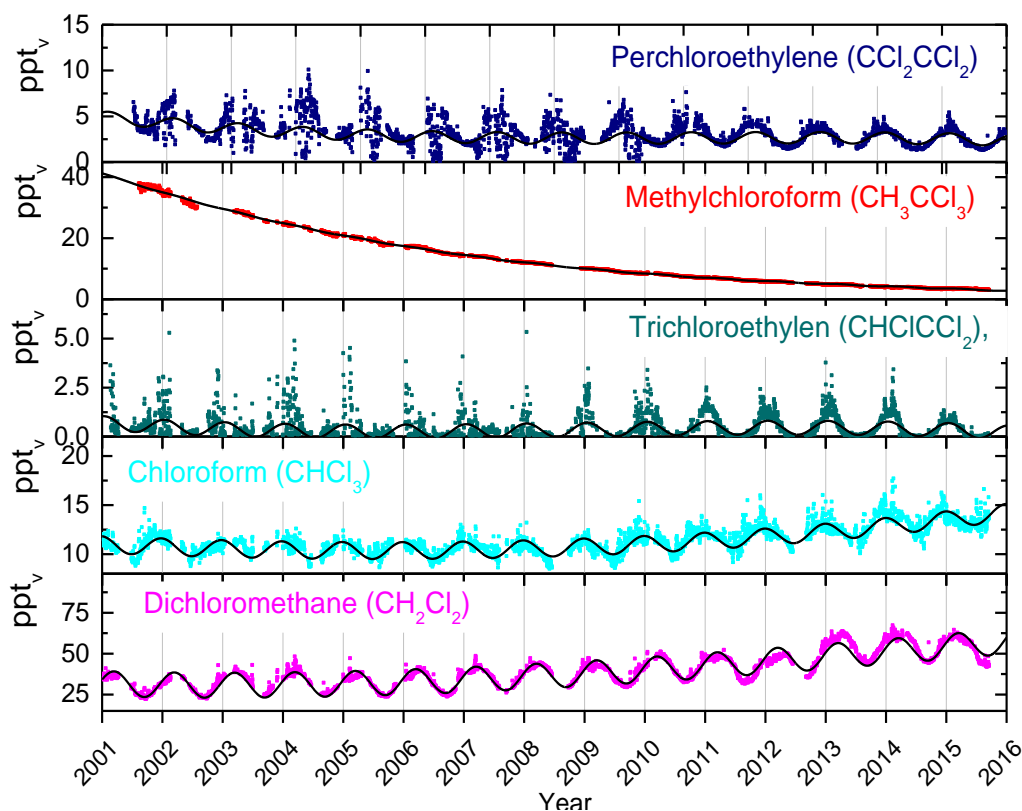


Figure 33: Daily average concentrations chlorinated hydrocarbons: From the upper panel: perchloroethylene (dark blue) methylchloroform (red), trichloroethylen (green), chloroform (light blue) and dichloromethane (pink) for the period 2001-2015 at the Zeppelin observatory. The solid lines are the empirical modelled background mixing ratio.

Methylchloroform (CH_3CCl_3) has continued to decrease, and accounted only for 1% of the total tropospheric chlorine in 2008, a reduction from a mean contribution of 10% in the 1980s (WMO, 2011). Globally averaged surface mixing ratios were around 10.5 ppt in 2008 (WMO, 2011) versus 22 ppt in 2004 (WMO, 2011). The measurements at Zeppelin show that the component has further decreased to 3.2 ppt, a reduction of more than 90% since the measurement start in 2001 and now contribute negligible to the atmospheric chlorine burden.

The measurements of methyl tetrachloride (CCl_4) is shown in Figure 34.

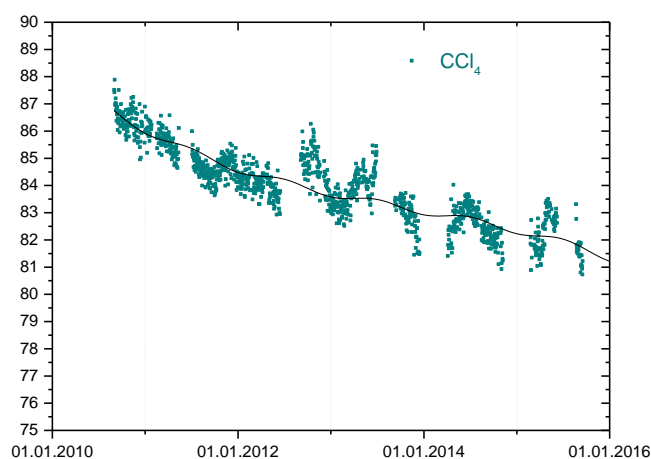


Figure 34: Daily average concentrations of carbon tetrachloride, CCl_4 , measured at Zeppelin Observatory. The solid lines are the empirical modelled background mixing ratio.

It is worth noting the strong recent increase in dichloromethane (violet), and chloroform (light blue), and the relaxation the last few years. Dichloromethane, has a lifetime of less than 6 months, and respond rapidly to emissions changes, and about 90 % has industrial origin. Its main applications include use in paint strippers, degreasers and solvents; in foam production and blowing applications; and as an agricultural fumigant (WMO et al., 2011). The most recent estimation for its natural components suggests it is comprised of a 10% combined biomass burning and marine source. At Zeppelin, the increase since 2001 is about 76%. The concentration is currently 54.1 ppt, a slight decrease since 2014. Strong seasonal variations are observed for chloroform (light blue) due to a relatively short lifetime of 1 year, thus the response to emission changes are also for this compound rapid.

The annual mean value of chloroform has increased with as much as 27% since 2005 at Zeppelin, this is also observed at other sites (e.g. Mauna Loa at Hawaii and Barrow in Alaska). From known emissions of this compound this increase is not expected, and the reason for this increase is not yet clear, it might also be related to natural sources. The concentration of trichloroethylene is very low and the annual variability is quite high, this may partly be due to uncertainty in the measurements and missing data

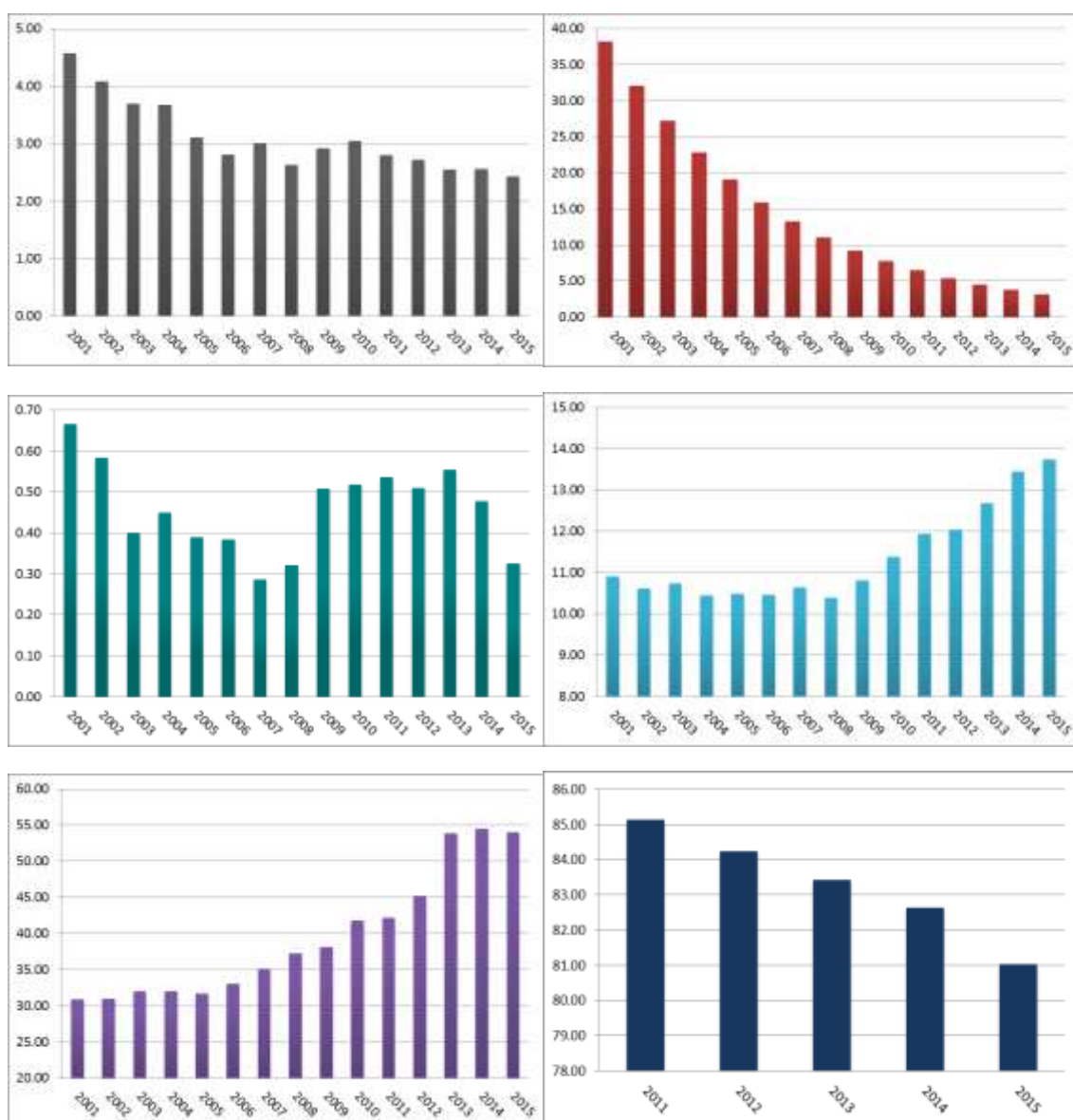


Figure 35: Annual means of the chlorinated hydrocarbons. From upper panel: perchloroethylene (grey), trichloromethane (red), mid panels; trichloroethylene (green), chloroform (light blue) and lower panel dichloromethane (violet) and carbon tetrachloride (dark blue) for the period 2001-2015. All units are ppt.

Key findings Other Chlorinated greenhouse gases, including Methylchloride and Methylbromide (section 2.1.6 and 2.1.7) : The following five chlorinated gases are measured at the Zeppelin Observatory: methylchloride (CH_3Cl), dichloromethane (CH_2Cl_2), chloroform (CHCl_3), trichloromethane (CHCl_3), methylchloroform (CH_2CCl_2), perchloroethylene (C_2Cl_4). Three of these gases have increased the last years and a considerable increase in chloroform is evident at Zeppelin of 180% compared to 2001. The reason for this is unclear. **Methylchloroform shows a decrease, and the concentrations are now very low. Methylchloride and Methylbromide at Zeppelin are also reduced as a direct result of the Montreal protocol.**

2.2.6 Perfluorinated (PFCs) compounds at Zeppelin Observatory

Perfluorinated compounds belong to a group of long-lived greenhouse gases, and their contribution to the Earth's radiative forcing has increased over the past several decades. The impact of these highly fluorinated compounds on climate change is a concern because of their exceptionally long atmospheric lifetimes, as well as their strong absorption in the infrared "window" region (Baasandorj et al, 21012).

Up to 2015, the national monitoring programme only included measurements of SF₆. However, other perfluorinated compounds are also very powerful greenhouse gases with atmospheric lifetimes as high as 50 000 years (See Table 3), and with increasing levels in the atmosphere. NILU has from 2010 extended the monitoring of perfluorinated compounds at Zeppelin as we have new and improved instrumentation. Several of these compounds are included in the national monitoring programme from 2015, with analysis back in time until September 2010. Hence, harmonised time series for the period September 2010-2015 is presented here for 4 new perfluorinated compounds.

2.2.6.1 Sulphurhexafluoride (SF₆)

Sulphurhexafluoride, SF₆, is an extremely strong greenhouse gas emitted to the atmosphere mainly from the production of magnesium and electronics industry. Measurements of this component has been a part of the programme since 2001. The atmospheric lifetime of this compound is as much as 3200 years, and the global warming potential is 23500, which means that the emission of 1 kg of this gas has a warming potential which is 23 500 times stronger than 1 kg emitted CO₂ (Myhre et al, 2013b).

The daily averaged concentration of SF₆ is presented in Figure 36.

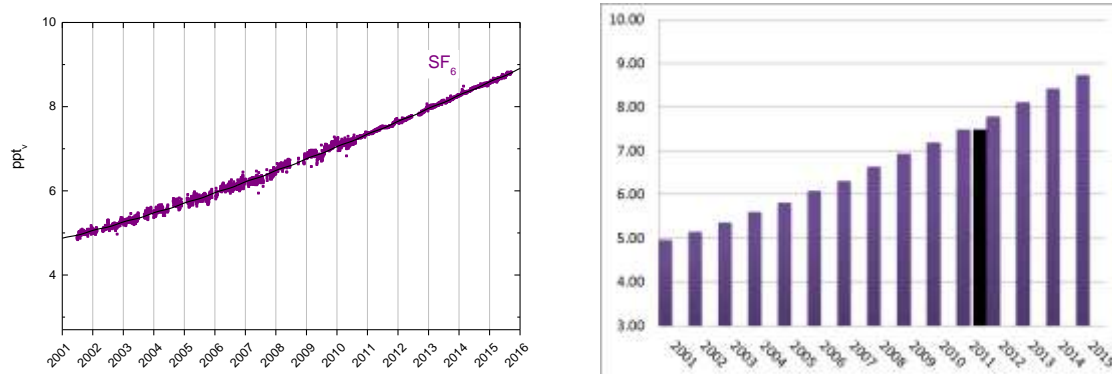


Figure 36: Daily average concentrations of SF₆ for the period 2001-2015 in the left panel, and the development of the annual mean concentrations in the right panel.

The compound is increasing with a rate of 0.27 pptv/year, and has increased as much as 70% since the start of our measurements in 2001. The instrumentation before 2010 is not the best suited for measurements of SF₆ thus there are higher uncertainties for this compound's mixing

ratios than for most of the other compounds reported in the first years (see Appendix I). The variations through the years are not due to seasonal variations, but rather to instrumental adjustments. The improvement with the new instrumentation in 2010 is very easy to see for this component, and the quality of the measurements has increased largely.

2.2.6.2 Perfluorocarbons or PFC's: PFC-14, PFC-116, PFC-218, PFC-318

Perfluorocarbons or PFCs are compounds that contain only carbon and fluorine. Four of these compounds are currently measured and reported at Zeppelin: PFC-14 (CF_4) PFC-116, PFC-218, and PFC-318. The most potent greenhouse gas is hexafluoroethane, PFC-116, which has an atmospheric lifetime of 10 000 years and a GWP of 11 100. The gas is used as an etchant in e.g. semiconductor manufacturing. The aluminium and the semiconductor manufacturing industries are the major emitters of PFC-116. Octafluoropropane, PFC-218, which has an atmospheric lifetime of 2600 years and a GWP of 8900, is also used in the electronics industry as a plasma etching material. In medicine, PFC-218 microbubbles reflect sound waves well and is used to improve the ultrasound signal backscatter. Octafluorocyclobutane, PFC-318, with a life time of 3200 years and a GWP of 9540, is the third most abundant PFC in the atmosphere (Oram et al, 2012). Although a number of potential sources of PFC-318 have been reported, including the electronics and semi-conductor industries, there remains a large discrepancy in the atmospheric budget. Tetrafluoromethane (CF_4) PFC-14, is the most persistent greenhouse gas of these compounds with an atmospheric lifetime of 50 000 years and a greenhouse warming potential of 6630. It is used as a low temperature refrigerant, in electronics microfabrication, and in neutron detectors.

The daily averaged concentrations of these compounds are shown in Figure 37.

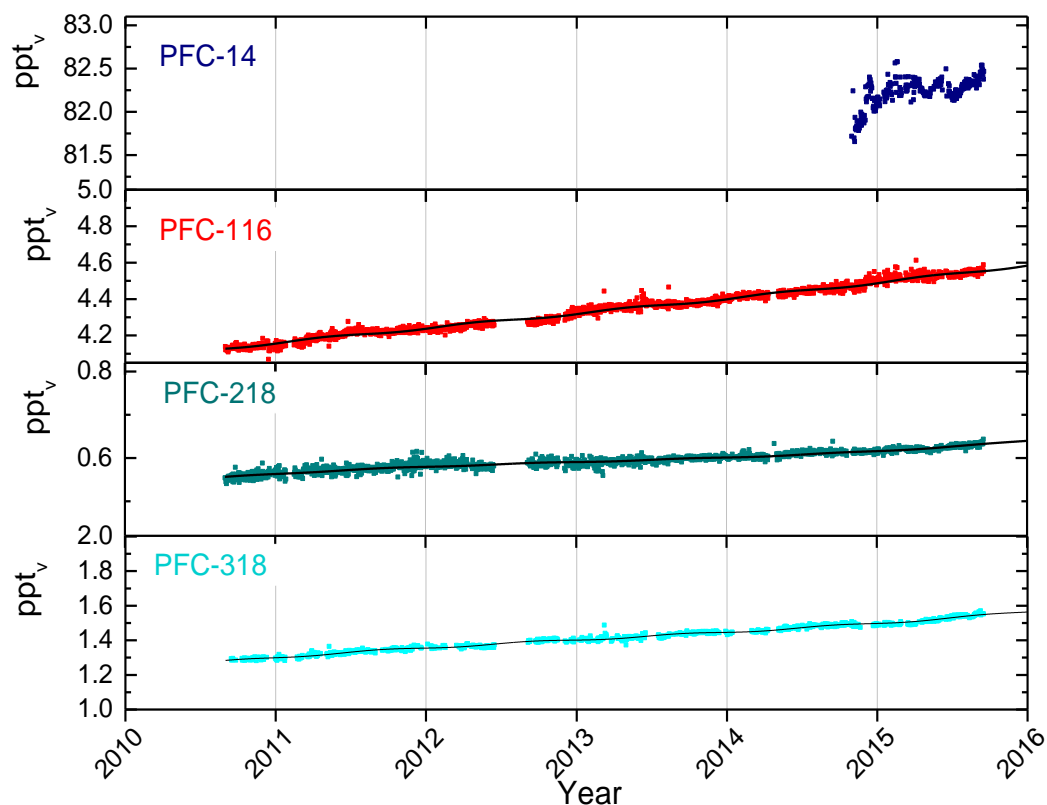


Figure 37: Daily average concentrations perfluorocarbons: From the upper panel: PFC-14 (dark blue) PFC-116 (red), PFC-218 (green), PFC-316 (light blue) for the period 2010-2015 at the Zeppelin observatory. PFC-14 is only ranging back to autumn 2014. The solid lines are the empirical modelled background mixing ratio.

The development of the annual means of these compounds are shown in Figure 38 are relatively stable over the measured period, with a slight increase. It is important to note the very low concentrations. However, PFC-14 has considerably higher concentration with an annual mean of 80.06 ppt in 2015. With a lifetime of 50 000 years, and GWP of 6630 this is a particularly important compound to follow.

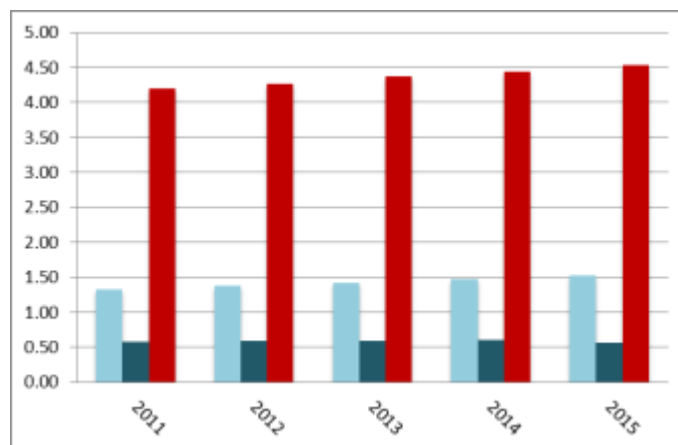


Figure 38: Annual mean concentrations perfluorocarbons hydrocarbons: PFC-116 (red), PFC-218 (green), PFC-316 (light blue) for the period 2010-2015 at the Zeppelin observatory. PFC-14 is only ranging back to autumn 2014. The solid lines are the empirical modelled background mixing ratio.

No valid annual mean are available for 2014 for this as there were only measurements the last months, the same apply to the other PFCs in 2010.

Nitrogen trifluoride, NF_3 , has a lifetime of 500 years and a GWP as high as 16100, meaning that it is an extremely strong greenhouse gas. It is e.g. used in the manufacturing of new generation solar panels, flat-screen televisions, touch-sensitive screens, and electronic processors. The use of NF_3 has widely increased in the past because of the rising demand in flat-screen televisions and microelectronics. The instrument at Zeppelin we re-build and optimized 2015 and 2016 to also provide measurements of this compounds. This will be included in the report in 2017.

Key findings SF_6 and PFC-14, PFC-116, PFC-218, PFC-318: Generally, these are extremely potent greenhouse gas, but their concentrations are still low. The measurements show that the concentration of SF_6 has increased as much as 70% since 2001. The PFCs are new and reported for first time this year, and they show a weak or no change since 2014.

3. Aerosols and climate: Observations from Zeppelin and Birkenes Observatories

Atmospheric aerosol influences climate by scattering incoming visible solar radiation back into space before it can reach the ground, be absorbed there and warm the earth surface. This so called direct aerosol climate forcing results mostly in cooling, but can be moderated if the aerosol itself absorbs solar radiation, e.g. if it consists partly of light absorbing carbon or light absorbing minerals. In this case, the aerosol warms the surrounding atmosphere, the so-called semi-direct effect. Atmospheric aerosol particles also affect the reflectivity and lifetime of clouds, which is termed the indirect aerosol climate effect. Here as well, the effect can be cooling as well as warming for climate, but in most cases, the cloud reflectivity and lifetime are increased, leading again to a cooling effect (see Figure 3). Figure 39 gives an overview of the main natural and anthropogenic sources of atmospheric aerosols.

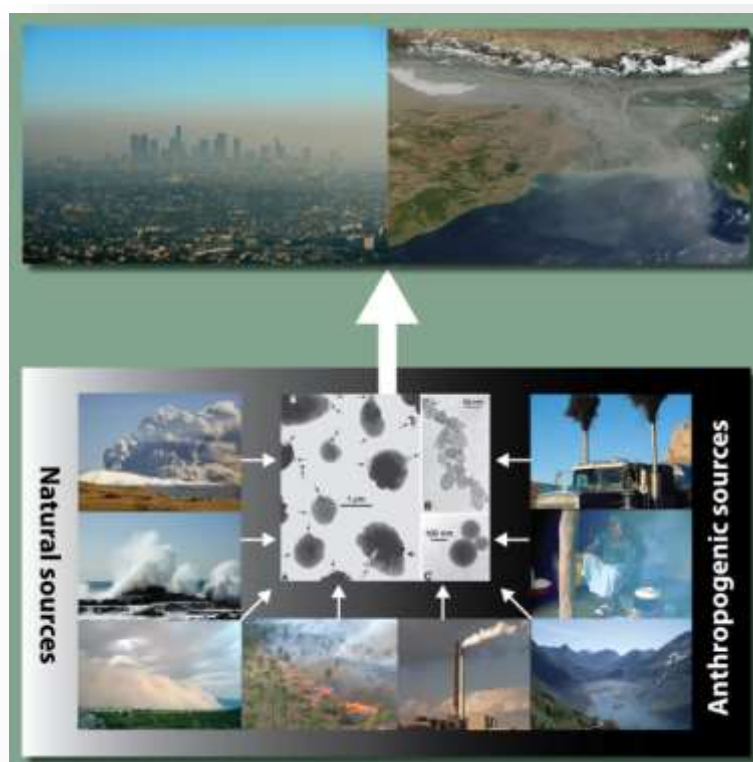


Figure 39: Illustration of the main natural and anthropogenic sources of atmospheric aerosols taken from Myhre et al (2013b). Top: local and large scale air pollution. Sources include (bottom, counter clockwise) volcanic eruptions (producing volcanic ash and sulphate), sea spray (sea salt and sulphate aerosols), desert storms (mineral dust), savannah biomass burning (BC and OC), coal power plants (fossil fuel BC and OC, sulphate, nitrate), ships (BC, OC, sulphates, nitrate), cooking* (domestic BC and OC), road transport (sulphate, BC, VOCs yielding OC). Additionally, Biogenic VOC to SOA and primary biological (e.g. pollen) from vegetation is crucial. Center: Electron microscope images of (A) sulphates, (B) soot, (C) fly ash, a product of coal combustion (Posfai et al., 1999).

Uncertainties in assessing aerosol climate forcing hamper the attribution of changes in the climate system. IPCC AR5 (IPCC, 2013) has high confidence in stating that atmospheric aerosol in the past has offset a significant fraction of greenhouse gas radiative warming, although the magnitude is connected with uncertainty. Due to the decline of aerosol concentrations as reported in Tørseth et al (2012), Collaud Coen et al., (2013), and Asmi et al., (2013), and summarized in Hartmann et al, 2013) the total anthropogenic radiative forcing will be even larger in the future.

IPCC AR5 mentions progress since AR4 concerning observations of climate relevant aerosol properties such as particle size distribution, particle hygroscopicity, chemical composition, mixing state, optical and cloud nucleation properties. This includes the parameters covered by the Norwegian climate monitoring programme, and underlines the importance of these observations. IPCC AR5 also mentions a lack of long time series on these parameters and stresses that existing time series need to be continued for maximising their informative value. This is the core of the EU project ACTRIS, now continued in ACTRIS-2, that NILU is highly involved in.

Due to hosting both, the data centre of the European Monitoring and Evaluation Programme (EMEP), ACTRIS (Aerosols, Clouds, and Trace gases Research InfraStructure Network) and the WMO Global Atmosphere Watch (GAW) World Data Centre for Aerosol (WDCA), NILU has a position connecting the community for measuring air quality and climate relevant atmospheric aerosol properties with the community using this data to constrain models for assessing and predicting the aerosol climate effects. This community is represented by the AeroCom project, an initiative for comparing these models among each other and with various data sources, which is hosted by the Norwegian Meteorological Institute. It is important to highlight and mention that NILU's work in hosting the WMO GAW World Data Centre for Aerosol, among many other synergy effects, ensures a rather efficient dissemination of the data on atmospheric aerosol properties collected within the Norwegian climate monitoring programme, and increases its visibility. In the reporting period, the AeroCom Phase III project, a collaboration between the Norwegian Meteorological Institute, NILU, and the CIENS institute CICERO, funded by the Norwegian Research Council, continued with starting designated tasks using the results of the Norwegian programme for monitoring climate relevant aerosol properties. The tasks involve confronting climate models in AeroCom with data collected at atmospheric observatories such as those operated by Norway. Compared parameters will include the aerosol particle size distribution, as well as the optical properties scattering and absorption, in order to improve the accuracy of the climate models. Further projects relevant in this context that started in the reporting period and where the Norwegian atmospheric monitoring programme is involved through NILU include the above mentioned ACTRIS-2 project, and the *Environmental Research Infrastructures Providing Shared Solutions for Science and Society* (ENVRI^{plus}) project. Among others, ACTRIS-2 will develop a primary standard for calibrating instruments measuring aerosol absorption, one of the properties of atmospheric black carbon, and develop quality standards for measuring the aerosol particle size distribution in the coarse size range ($D_p > 1 \mu\text{m}$) in order to further improve assessments of aerosol climate forcing. ENVRI^{plus} is an umbrella project for all geoscientific research infrastructures funded or supported by the EU. One of its objectives will be to put data from the atmospheric, marine, tectonic, and biosphere domains into a common context by making the data interoperable, i.e. visible in common services. The efforts started with achieving this goal first within the atmospheric domain.

NILU continues to operate 3 observatories measuring aerosol properties relevant for quantifying the direct and indirect aerosol climate effects: 1) Zeppelin Mountain / Ny Ålesund (in collaboration with the Norwegian Polar Institute and Stockholm University); 2) Birkenes Atmospheric Observatory, Aust-Agder, Southern Norway; 3) Troll Atmospheric Observatory, Antarctica (observatory operated by NILU, main station operated by Norwegian Polar Institute). The station locations represent the focal areas of the polar regions, which are more vulnerable to climate change, as well as the regions where the largest fraction of the Norwegian population lives. Recent developments at these stations include:

1. **Zeppelin Mountain:** Within the Swedish - Norwegian co-operation operating the atmospheric observatory on Zeppelin mountain, Stockholm University maintains a set of instruments measuring the fine-range ($D_p < 1 \mu\text{m}$) particle number size distribution, as well as the aerosol particle scattering and absorption coefficients. Stockholm University has had problems with timely delivery of data due to funding limitations on the Swedish side. Beginning in 2015, these issues should have been resolved due to additional funding from the Norwegian side covering the Swedish rental of the lab facilities at the station. Unfortunately, data delivery by Stockholm University is still delayed. The last data reported for the Swedish instruments at Zeppelin are for the year 2014, and the data delivery was incomplete, i.e. didn't cover all instruments. Through the additional Norwegian funding for Zeppelin observatory, a number of additional measurements have been or are planned to be installed. Due to this funding, NILU is now operating a latest generation aethalometer at Zeppelin since June 2015. The Magee AE33 instrument is a filter absorption photometer providing the spectral aerosol particle absorption coefficient at 7 wavelengths from the UV to the infra-red. The instrument is designed to be less prone to systematic uncertainties than the previous instrument generation, and complements existing observations of that type at Zeppelin. The new instrument is due to replace a previous generation instrument operated at Zeppelin by the Greek Demokritos Research Institute (Athens). Both instruments are operated in collaboration between Greece and Norway. Another instrument now operated by NILU at Zeppelin is a time-of-flight Aerosol Chemical Speciation Monitor (ACSM-ToF) that will yield the particle chemical speciation with high (~hourly) time resolution. Moreover, NILU installed a Mobility Particle Size Spectrometer (MPSS) at Zeppelin that now measures the fine-range particle number size distribution in near-real-time, with data publicly available in NILU's EBAS database within 1 hour of measurement. During autumn 2016, this MPSS will be extended to also measure the particle size distribution of the fine-range non-volatile aerosol as a proxy of the absorbing aerosol fraction.
2. **Birkenes Atmospheric Observatory:** In 2015, operation of the extended aerosol instrument set at Birkenes resumed according to the quality standards of WMO GAW and the European infrastructure project ACTRIS. These quality standards require networked instruments to participate in inter-comparisons at the joint GAW and ACTRIS aerosol calibration centre in Leipzig, Germany, in regular intervals. This measure has proven to be necessary in order to ensure comparability of observations within the network. The frequency of these inter-comparisons, once every 2-3 years, is balanced with minimising the downtime associated with these quality assurance measures. In 2015, instruments targeting the direct aerosol climate effect were in the focus of inter-comparisons. Both the integrating nephelometer and the newer filter absorption photometer, measuring the spectral aerosol particle scattering and

absorption coefficients respectively, were scheduled for being inter-compared, with satisfactory outcome in both cases. A further improvement of the Birkenes aerosol observation programme is scheduled for late 2016 / early 2017. The station will be equipped with a new generation filter absorption photometer measuring the particle absorption coefficient with an extended spectral range (from ultraviolet to infrared) as compared to before (from blue to red). The intention behind this upgrade is to better distinguish sources of absorbing aerosol between fossil and biomass combustion, which are supposed to have different spectral absorption signatures in the extended wavelength range.

- 3. Troll Atmospheric Observatory:** Work around Troll Atmospheric Observatory continued to follow up on a 2014 publication (Fiebig et al., 2014) funded by a base funding project controlled by the Norwegian Research Council (Strategisk Instituttssatsing, SIS). The article investigates the annual cycle of the baseline aerosol at Troll as observed in the particle number size distribution and aerosol scattering coefficient data collected at Troll. It is shown that the baseline aerosol annual cycles in both parameters have the same physical origin. A comparison with data collected at the Antarctic stations South pole and Dome C, yields that the baseline air annual cycle observed at Troll is common to the whole Central Antarctic plateau. Following the Troll baseline air masses backwards with the Lagrangian transport model FLEXPART, the article demonstrates that these air masses descend over Antarctica after being transported in the free troposphere and lower stratosphere from mid-latitudes (there uplifted in fronts) or from the inter tropical convergence zone (uplifted by convection). The article shows further that the aerosol particles contained in Antarctic baseline air are formed in situ by photochemical oxidation of precursor substances. A project following up on the discussed previous findings was applied for and approved by the NFR Norwegian Antarctic Research Expeditions (NARE) programme. Among others, the project investigates the Antarctic background aerosol further by collecting an ultra-long exposure filter sample for chemical analysis despite the low concentrations, and use the cluster analysis method developed with Birkenes to identify the source regions and aerosol types found at Troll. This work is intended to further improve our knowledge about the aerosol and aerosol processes in pristine regions of the globe, which are often used as proxy for pre-industrial aerosol. Uncertainty about the climate effect of pre-industrial aerosol is still one of the main sources of uncertainty in climate predictions (Carslaw et al., 2013).

Table 4: Aerosol observations at Zeppelin, Birkenes and Troll Observatory following the GAW recommendations. Parameters in green are funded by the Norwegian Environment Agency and included in this report.

	Zeppelin/Ny-Ålesund	Birkenes	Troll
Particle Number Size Distribution (fundamental to all aerosol processes)	fine mode ($0.01 \mu\text{m} < D_p < 0.8 \mu\text{m}$), NILU and in collaboration with Stockholm University	fine and coarse mode ($0.01 \mu\text{m} < D_p < 10 \mu\text{m}$)	fine mode ($0.03 \mu\text{m} < D_p < 0.8 \mu\text{m}$)
Aerosol Scattering Coefficient (addressing direct climate effect)	spectral at 450, 550, 700 nm, in collaboration with Stockholm University	spectral at 450, 550, 700 nm	spectral at 450, 550, 700 nm
Aerosol Absorption Coefficient (addressing direct climate effect)	single wavelength at 525 nm, (Stockholm University); single wavelength at 670 nm (Stockholm University); 7-wavelength (Demokritos Athens); 7-wavelength (NILU)	single wavelength (525 nm) and spectral at 3 wavelengths	single wavelength at 525 nm and spectral at 3 wavelengths.
Aerosol Optical Depth (addressing direct climate effect)	spectral at 368, 412, 500, 862 nm in collaboration with WORCC	spectral at 340, 380, 440, 500, 675, 870, 1020, 1640 nm, in collaboration with Univ. Valladolid	spectral at 368, 412, 500, 862 nm
Aerosol Chemical Composition (addressing direct + indirect climate effect)	main components (ion chromatography), heavy metals (inductively-coupled-plasma mass-spectrometry)	main components (daily resolution, offline filter-based, ion chromatography), heavy metals (inductively-coupled-plasma mass-spectrometry)	main components (ion chromatography), discontinued from 2011 due to local contamination.
Aerosol Chemical Speciation (direct + indirect climate effect, source attribution, transport)	Particle main chemical species (hourly resolution, online mass spectrometry)	Particle main chemical species (hourly resolution, online mass spectrometry)	---
Particle Mass Concentration	---	$PM_{2.5}$, PM_{10}	PM_{10} , discontinued from 2011 due to local contamination
Cloud Condensation Nuclei (addressing indirect climate effect)	size integrated number concentration at variable supersaturation in collaboration with Korean Polar Research Institute	Size integrated number concentration at variable supersaturation	---

An overview of all aerosol parameters currently measured at the 3 observatories can be found in Table 4. Parameters where observations are funded by Miljødirektoratet (and which are covered in this report) are written in green type.

3.1 Physical and optical aerosol properties at Birkenes Observatory

3.1.1 Optical Aerosol Properties Measured In Situ at the Surface

The comprehensive set of instruments observing optical aerosol properties, i.e. those describing the direct effect of aerosol on climate, in situ and close to the surface at Birkenes has now been in operation for over 6 years. Figure 40 summarises the essence of these observations for the years 2010 - 2015 in time series of the observations themselves and relevant directly derived parameters. All properties are measured for particles with aerodynamic diameter $D_{p,aero} < 10 \mu\text{m}$ and at relative humidity below 40%, thus avoiding water uptake by the aerosol particles, for best comparability between stations in the network. This protocol follows the recommendations of the WMO GAW aerosol network, and is identical with the recommendations of the relevant European networks (EUSAAR, ACTRIS).

Panel a) of Figure 40 displays the time series of the spectral scattering coefficient σ_{sp} at 450, 550, and 700 nm wavelength, covering the visible spectral range. Thin lines represent daily average values for the respective wavelength, whereas the heavy green line represents the running 8-week median for easier visibility of seasonal averages (green wavelength at 550 nm only for clarity). The σ_{sp} time series exhibits significant variability on the time scale of days, illustrating that particle load in an air mass varies significantly with air mass type and thus air mass origin, i.e. with the synoptic weather situation on a time scale of 1 - 3 days. When focussing on the graph of the running median, a slight seasonal variation can be detected, with values higher in summer than winter.

For spectral optical aerosol properties, information is contained not only in the absolute level of values, but also in the values at different wavelengths relative to each other. This information is often hidden in graphs due to rapid variations of the absolute values. In order to make this spectral information more readily accessible, the Ångström coefficient has been defined, that can be calculated for all optical aerosol properties. Higher values of \hat{a}_{sp} correlate with higher concentration ratios of particle surface in the fine size range ($D_p < 1 \mu\text{m}$) as compared to the coarse size range ($D_p > 1 \mu\text{m}$). Moreover, the relative size of particles determining an optical aerosol property decreases with wavelength, i.e. smaller wavelengths “look at” smaller particles in relative terms, larger wavelengths “look at” larger particles. Already with these simple qualitative rules, many features exhibited by spectral aerosol optical property data in general and Ångström coefficient data in particular can be interpreted meaningfully.

Panel b) of Figure 40 shows the time series of the scattering Ångström coefficient \hat{a}_{sp} , calculated from $\sigma_{sp}(\lambda)$, again as daily averages (thin line) and running 8-week median (heavy line). As with σ_{sp} , the strongest variability is associated to a time scale of 1-3 days, indicative of changes associated with air mass type, origin, and synoptic weather situation. Looking at the running median however, the seasonal cycle is more pronounced for \hat{a}_{sp} as for σ_{sp} , with \hat{a}_{sp} values around 1.1 in winter and 1.8 in summer. As explained above, this indicates a stronger contribution of smaller particles, i.e. particles with D_p smaller than about 120 nm, to σ_{sp} in summer than in winter. This is consistent with number concentrations of particles in this size range exhibiting a similar seasonal cycle, as will be discussed below. The time series of σ_{sp} and \hat{a}_{sp} don't show any visible underlying trend, which is consistent with the findings for other

European continental background stations at Jungfraujoch (Switzerland, mountain top), Hohenpeissenberg (Southern Germany, elevated boundary layer), and Pallas (Northern Finland, boreal background) (Collaud Coen et al., 2013). Also the range of σ_{sp} values encountered, 3 - 50 Mm^{-1} with an annual average of about 12.5 Mm^{-1} , is consistent with findings at comparable stations (Delene & Ogren, 2002).

The observations of the particle absorption coefficient σ_{ap} at Birkenes were upgraded in 2012. In addition to the filter absorption photometer custom-built by Stockholm University, measuring at only one wavelength (525 nm) since late 2009, a second instrument has been installed. The new instrument uses the same physical principle, but measures σ_{ap} at 3 wavelengths (470, 522, 660 nm) with considerable less electronic noise and significantly better long-term stability. Panel c) of Figure 40 displays the σ_{ap} time series of the older, one wavelength filter absorption photometer, with its wavelength recalculated to the same green

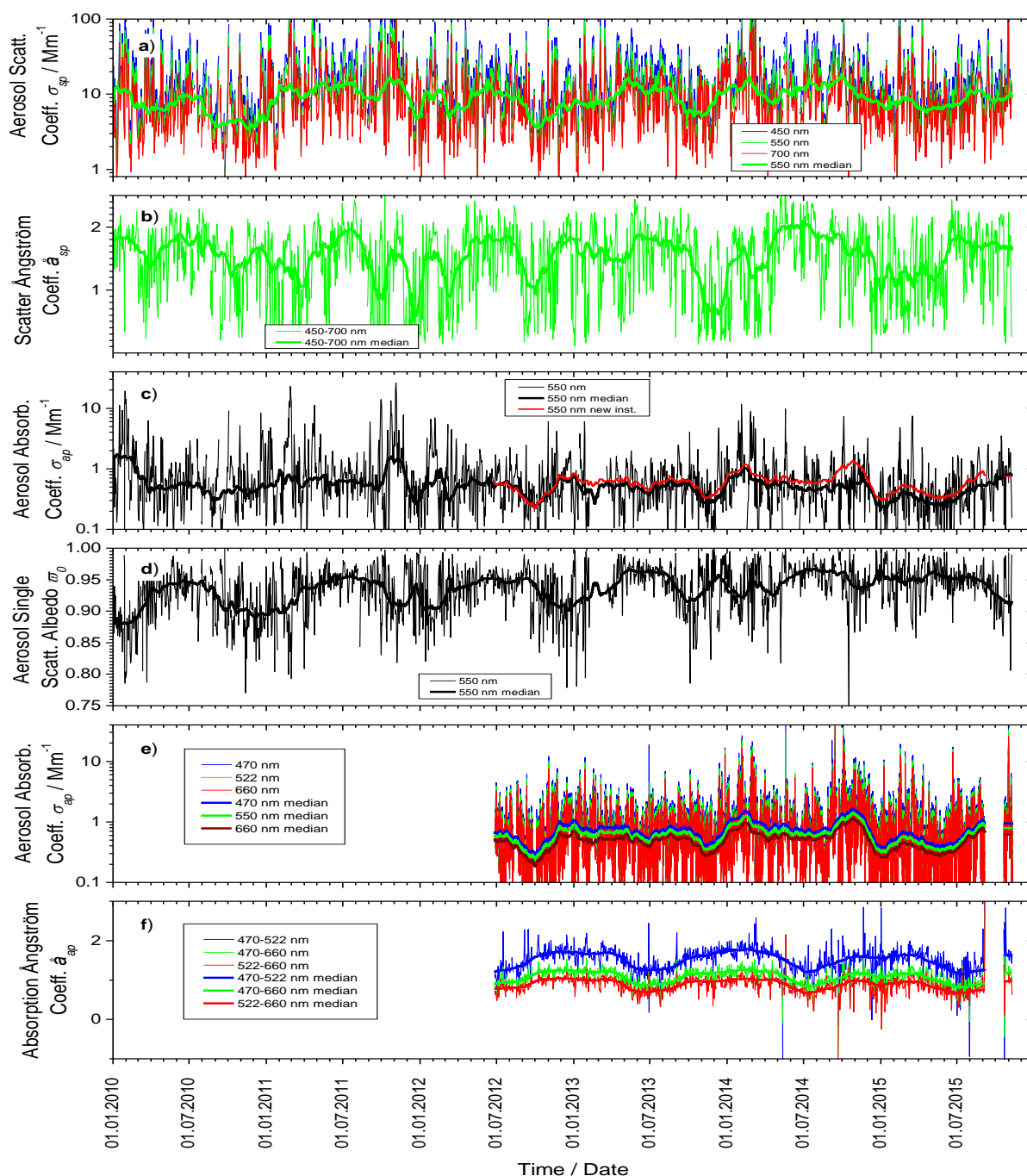


Figure 40: Time series of aerosol particle optical property daily means measured for 2010 - 2015 at Birkenes. Panel a) shows the aerosol scattering coefficient σ_{sp} at 450, 550, and 700 nm wavelength measured by integrating nephelometer. Panel c) depicts the aerosol absorption coefficient σ_{ap} at 550 nm wavelength measured by filter absorption photometer, shifted from the instrument wavelength at 525 nm to 550 nm for consistent comparison assuming an absorption Ångström coefficient of -1. Panels b) and d) show the scattering Ångström coefficient \hat{a}_{sp} and the single scattering albedo τ_0 as derived properties, respectively. Panels e) and f) display the data of the more recently installed multi-wavelength absorption photometer, absorption coefficient σ_{ap} in panel e) and absorption Ångström coefficient \hat{a}_{ap} in panel f). All plots also depict the running 8-week medians of the respective properties as heavy lines to visualize seasonal variations.

wavelength as observed by the nephelometer (550 nm), thin line daily averages, heavy line running 8-week median. The plot also displays the σ_{ap} running median time series observed by

the new filter absorption photometer (also recalculated to 550 nm wavelength) as an indicator for the goodness of overlap between the 2 instruments measuring the same property. Apart from the variation with synoptic transport and air mass origin, σ_{ap} does not seem to exhibit significant seasonal variation. The values of σ_{ap} fall in the range of 0.3 - 4 Mm^{-1} with annual means around 1 Mm^{-1} , whereas ϖ_0 varies between 0.86 - 0.96. When comparing the median time series of old (panel c) heavy black line) and new filter absorption photometer (panel c) red line), the very good co-variation of the two instruments measuring the same property is rather re-confirming, especially in the begin of the comparison period. Towards the end of the comparison period so far available, the systematic deviation of both instruments in absolute terms is increasing. Both instruments have participated in inter-comparison workshops at the joint calibration centre for aerosol physics for WMO GAW and the European ACTRIS Research Infrastructure at the Institute for Tropospheric Research, Leipzig, Germany. The older instrument's inter-comparison dates back to 2013, the new instrument participated in 2015. Due to late arrival of the results for the new instrument close to the deadline for this report, it wasn't possible yet to join the data of both instruments into one common σ_{ap} time series for Birkenes. However, judging from the known stability properties of both instruments, experiences of other stations in the WMO GAW network, and the increasing age of the older instrument, which was first deployed in 2006 at the old Birkenes station, it appears likely that the observations of σ_{ap} at Birkenes were upgraded just in time.

In order to cover the largest possible time period, panel d) of Figure 40 shows the time series of the aerosol particle single scattering albedo ϖ_0 based on the time series of the older filter absorption photometer, again daily averages (thin line) and 8-week running median (heavy line). When looking at the fraction of incident light interacting with the particle phase of an aerosol, the single scattering albedo ϖ_0 quantifies the fraction of light scattered by the particles rather than absorbed. It thus quantifies how absorbing the average aerosol particle is and does not scale with the absolute amount of particles, with ϖ_0 values decreasing with increasing absorption of the average particle. For a purely scattering aerosol, ϖ_0 is 1, and decreases with increasing fraction of light absorbing components in the aerosol particle phase. The most prominent features in the ϖ_0 time series are the pronounced annual cycle, with lower ϖ_0 values and higher particle absorption in winter, and the underlying increasing tendency in ϖ_0 , i.e. decreasing tendency in absorption of the average particle, until 2014, which seems to level out thereafter. The annual cycle in ϖ_0 has been discussed in previous reports of the Birkenes aerosol dataset, and has been connected to the combustion of biomass in wood stoves for domestic heating in the winter season. Bearing in mind the uncertainty of a trend based on a 6-year time series, ϖ_0 has increased at Birkenes by 4.2% over the years 2010 - 2014 disregarding the annual cycle. A tendency towards less aerosol absorption has also been observed for stations in the continental U.S. and Alaska (Barrow), but only few stations in continental Europe (Hohenpeissenberg, Germany) (Collaud Coen et al., 2013). The underlying increasing tendency in ϖ_0 is likely connected to policy measures oriented towards improving air quality. Over the past decades, regulations limiting the particle emissions of motorised vehicles came into effect, and old wood stoves have been replaced with newer ones that use secondary combustion technology to reduce emissions. Motorised transport as well as domestic heating involve combustion processes, which are also source of absorbing aerosol particles due to unavoidably incomplete combustion. Reduction of these emissions has likely co-reduced emissions of absorbing particles, leading to the observed increasing tendency in ϖ_0 . As of 2014, the increasing tendency of ϖ_0 seems to level out, but more data is needed for a conclusion on this. It is likely that the tendency towards

less absorbing aerosol observed in Birkenes will decrease in the years to come, simply because further reductions will be harder to achieve. It needs to be pointed out that firm attributions of the reasons for both, annual cycle and tendency in ϖ_0 , cannot be established in the scope of this report. For this, advanced statistical methods such as cluster analysis and positive matrix factorisation need to be used in connection with modelling the transport of air masses observed at Birkenes back to their sources regions.

Panels e) and f) of Figure 40 are based on data of the new filter absorption photometer, measuring σ_{ap} spectrally at 3 wavelengths, as opposed to 1 wavelength with the older instrument. Panel e) shows the time series of σ_{ap} for all 3 wavelengths in the same way as before (thin line daily means, heavy line running 8-week median). In the same way, panel f) depicts the time series of the absorption Ångström coefficient \hat{a}_{ap} for all 3 wavelength pairs provided by the new instrument. Not surprisingly, the σ_{ap} time series for the new filter absorption photometer exhibits the same general features as for the old one, with the graphs for all 3 wavelengths following each other. Changes in the relative differences between σ_{ap} values at different wavelengths are visible, but difficult to quantify in this plot. This is facilitated by the absorption Ångström coefficient \hat{a}_{ap} data displayed in panel f). For \hat{a}_{ap} , the information on relative particle size concerns not the overall aerosol particle phase, but the fraction of absorbing particles. Thus, considering \hat{a}_{ap} data allows to investigate changes in source and transport of the absorbing particle fraction in the aerosol. When looking at the \hat{a}_{ap} data in panel f) of Figure 40, an annual cycle is apparent that is opposite of the annual cycles seen in scattering Ångström coefficient \hat{a}_{sp} and single scattering albedo ϖ_0 . Both \hat{a}_{sp} and ϖ_0 increase in summer as compared to winter, \hat{a}_{sp} because of a summer increase in small particles due to particle formation from biogenic precursors, ϖ_0 because of fewer combustion emissions in summer than in winter. For \hat{a}_{ap} , values increase in winter as compared to summer, indicating, in relative terms, higher abundance of smaller absorbing particles in winter than in summer. This observation is consistent with assuming emissions from domestic heating by wood stoves to contribute to the Birkenes winter aerosol, which is the explanation for the decreased winter values of ϖ_0 . The size of the absorbing aerosol particles increases with aerosol age. Consequently, a smaller size of the absorbing particles indicates a younger combustion aerosol and a closer combustion source, which is consistent with a scattered distribution of houses using wood stoves for heating, i.e. typical for Southern Norway. The previous instrument upgrade of aerosol absorption measurements in Birkenes has thus provided another indication for the contribution of wood stove emissions to the Birkenes winter aerosol. Further information can be expected from the additional upgrade extending the spectral range of particle absorption observations scheduled for late 2016 / early 2017. Another important puzzle piece in distinguishing sources of absorbing aerosol particles would be the size distribution of the non-volatile particle fraction as a proxy of the size distribution of absorbing particles. This property could be measured with a relatively simple addition to the existing instruments at Birkenes, similar to the new instrument to be deployed by NILU at Zeppelin.

3.1.2 Physical Aerosol Properties Measured In Situ at the Surface

Figure 41 shows the time series of the particle number size distribution (PNSD) measured at Birkenes in 2015, separated into 4 different panels by season. In this plot type, the x-axis holds the time of the observation, whereas the y-axis holds the particle diameter D_p on a logarithmic scale. The logarithmic colour scale holds the particle concentration, normalised

to the logarithmic size interval, $dN / d \log D_p$. The use of logarithmic axis is common when displaying PNSD information since both, particle diameter and particle concentration, tend to span several orders of magnitude while containing relevant information over the whole scale. In this report, the PNSD reported for Birkenes covers for the first time the whole size range between 0.01 - 10 μm by combining the information of 2 instruments, one each focussing on the fine and coarse size ranges, into a common PNSD product (see appendix for details). Where existing, operating procedures and quality standards defined by the WMO Global Atmosphere Watch Programme and the European research infrastructure ACTRIS have been used (Wiedensohler et al., 2012).

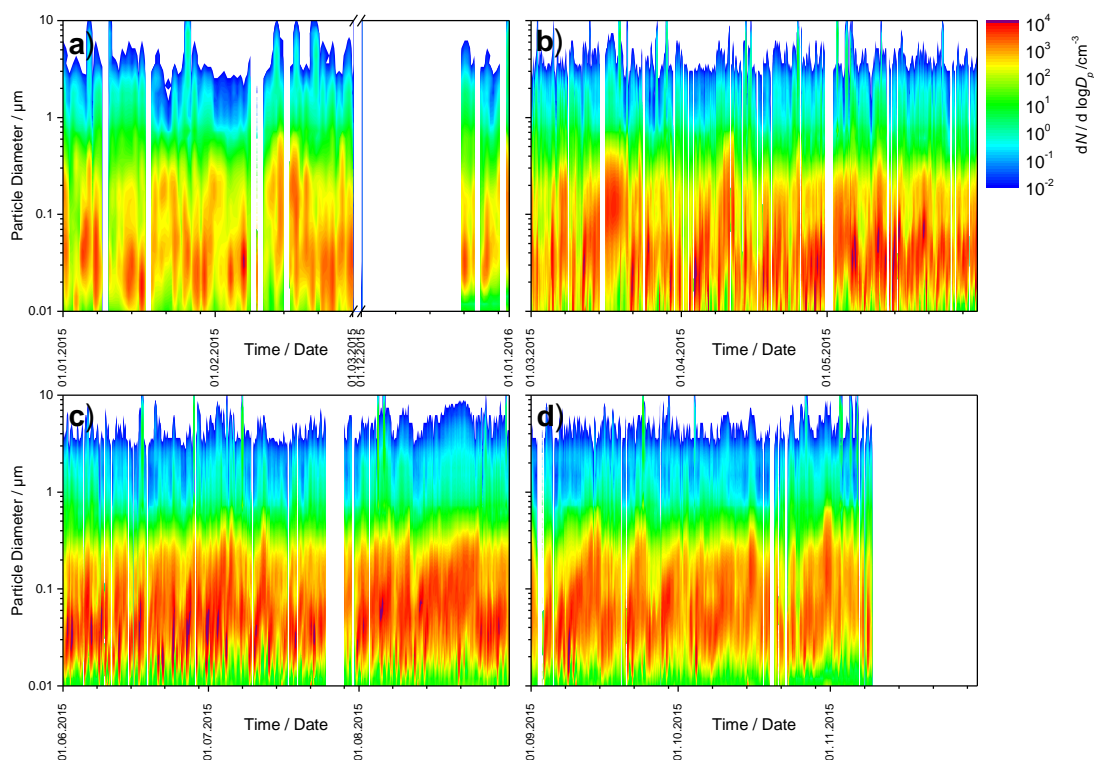


Figure 41: 2015 time series of particle number size distribution at Birkenes, panel a) winter, panel b) spring, panel c) summer, panel d) autumn.

There doesn't exist any unique connection between the PNSD and air mass type, but the PNSD still is normally fairly characteristic for the air mass, and can serve, together with the single scattering albedo ω_0 , and the scattering Ångström coefficient \hat{a}_{sp} , as valuable indication of air mass origin, which at Birkenes shifts with the synoptic weather situation. Consequently, the information content of a PNSD time series plot is too high to be discussed in detail in this overview-type annual report. The PNSD and ω_0 observations reconfirm previous findings on the dominant air mass types at Birkenes, which consist of: 1) clean Arctic background aerosol; 2) Central and Eastern European aerosol; 3) Arctic haze; 4) biogenic aerosol, i.e. vegetation emitted precursor gases condensing to the particle phase by photooxidation; 5) wood combustion aerosol from domestic heating.

In order to condense the information in the PNSD time series, Figure 42 shows the time series of selected PNSD integrals, i.e. the concentration of particles falling into selected size intervals. The size intervals are chosen to represent characteristic processes governing the

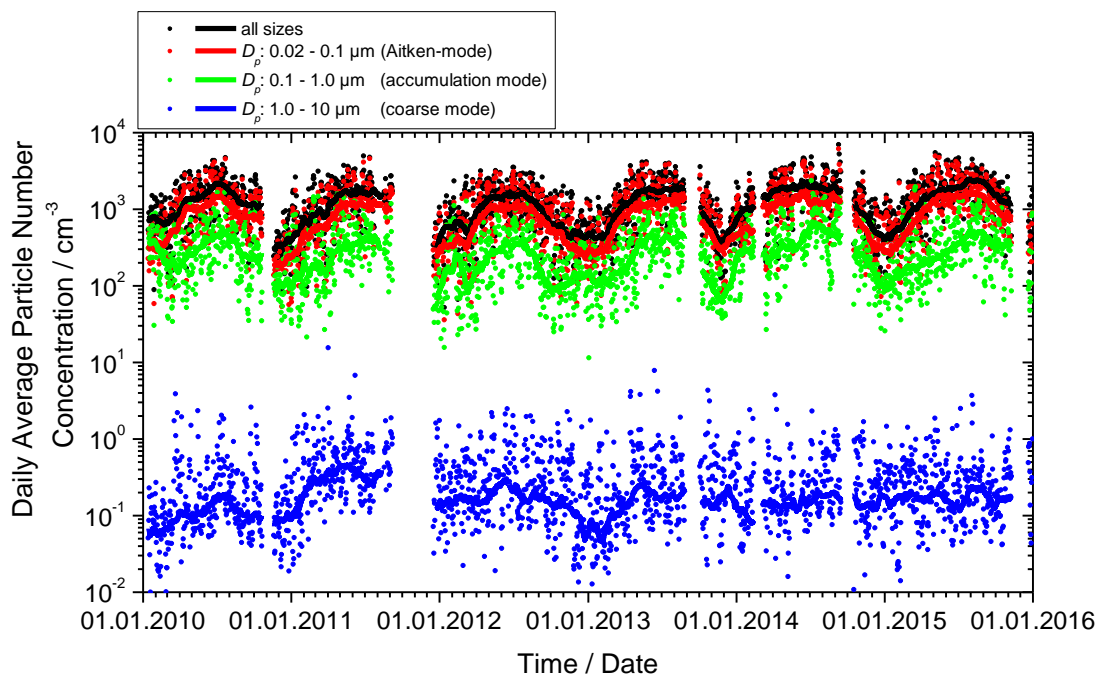


Figure 42: 2010-2015 time series of particle number concentration integrated over selected size ranges representing the different physical processes governing the atmospheric aerosol. The dotted graphs represent daily averages of the respective size range, the lines the 8-week running median.

atmospheric aerosol (see appendix for more details): 1) the Aitken-mode size range, 0.02 - 0.1 μm ; 2) the accumulation mode size range, 0.1 - 1 μm ; 3) the coarse mode size range, 1 - 10 μm . The time series in Figure 42 represent daily averages over these PNSD integrals for the whole period since the Birkenes station upgrade in 2010, as well as the corresponding running 8-week medians to highlight seasonal variations. The respective size range integral particle concentrations, N_{ait} for the Aitken mode, N_{acc} for the accumulation mode, and N_{coa} for the coarse mode, are also included in Table 5 to show the respective seasonal and annual average concentrations.

As to be expected, the particle concentration in the Birkenes aerosol in absolute terms is dominated by the Aitken mode particles, followed by the accumulation mode. Also the most prominent feature in Figure 42 is exhibited by the particle concentrations in these 2 modes, a clear annual cycle caused by the same underlying physical process. In summer, the vegetation emits gaseous aerosol precursors, which are photooxidised and condense onto Aitken-mode particles or form those directly. These particles coagulate, increasing the concentration of accumulation mode particles. These same processes increasing N_{ait} and N_{acc} in summer are also responsible for increasing the scattering Ångström coefficient \hat{a}_{sp} in summer. The processes controlling N_{coa} are decoupled from those controlling N_{ait} and N_{acc} . Coarse mode particles are formed from bulk material, their concentration is affected by wind speed (levitating dust, spores, pollen), snow cover, and rain (both inhibiting dust levitation).

3.1.3 Birkenes Aerosol Properties Measured In Situ at the Surface: Summary

In terms of particle concentration, the year 2015 is similar to 2014, but somewhat distinct from the previous years. As can be seen from Table 5, the particle concentrations in Aitken

Table 5: 2010 - 2015 seasonal and annual means of size distribution integrals, scattering coefficient, absorption coefficient, and single scattering albedo.

Year	Season	N_{ait} / cm^{-3}	N_{acc} / cm^{-3}	$N_{coarse} / \text{cm}^{-3}$	$N_{total} / \text{cm}^{-3}$	$\sigma_{sp} (550 \text{ nm}) / \text{Mm}^{-1}$	$\sigma_{ap} (550 \text{ nm}) / \text{Mm}^{-1}$	$\omega_0 (550 \text{ nm})$
2009/10	Winter	440	384	0.087	824	16.82	3.09	0.88
2010	Spring	1030	324	0.311	1354	12.33	0.78	0.93
2010	Summer	1511	488	0.323	1999	11.30	0.70	0.94
2010	Autumn	835	299	0.260	1135	7.26	0.71	0.90
2010	Whole Year	973	362	0.256	1336	11.52	1.24	0.91
2010/11	Winter	454	285	0.311	739	16.96	2.18	0.89
2011	Spring	1127	369	0.639	1496	18.67	1.26	0.93
2011	Summer	1391	438	0.572	1829	15.43	0.74	0.95
2011	Autumn	1594	464	0.966	2059	29.74	2.87	0.92
2011	Whole Year	1047	371	0.565	1418	20.26	1.69	0.93
2011/12	Winter	424	213	0.305	637	11.29	1.00	0.91
2012	Spring	1107	271	0.386	1378	15.10	0.86	0.93
2012	Summer	1314	392	0.485	1706	12.62	0.67	0.95
2012	Autumn	661	152	0.365	814	9.80	0.65	0.92
2012	Whole Year	889	263	0.375	1152	12.22	0.83	0.92
2012/13	Winter	383	183	0.183	566	12.48	0.92	0.90
2013	Spring	1190	352	0.411	1543	17.03	0.68	0.95
2013	Summer	1519	447	0.467	1967	13.81	0.56	0.96
2013	Autumn	701	162	0.417	864	8.89	0.64	0.91
2013	Whole Year	1020	304	0.391	1324	13.73	0.67	0.94
2013/14	Winter	699	333	0.347	1033	22.89	1.45	0.93
2014	Spring	1464	402	0.334	1866	12.95	1.09	0.93
2014	Summer	1723	625	0.343	2349	15.85	0.57	0.96
2014	Autumn	1122	446	0.385	1568	18.76	0.91	0.94
2014	Whole Year	1279	456	0.338	1735	16.99	0.99	0.94
2014/15	Winter	549	192	0.307	741	13.98	0.61	0.94
2015	Spring	1425	332	0.348	1757	12.72	0.68	0.94
2015	Summer	1979	559	0.395	2539	12.45	0.62	0.95
2015	Autumn	1130	422	0.257	1553	15.69	0.84	0.92
2015	Whole Year	1326	390	0.340	1717	14.36	0.67	0.94

and accumulation mode N_{ait} and N_{acc} are higher in winter, spring, and summer as compared to previous years. These deviations are caused by the unusual meteorological conditions in the reporting year, with winter temperatures falling rarely below freezing, very early onset of spring, and high summer temperatures. These conditions caused stronger and prolonged biogenic emissions of aerosol precursor substances, leading to the observed higher particle concentrations on seasonal and annual average for Aitken and accumulation mode size range

The seasonal and absolute trend in the optical aerosol properties over the years reflects discussed in Figure 40. The average winter aerosol particles becomes less absorbing over the years, and the differences between the average winter and summer aerosol particles in this respect decrease.

3.1.4 Column-Integrated Optical In Situ Aerosol Properties Measured by Ground-Based Remote Sensing

Ground-based remote sensing of the optical characteristics of aerosols in the atmospheric total column is conducted with multi-wavelength sun-photometers. A sun-photometer is oriented towards the sun to detect the solar radiation attenuated along the slant path from the top-of-atmosphere to the ground. The atmospheric aerosol load leads to a decrease in the solar radiation transmitted through the atmosphere. This decrease depends on the aerosol optical depth (AOD), which is given by the integral of the volume aerosol extinction coefficient along the vertical path of the atmosphere. The wavelength dependence of AOD, described by the Ångström exponent (Å) is a qualitative indicator of the particle size and contains information about the aerosol type. The larger the Ångström exponent, the smaller the size of the particles measured.

Photos of instruments used for monitoring of spectral resolved AOD at Birkenes and Ny-Ålesund (see below), their main characteristics are given in Appendix II, and detailed Tables with monthly data for all years are given in Appendix I.

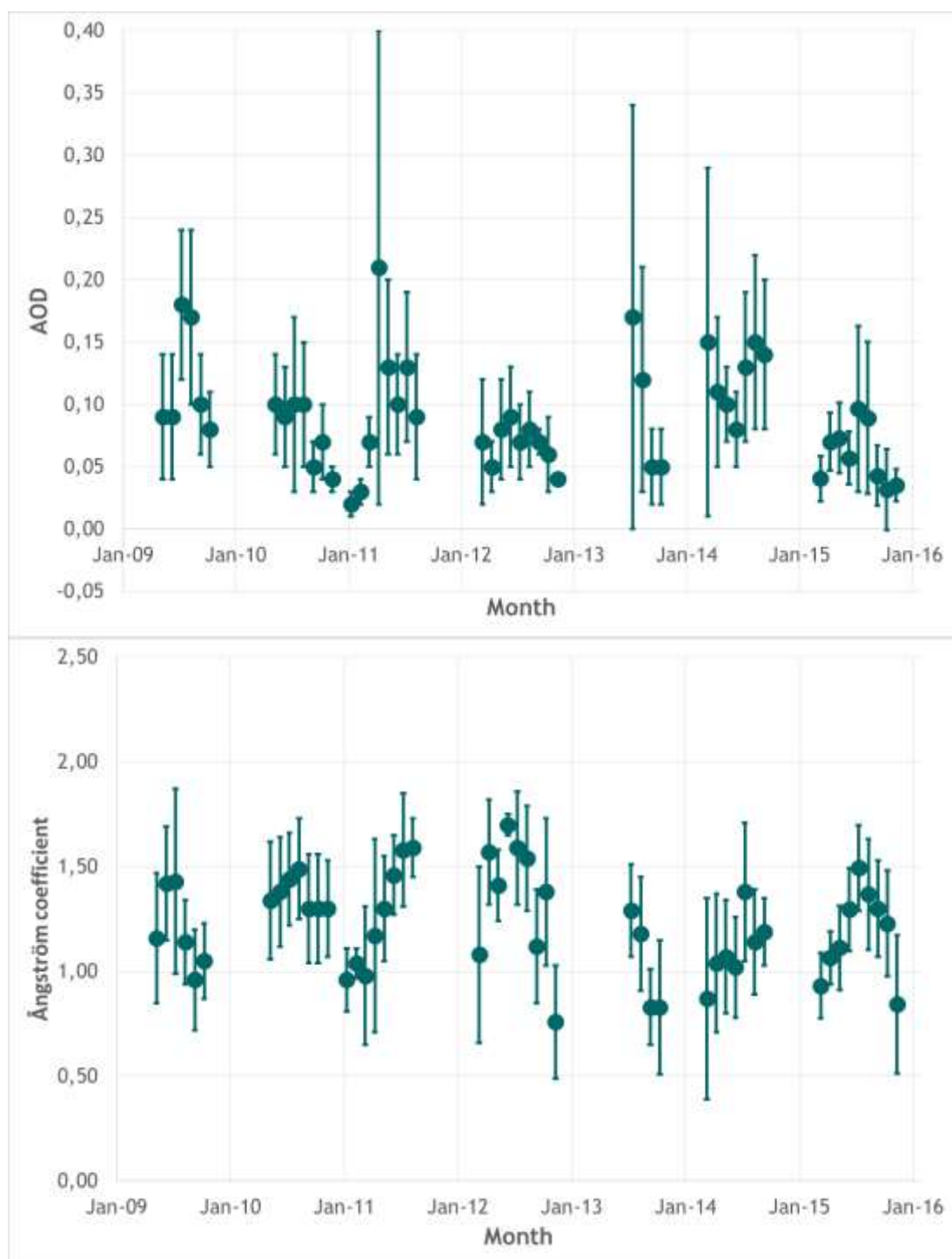


Figure 43: 2009 - 2015 time series of aerosol optical depth (AOD) at 500 nm wavelength in the atmospheric column above Birkenes (upper panel) and Ångström coefficient describing the AOD wavelength dependence (lower panel). Mean values and standard deviations are given.

AOD measurements started at the Birkenes Observatory in spring 2009, utilizing an automatic sun and sky radiometer (CIMEL type CE-318, instrument #513). The retrieval method is that of the AERONET version 2 direct sun algorithm (for details: <http://aeronet.gsfc.nasa.gov>). Quality assured (Level 2) data are available for the seven years of operation, 2009 - 2015. The Cimel instrument was not calibrated in 2015, but the calibration in October and November 2014 and a more recent one in summer 2016 was used for data calibration. Therefore, quality

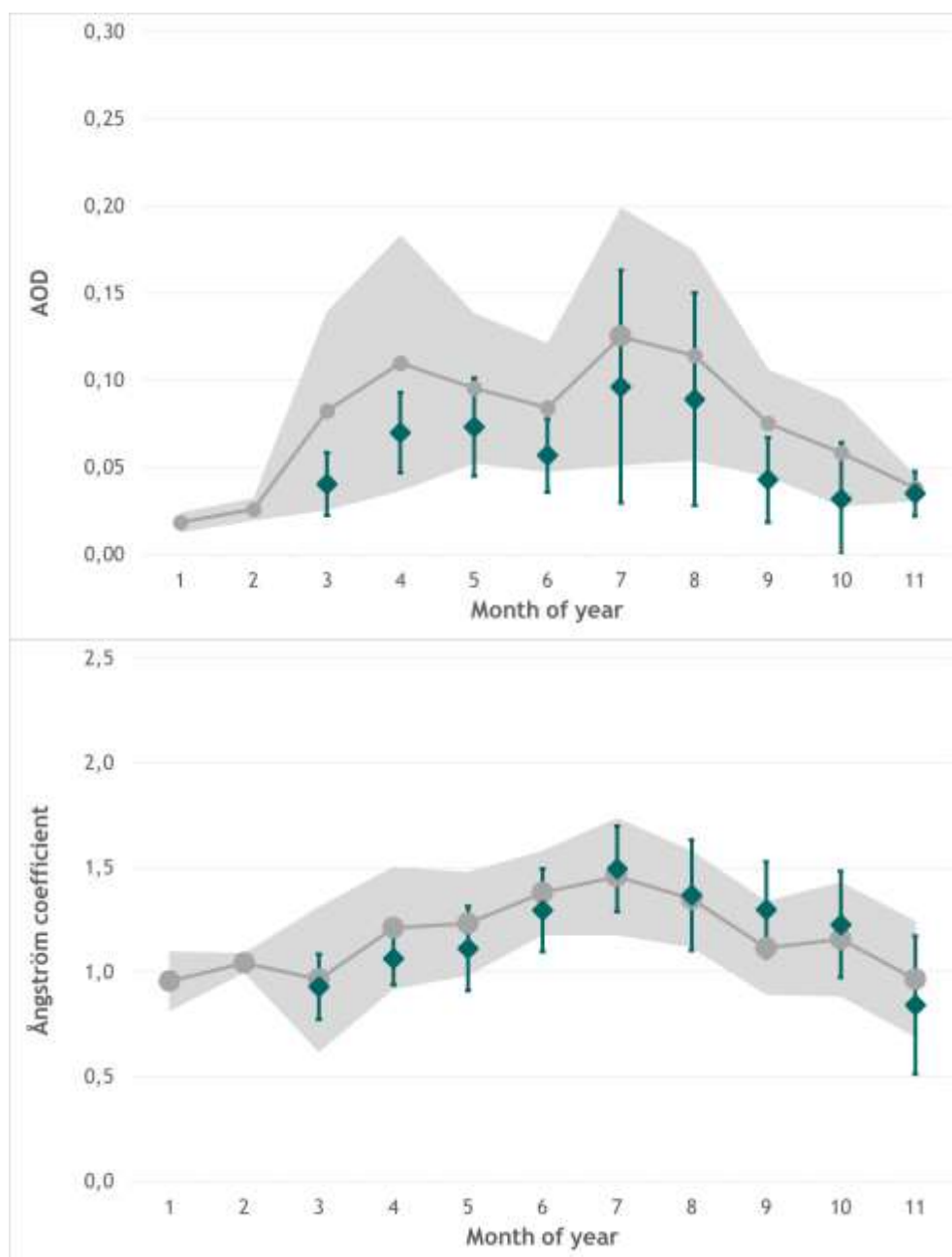


Figure 44: Monthly mean aerosol optical depth (AOD) at 500 nm wavelength in the atmospheric column above Birkenes (upper panel) and Ångström coefficient describing the AOD wavelength dependence (lower panel). Mean values and standard deviations are given.

assured AERONET level 2 data are available for the whole period when solar elevation allows reasonable data, in 2015 from March to November.

The AOD and Ångström coefficient time series and seasonal variations are shown Figure 43 and Figure 44. The 2015 monthly mean and mean values for all years are shown in Table 6. Data for all years are given in Appendix I. There are no obvious trends visible in the seven years of observations. Data gaps are caused by lack of sun light hours during the winter months (from last part of November through first part of February). In general, AOD measured at Birkenes are relatively low, compared to central European observations. E.g., AERONET climatological values for Cabauw, the Netherlands, vary between 1.2 ± 0.06 in December and 3.1 ± 0.19 in April). In 2015, AOD values at Birkenes were very low, even compared to previous

years at this station. The highest monthly average AOD of 0.096 was observed in July, while monthly means in March and throughout autumn were 0.04 or even lower. The largest spreads of daily values within a month were observed in July and August (standard deviations of 0.67 and 0.61, respectively). In these months, a small number daily mean AOD values of more than 0.15 were recorded, and on one day in July (day 193) even values of up to 0.7 were measured (which were discarded due to too few single values to calculate a daily means. AOD values for 2015 are at the lower end of the spread observed during the years 2009 - 2014, comparable to observations in 2012. All monthly means are smaller than the multi-year average. The low-AOD period with values of 0.04 or less in autumn 2015 is the longest observed since the start of observations at Birkenes.

Ångström exponent monthly means are close to the long-term means observed at Birkenes and also follows the seasonal variation of previous years, with monthly means close to 1.0 in the first half of the year, maximum values close to 1.5 in late summer and decreasing values again in autumn. All 2015 monthly means are within the standard deviations of all years at the station.

Table 6: Monthly mean values for 2014 and mean for the time period 2009-2014, plus standard deviations, for aerosol optical depth (AOD) and Ångström coefficient observed in Birkenes. In addition, the number of days with cloud free and quality assured observations are given.

Month/Year	Jan	Feb	Mar	Apr	May	Jun	Jul	Aug	Sep	Oct	Nov
Aerosol optical depth (AOD)											
2015			0.04 ±0.02	0.07 ±0.02	0.07 ±0.03	0.06 ±0.02	0.10 ±0.07	0.09 ±0.06	0.04 ±0.02	0.03 ±0.03	0.04 ±0.01
Mean 09-15	0.02 0.01	0.03 ±0.01	0.08 ±0.06	0.11 ±0.07	0.10 ±0.04	0.08 ±0.04	0.13 ±0.07	0.11 ±0.06	0.08 ±0.03	0.06 ±0.03	0.04 ±0.01
Ångström coefficient (Å)											
2015			0.93 ± 0.16	1.06 ± 0.13	1.11 ± 0.20	1.30 ± 0.20	1.49 ± 0.20	1.37 ±0.26	1.30 ±0.23	1.23 ±0.25	0.84 ±0.33
Mean 09-15	0.96 ±0.14	1.04 ±0.05	0.97 ±0.35	1.21 ±0.29	1.23 ±0.25	1.38 ±0.20	1.46 ±0.28	1.35 ±0.23	1.12 ±0.22	1.16 ±0.27	0.97 ±0.28
Number of days with cloud-free and quality assured observations (AERONET level 2)											
2015			6	1	14	21	21	16	9	11	3
Total 09-15	7	2	49	54	93	114	127	107	68	52	11

3.2 Physical and optical aerosol properties at Zeppelin Observatory

3.2.1 Aerosol Properties Measured In Situ at the Surface at Zeppelin Observatory

Figure 45 summarises the first few months of spectral aerosol particle absorption coefficient σ_{ap} data collected at Zeppelin Observatory since deployment of the new aethalometer in June 2015. The top panel displays daily averaged data for all 7 wavelengths (thin lines), as well as running 8-week medians (heavy lines), here only for 3 wavelengths to improve readability of the graph. The middle panel shows graphs of the absorption Ångström coefficient \hat{a}_{ap} for 3 wavelength pairs representing short wave end, long wave end, and full range of the measured wavelength spectrum. The \hat{a}_{ap} data are plotted as 8-week median only since daily averages

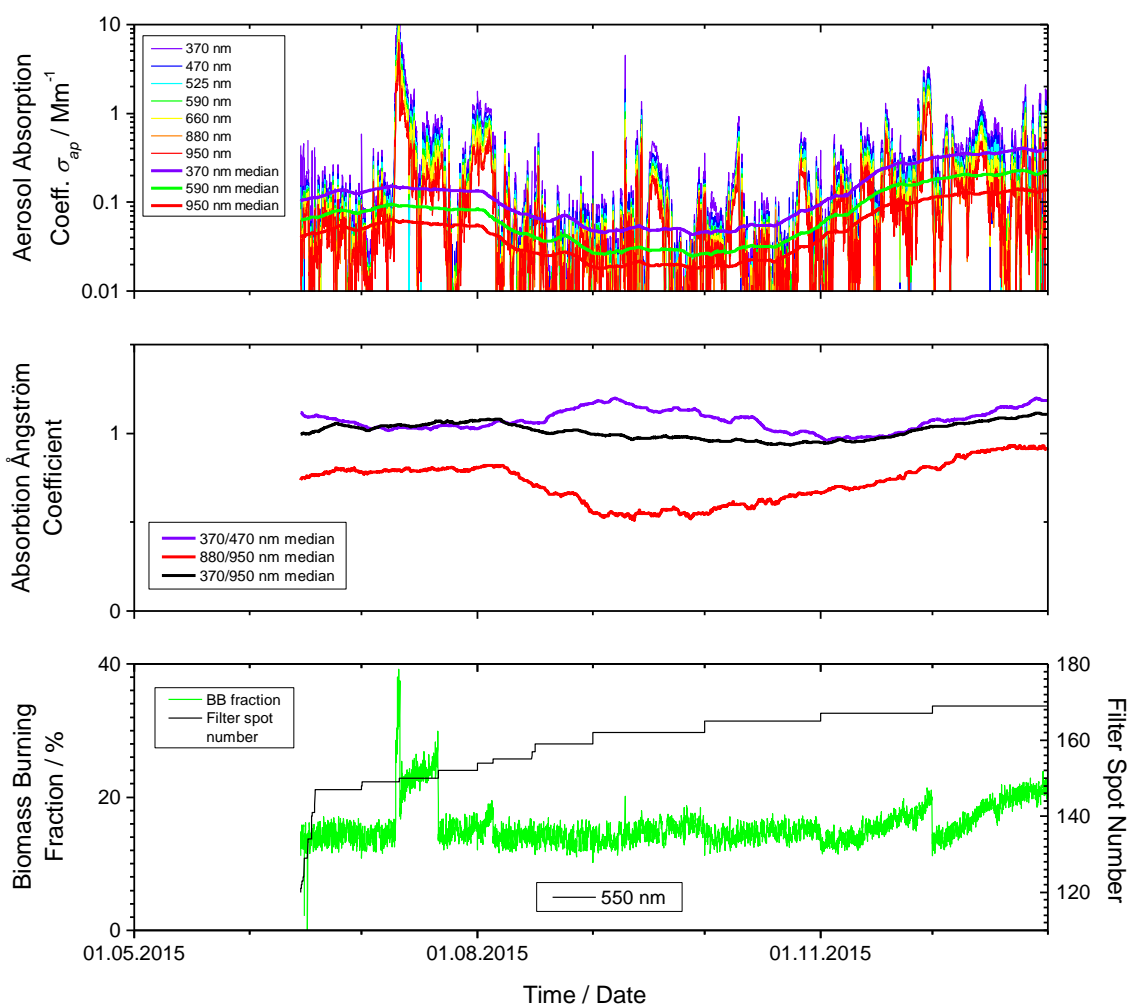


Figure 45: Time series graphs of the first months of data collected by the new filter absorption photometer at Zeppelin Observatory since deployment in June 2015. Top: daily means of absorption coefficient at all 7 measured wavelengths (thin lines), and 8-week running medians for top, middle and bottom of observed spectral range (heavy lines). Middle: 8-month running medians of absorption Ångström coefficient, top, bottom, and whole observed spectral range. Bottom: fraction of biomass burning aerosol contributing to particle absorption as calculated by instrument, together with ID number of filter spot.

are too noisy due to the low particle load commonly observed at Zeppelin. The bottom panel of Figure 45 depicts the fraction of biomass burning aerosol contributing to the sampled aerosol as calculated by the instrument. To calculate the biomass burning fraction, the instrument uses the different spectral absorption characteristics of aerosol from fossil as compared to biofuel combustion (Sandradewi et al., 2008). When interpreting this parameter, caution needs to be exercised. The assumed absorption models for fossil and biofuel combustion emissions have been derived for conditions in rural Switzerland. These conditions are certainly not representative for Arctic aerosol. However, if interpreted in a qualitative way, the parameter may give a first indication of changes in the properties of the absorbing aerosol particle fraction.

Even though the time series of the aethalometer at Zeppelin spans only half a year at this point, a few interesting features can be detected already now. The time series of σ_{ap} (top panel of Figure 45) exhibits the same annual cycle as described already in the data of the aethalometer instrument collected in earlier years (Eleftheriadis et al., 2009), with lower values in summer and higher ones in winter. These variations have been attributed to changes in combustion aerosol source strength caused by emissions from domestic heating in the relevant source regions, e.g. Northern and Central Russia (Law & Stohl, 2007). This pattern is moderated by incidents of emissions from big forest fires reaching the Arctic, which can increase aerosol particle absorption in episodes also in summer (e.g. Stohl et al., 2007). This pattern is mirrored in the time series of the biomass burning fraction calculated by the MAGEE AE33 instrument, which increases for episodes summer and towards winter. However, obvious artefacts can be detected in the calculation of the biomass burning fraction, which increases also with aerosol loading on the filter, and drops when the filter spot is changed (see filter spot number also plotted in bottom panel of Figure 45).

Probably most interesting in the data provided by the new filter absorption photometer is the aerosol absorption Ångström coefficient \tilde{a}_{ap} , which seems to display its own annual cycle. Towards autumn, \tilde{a}_{ap} increases in the ultraviolet (UV) range, and decreases in the infrared (IR) range. In descriptive terms, this means that the absorbing aerosol fraction in autumn decreases in particle size as seen by UV light (which weighs smaller particles more), and increases in particle size as seen by IR light (which weighs larger particles more). An explanation of this puzzling phenomenon needs to await further measurements at Zeppelin. Also funded by the extraordinary grant of the Norwegian Ministry of Climate and Environment, an instrument observing the size distribution of the non-volatile particle fraction as a proxy of the absorbing particle fraction will be installed at Zeppelin by NILU in autumn 2016.

3.2.2 Column-Integrated Optical In Situ Aerosol Properties Measured by Ground-Based Remote Sensing at Ny-Ålesund

In 2002, Physikalisch-Meteorologisches Observatorium Davos/ *World Radiation Center* (PMOD/WRC) in collaboration with NILU, started AOD observations in Ny-Ålesund (at the Sverdrup station, 46 m a.s.l.) as part of the global AOD network on behalf of the WMO GAW program. A precision filter radiometer (PFR) measures the extinction in four narrow spectral bands at 368 nm, 415 nm, 500 nm and 862 nm. Data quality control includes instrumental control like detector temperature and solar pointing control as well as objective cloud screening. Ångström coefficients are derived for each set of measurements using all four PFR

channels. Calibration is performed annually at PMOD/WRC. Quality assured data are available at the World Data Center of Aerosols (WDCA), hosted at NILU (see <https://ebas.nilu.no>).

In Ny-Ålesund, the solar elevation is less than 5° before 4 March and after 10 October, limiting the period with suitable sun-photometer observations to the spring-summer-early autumn seasons (NILU contributes to a Lunar Arctic initiative to fill the gap in the wintertime AOD climatology by using Lunar photometer, see Appendix II). In 2015, sun-photometer observations started on 20 March and lasted until 18 September; reliable AOD values are available on 76 days. The AOD and Ångström coefficients time series of monthly means and standard deviation are shown in Figure 46, while the 2015 values on the background of the average data and their standard deviation from the whole 14-year period are shown in Figure 47. The 2015 monthly mean values and standard deviations for all years are given in Table 7. Data for all years are given in Appendix I.

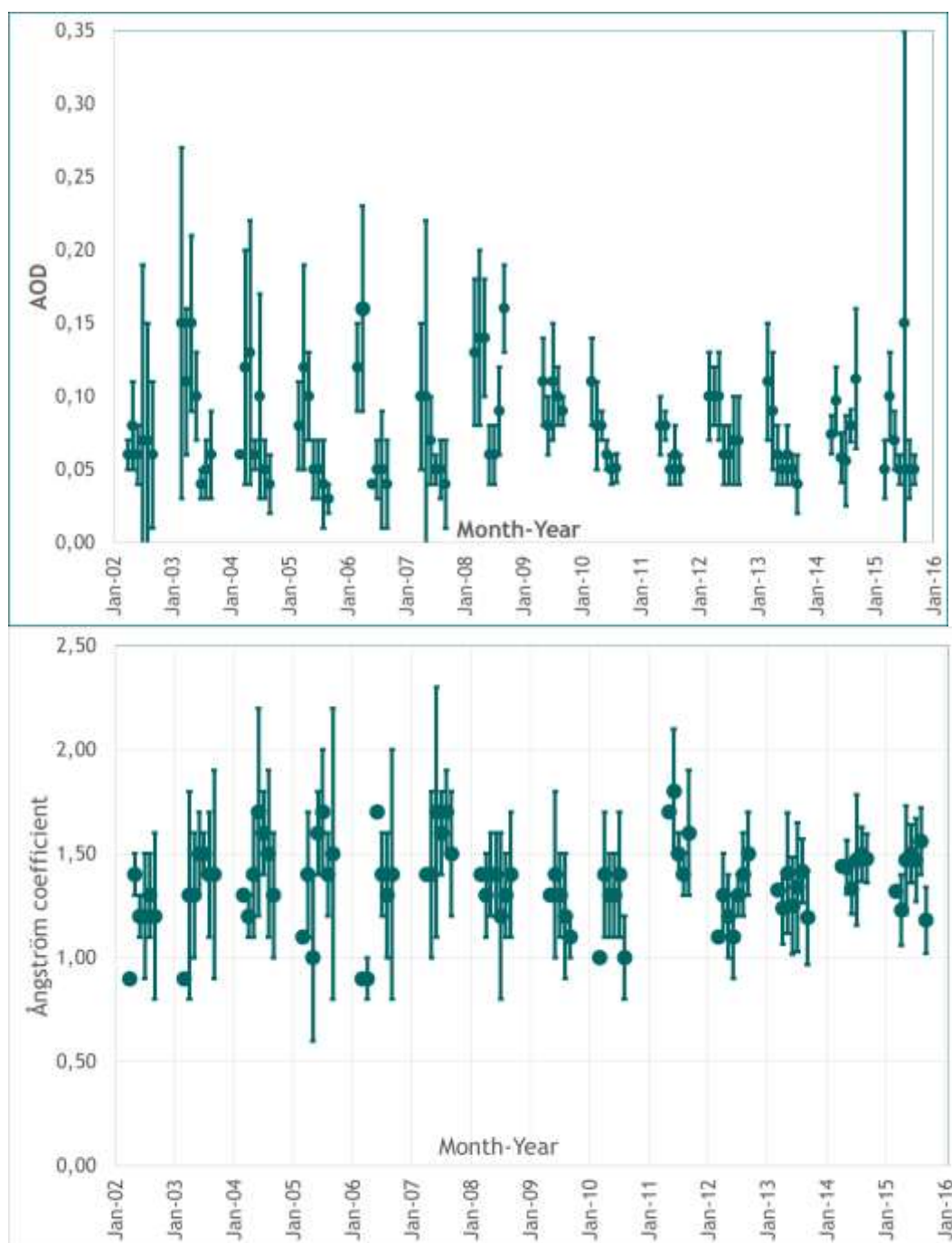


Figure 46: 2002 - 2015 time series of aerosol optical depth (AOD) at 500.5 nm wavelength in the atmospheric column above Ny-Ålesund (upper panel) and Ångström coefficient (lower panel). Monthly mean values and standard deviations are given.

In all months except July, monthly mean AOD values are equal to or smaller than the long-term mean; in March the value is outside the standard deviation of previous years. The most prominent feature in AOD is a short episode in July (9 - 12) with daily means of up to 0.7 and single measurement values of up to 1.2. This period increases the monthly means to 0.15 and the standard deviation to 0.2. A preliminary analysis of the event by Zielinski et al. concluded that this event was due to the advection of air masses from massive forest fires in Alaska; it will be further analysed and published in the near future. Besides comparison with other

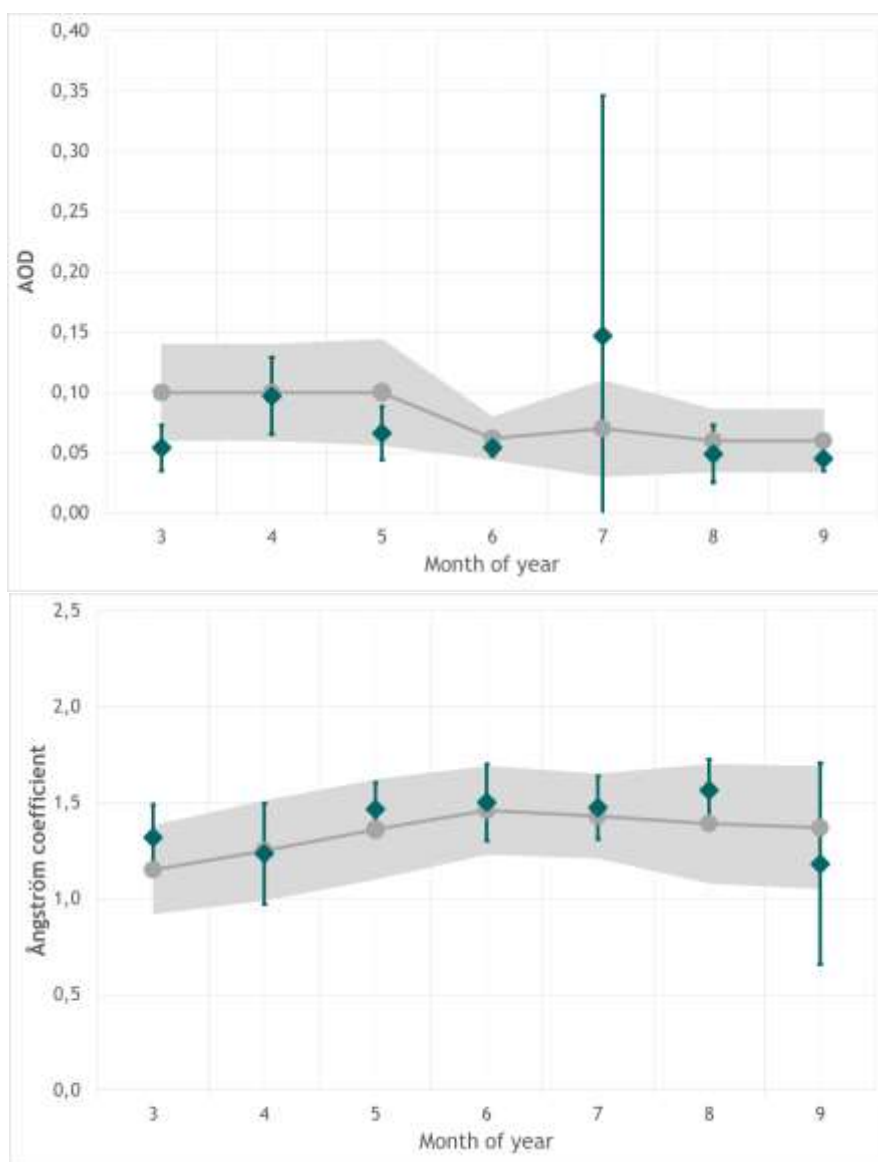


Figure 47: Seasonal variation of the aerosol optical depth (AOD) (upper panel) and Ångström coefficient (lower panel) observed in Ny-Ålesund. Values marked in grey are the mean and standard deviations for the time period 2009-2015; the 2015 monthly mean and standard deviations are shown in green.

measurements in Ny-Ålesund and Hornsund, also the Ångström exponent values from this period confirm the validity of the measurements. Ångström coefficient monthly means were very stable throughout almost the whole measurement period close to a value of 1.4. However, both in April and September significantly lower values (< 1.0) were observed; the smallest daily means of 0.25 was recorded in mid-September. Generally, in Ny-Ålesund seasonal variation of the Ångström coefficient is very weak, and the monthly mean Ångström coefficients in 2015 lie within the standard deviation range of the long-term monthly means, except September. This period with extremely low AE should be studied in more detail as well.

Table 7: Monthly mean values for 2014 and mean for the time period 2002-2014 for March to September, plus standard deviations, for aerosol optical depth (AOD) and Ångström coefficient observed in Ny-Ålesund. In addition, the number of days with cloud free and quality assured observations are given.

Month/Year	Mar	Apr	May	Jun	Jul	Aug	Sep
Aerosol optical depth (AOD)							
2015	0.05 ±0.02	0.10 ±0.03	0.07 ±0.02	0.05 ±0.01	0.15 ±0.20	0.05 ±0.02	0.05 ±0.01
Mean 2002-2015	0.10 ±0.06	0.10 ±0.06	0.10 ±0.06	0.06 ±0.04	0.07 ±0.03	0.06 ±0.03	0.06 ±0.03
Ångström coefficient (Å)							
2015	1.32 ±0.17	1.23 ±0.26	1.47 ±0.14	1.50 ±0.20	1.47 ±0.6	1.56 ±0.16	1.18 ±0.52
Mean 2002-2015	1.15 ±0.23	1.25 ±0.26	1.36 ±0.26	1.46 ±0.23	1.43 ±0.22	1.39 ±0.31	1.37 ±0.32
Number of days with cloud-free and quality assured observations							
2015	5	17	15	9	17	13	6
Total 2002- 2015	61	160	153	145	167	125	111

4. References

- Aas, W., Platt, S., Solberg, S., Yttri, K.E. (2016) Monitoring of long-range transported air pollutants in Norway, annual report 2015. Kjeller, NILU (Miljødirektoratet rapport, M-562/2016) (NILU OR, 13/2016).
- Asmi, A., Collaud Coen, M., Ogren, J. A., Andrews, E., Sheridan, P., Jefferson, A., Weingartner, E., Baltensperger, U., Bukowiecki, N., Lihavainen, H., Kivekäs, N., Asmi, E., Aalto, P. P., Kulmala, M., Wiedensohler, A., Birmili, W., Hamed, A., O'Dowd, C., G Jennings, S., Weller, R., Flentje, H., Fjaeraa, A. M., Fiebig, M., Myhre, C.E.L., Hallar, A. G., Swietlicki, E., Kristensson, A., Laj, P. (2013) Aerosol decadal trends - Part 2: In-situ aerosol particle number concentrations at GAW and ACTRIS stations. *Atmos. Chem. Phys.*, 13, 895-916. doi:10.5194/acp-13-895-2013.
- Baasandorj, M., Hall, B. D., Burkholder, J. B. (2012) Rate coefficients for the reaction of O(¹D) with the atmospherically long-lived greenhouse gases NF₃, SF₅CF₃, CHF₃, C₂F₆, C₄F₈, n-C₅F₁₂, and n-C₆F₁₄. *Atmos. Chem. Phys.*, 12, 11753-11764. doi:10.5194/acp-12-11753-2012.
- Coen, M.C., Andrews, E., Asmi, A., Baltensperger, U., Bukowiecki, N., Day, D., Fiebig, M., Fjaeraa, A. M., Flentje, H., Hyvärinen, A., Jefferson, A., Jennings, S. G., Kouvarakis, G., Lihavainen, H., Myhre, C.E.L., Malm, W. C., Mihapopoulos, N., Molenaar, J. V., O'Dowd, C., Ogren, J. A., Schichtel, B. A., Sheridan, P., Virkkula, A., Weingartner, E., Weller, R., Laj, P. (2013) Aerosol decadal trends - Part 1: In-situ optical measurements at GAW and IMPROVE stations. *Atmos. Chem. Phys.*, 13, 869-894. doi:10.5194/acp-13-869-2013.
- Dalsøren, S. B., Myhre, C.E.L., Myhre, G., Gomez-Pelaez, A. J., Søvde, O. A., Isaksen, I. S. A., Weiss, R. F., Harth, C. M. (2016) Atmospheric methane evolution the last 40 years. *Atmos. Chem. Phys.*, 16, 3099-3126. doi:10.5194/acp-16-3099-2016.
- Delene, D.J., Ogren, J.A. (2002) Variability of aerosol optical properties at four North American surface monitoring sites. *J. Atmos. Sci.*, 59, 1135-1150.
- Etiopie, G., Ciccioli, P. (2009) Earth's Degassing: A Missing Ethane and Propane Source. *Science* 323, 478. doi:10.1126/science.1165904.
- IPCC (2013) Summary for policymakers. In: *Climate Change 2013: The Physical Science Basis. Contribution of Working Group I to the Fifth Assessment Report of the Intergovernmental Panel on Climate Change*. Ed. by Stocker, T.F., Qin, D., Plattner, G.-K., Tignor, M., Allen, S.K., Boschung, J., Nauels, A., Xia, Y., Bex, V., Midgley, P.M. Cambridge, Cambridge University Press. pp. 3-29.
- Hartmann, D.L., Klein Tank, A.M.G., Rusticucci, M., Alexander, L.V., Brönnimann, S., Charabi, Y., Dentener, F.J., Dlugokencky, E.J., Easterling, D.R., Kaplan, A., Soden, B.J., Thorne, P.W., Wild, M., Zhai, P.M. (2013) Observations: atmosphere and surface. In: *Climate Change 2013: The Physical Science Basis. Contribution of Working Group I to the Fifth Assessment Report of the Intergovernmental Panel on Climate Change*. Ed. by Stocker, T.F., Qin, D., Plattner, G.-K., Tignor, M., Allen, S.K., Boschung, J., Nauels, A., Xia, Y., Bex, V., Midgley, P.M. Cambridge, Cambridge University Press. pp. 159-254.
- Helmig D. et al. (2016) Reversal of global atmospheric ethane and propane trends largely due to US oil and natural gas production, *Nature Geosci.*, 9, 490-495. doi:10.1038/ngeo2721.

- Hewitt, C. Nicholas (ed.) (1999) *Reactive Hydrocarbons in the Atmosphere*. San Diego, CA, Academic Press. p. 313.
- Isaksen, I.S.A., Hov, Ø. (1987) Calculation of trends in the tropospheric concentration of O₃, OH, CO, CH₄ and NO_x. *Tellus*, 39B, 271-285.
- Mazzola, M., Vitale, V., Lupi, A., Wehrli, C., Kouremeti, N., Stone, R.S., Stebel, K. (2015) Moon-photometric aerosol optical depth measurements during polar night. Poster presented at the Lunar Photometry workshop, University of Valladolid, Spain, June 24 - 26, 2015.
- Myhre, C.E.L., Ferré, B., Platt, S.M., Silyakova, A., Hermansen, O., Allen, G., Pisso, I., Schmidbauer, N., Stohl, A., Pitt, J., Jansson, P., Greinert, J., Percival, C., Fjaeraa, A.M., O'Shea, S., Gallagher, M., Le Breton, M., Bower, K., Bauguitte, S., Dalsøren, S., Vadakkepuliambatta, S., Fisher, R., Nisbet, E., Lowry, D., Myhre, G., Pyle, J., Cain, M., Mienert, J. (2016) Large methane release from the Arctic seabed west of Svalbard, but small release to the atmosphere. *Geophys. Res. Lett.*, 43, 4624-4631. doi:10.1002/2016GL068999.
- Myhre, G., Myhre, C.E.L., Samset, B. H., Storelvmo, T. (2013a) Aerosols and their relation to global climate and climate sensitivity. *Nature Education Knowledge*, 4, 5,7. URL: <http://www.nature.com/scitable/knowledge/library/aerosols-and-their-relation-to-global-climate-102215345>
- Myhre, G., Shindell, D., Bréon, F.-M., Collins, W., Fuglestedt, J., Huang, J., Koch, D., Lamarque, J.-F., Lee, D., Mendoza, B., Nakajima, T., Robock, A., Stephens, G., Takemura, T., Zhang, H. (2013b) Anthropogenic and natural radiative forcing. In: *Climate Change 2013: The Physical Science Basis. Contribution of Working Group I to the Fifth Assessment Report of the Intergovernmental Panel on Climate Change*. Ed. by Stocker, T.F., Qin, D., Plattner, G.-K., Tignor, M., Allen, S.K., Boschung, J., Nauels, A., Xia, Y., Bex, V., Midgley, P.M. Cambridge, Cambridge University Press. pp. 659-740.
- Ng, N.L., Kröll, J.H., Chan, A.W.H., Chhabra, P.S., Flagan, R.C., Seinfeld, J.H. (2007) Secondary organic aerosol formation from m-xylene, toluene, and benzene. *Atmos. Chem. Physics*, 7, 3909-3922.
- Nicewonger, M.R., Verhulst, K.R., Aydin, M., Saltzman, E.S. (2016) Preindustrial atmospheric ethane levels inferred from polar ice cores: A constraint on the geologic sources of atmospheric ethane and methane. *Geophys. Res. Lett.*, 43, 214-221. doi:10.1002/2015GL066854.
- Oram, D. E., Mani, F. S., Laube, J. C., Newland, M. J., Reeves, C. E., Sturges, W. T., Penkett, S. A., Brenninkmeijer, C. A. M., Röckmann, T., and Fraser, P. J. (2012) Long-term tropospheric trend of octafluorocyclobutane (c-C₄F₈ or PFC-318), *Atmos. Chem. Phys.*, 12, 261-269. doi:10.5194/acp-12-261-2012.
- Prather, M., Ehhalt, D., Dentener, F., Derwent, R.G., Dlugokencky, E., Holland, E., Isaksen, I.S.A., Katima, J., Kirchhoff, V., Matson, P., Midgley, P.M., Wang, M. (2001) Atmospheric chemistry and greenhouse gases. In: *Climate Change 2001: The Scientific Basis, Contribution of Working Group I to the Third Assessment Report of the Intergovernmental Panel on Climate Change*. Ed. by: Houghton, J.T., Ding, Y., Griggs, D.J., Noguer, M., van der Linden, P.J., Dai, X., Maskell, K., Johnson, C.A. Cambridge, Cambridge University Press. pp. 239-287.

- Pisso, I., Myhre, C.E.L., Platt, S.M., Eckhardt, S., Hermansen, O., Schmidbauer, N., Mienert, J., Vadakkepuliambatta, S., Bauguitte, S., Pitt, J., Allen, G., Bower, K.N., O'Shea, S., Gallagher, M.W., Percival, C.J., Pyle, J., Cain, M., Stohl, A. (2016) Constraints on oceanic methane emissions west of Svalbard from atmospheric in situ measurements and Lagrangian transport modelling. *J. Geophys. Res.*, doi:10.1002/2016JD025590, under review.
- Repo, M.E., Susiluoto, S., Lind, S.E., Jokinen, S., Elsakov, V., Biasi, C., Virtanen, T., Pertti, J., Martikainen, P.J. (2009) Large N₂O emissions from cryoturbated peat soil in tundra. *Nature Geosci.*, 2, 189-192.
- Simmonds, P.G., Manning, A.J., Cunnold, D.M., Fraser, P.J., McCulloch, A., O'Doherty, S., Krummel, P.B., Wang, R.H.J., Porter, L.W., Derwent, R.G., Grealley, B., Salameh, P., Miller, B.R., Prinn, R.G., Weiss, R.F. (2006) Observations of dichloromethane, trichloroethene and tetrachloroethene from the AGAGE stations at Cape Grim, Tasmania, and Mace Head, Ireland. *J. Geophys. Res.*, 111, D18304. doi:10.1029/2006JD007082.
- Svendby, T.M., Edvardsen, K., Hansen, G.H., Stebel, K., Dahlback, A. (2015) Monitoring of the atmospheric ozone layer and natural ultraviolet radiation. Annual report 2014. Kjeller, NILU (Miljødirektoratet rapport, M-366/2015) (NILU OR, 18/2015).
- Svendby, T.M., Hansen, G.H., Edvardsen, K., Stebel, K., Dahlback, A. (2016) Monitoring of the atmospheric ozone layer and natural ultraviolet radiation. Annual report 2015. Kjeller, NILU. (Miljødirektoratet rapport, M-561/2016) (NILU report, 12/2016).
- Stebel, K., Vik, A.F., Myhre, C.E.L., Fjæraa, A.M., Svendby, T., Schneider, P. (2013) Towards operational satellite based atmospheric monitoring in Norway SatMoNAir. Kjeller, NILU, (NILU OR, 46/2013).
- Toledano, C., Cachorro, V., Gausa, M., Stebel, K., Aaltonen, V., Berjón, A., Ortiz de Galisteo, J.P., de Frutos, A.M., Bennouna, Y., Blindheim, S., Myhre, C.E.L., Zibordi, G., Wehrli, C., Kratzer, S., Hakansson, B., Carlund, T., de Leeuw, G., Herber, A., Torres, B. (2012) Overview of sun photometer measurements of aerosol properties in Scandinavia and Svalbard. *Atmos. Environ.*, 52, 18-28. doi: 10.1016/j.atmosenv.2011.10.022.
- Tomasi, C., Kokhanovsky, A. A., Lupi, A., Ritter, C., Smirnov, A., O'Neill, N. T., Stone, R. S., Holben, B. N., Nyeki, S., Wehrli, C., Stohl, A., Mazzola, M., Lanconelli, C., Vitale, V., Stebel, K., Aaltonen, V., de Leeuw, G., Rodriguez, E., Herber, A. B., Radionov, V. F., Zielinski, T., Petelski, T., Sakerin, S. M., Kabanov, D. M., Xue, Y., Mei, L., Istomina, L., Wagener, R., McArthur, B., Sobolewski, P. S., Kivi, R., Courcoux, Y., Larouche, P., Broccardo, S., Piketh, S. J. (2015) Aerosol remote sensing in polar regions. *Earth Sci. Rev.*, 140, 108-157. doi:10.1016/j.earscirev.2014.11.001.
- Thompson, R.L., Sasakawa, M., Machida, T., Aalto, T., Worthy, D., Lavric, J. V., Myhre, C.E.L., Stohl, A. (2016) Methane fluxes in the high northern latitudes for 2005-2013 estimated using a Bayesian atmospheric inversion. *Atmos. Chem. Phys. Discuss.*, doi:10.5194/acp-2016-660, in review.
- Thompson, R.L., Dlugockenky, E., Chevallier, F., Ciais, P., Dutton, G., Elkins, J. W., Langenfelds, R. L., Prinn, R. G., Weiss, R. F., Tohjima, Y., Krummel, P. B., Fraser, P., Steele, L. P. (2013) Interannual variability in tropospheric nitrous oxide. *Geophys. Res. Lett.*, 40, 4426-4431. doi:10.1002/grl.50721.

- Tørseth, K., Aas, W., Breivik, K., Fjæraa, A. M., Fiebig, M., Hjellbrekke, A. G., Myhre, C.E.L., Solberg, S., Yttri, K. E. (2012) Introduction to the European Monitoring and Evaluation Programme (EMEP) and observed atmospheric composition change during 1972-200. *Atmos. Chem. Phys.*, 12, 5447-5481. doi:10.5194/acp-12-5447-2012.
- Vik, A.F., Myhre, C.E.L., Stebel, K., Fjæraa, A.M., Svendby, T., Schyberg, H., Gauss, M., Tsyro, S., Schulz, M., Valdebenito, A., Kirkevåg, A., Seland, Ø., Griesfeller, J. (2011) Roadmap towards EarthCARE and Sentinel-5 precursor. A strategy preparing for operational application of planned European atmospheric chemistry and cloud/aerosol missions in Norway. Kjeller, NILU (NILU OR, 61/2011).
- Wiedensohler, A., Birmili, W., Nowak, A., Sonntag, A., Weinhold, K., Merkel, M., Wehner, B., Tuch, T., Pfeifer, S., Fiebig, M., Fjæraa, A.M., Asmi, E., Sellegri, K., Depuy, R., Venzac, H., Villani, P., Laj, P., Aalto, P., Ogren, J.A., Swietlicki, E., Williams, P., Roldin, P., Quincey, P., Hüglin, C., Fierz-Schmidhauser, R., Gysel, M., Weingartner, E., Riccobono, F., Santos, S., Gruning, C., Faloon, F., Beddows, D., Harrison, R., Monahan, C., Jennings, S.G., O'Dowd, C.D., Marinoni, A., Horn, H.-G., Keck, L., Jiang, J., Scheckman, J., McMurry, P.H., Deng, Z., Zhao, C.S., Moerman, M., Henzing, B., de Leeuw, G., Löschau, G., Bastian, S. (2012) Mobility particle size spectrometers: harmonization of technical standards and data structure to facilitate high quality long-term observations of atmospheric particle number size distributions. *Atmos. Meas. Tech.*, 5, 657 - 685. doi:10.5194/amt-5-657-2012.
- WMO (2016) Greenhouse Gas Bulletin. The state of greenhouse gases in the atmosphere using global observations through 2015. Geneva, World Meteorological Organization (GHG Bulletin No. 12, 24 October 2016). URL: http://library.wmo.int/pmb_ged/ghg-bulletin_12_en.pdf
- WMO (2015) Greenhouse Gas Bulletin. The state of greenhouse gases in the atmosphere using global observations through 2014. Geneva, World Meteorological Organization (GHG Bulletin No. 11, 9 November 2015). URL: http://library.wmo.int/pmb_ged/ghg-bulletin_11_en.pdf
- WMO (2014) Greenhouse Gas Bulletin. The state of greenhouse gases in the atmosphere using global observations through 2013. Geneva, World Meteorological Organization (GHG Bulletin No. 10, 9 September 2014). URL: http://library.wmo.int/opac/index.php?lvl=notice_display&id=16396#.VGHPz5-gQtK
- WMO (2013) Greenhouse Gas Bulletin. The state of greenhouse gases in the atmosphere using global observations through 2012. Geneva, World Meteorological Organization (GHG Bulletin No. 9, 6 November 2013). URL: http://www.wmo.int/pages/prog/arep/gaw/ghg/documents/GHG_Bulletin_No.9_en.pdf
- WMO (2012) Greenhouse Gas Bulletin. The state of greenhouse gases in the atmosphere using global observations through 2011. Geneva, World Meteorological Organization (GHG Bulletin No. 8, 19 November 2012). URL: http://www.wmo.int/pages/prog/arep/gaw/ghg/documents/GHG_Bulletin_No.8_en.pdf
- WMO (2011) Scientific assessment of ozone depletion: 2010. Geneva, World Meteorological Organization (Global ozone research and monitoring project, Report No. 52).

Xiong, X., Barnet, C. D., Maddy, E., Sweeney, C., Liu, X., Zhou, L., Goldberg, M. (2008) Characterization and validation of methane products from the atmospheric infrared sounder AIRS. *J. Geophys. Res.*, 113, G00A01. doi:10.1029/2007JG000500.

Xu, Y., Zaelke, D., Velders, G.J.M., Ramanathan, V. (2013) The role of HFCs in mitigating 21st century climate change. *Atmos. Chem. Phys.*, 13, 6083-6089. doi:10.5194/acp-13-6083-2013.

APPENDIX I: Data Tables

Table A 1: Annual mean concentration for all greenhouse gases included in the programme at Zeppelin and Birkenes. All concentrations are mixing ratios in ppt, except for methane and carbon monoxide (ppb) and carbon dioxide (ppm). The annual means are based on a combination of the observed methane values and the modelled background values; during periods with lacking observations, we have used the fitted background mixing ratios in the calculation of the annual mean. All underlying measurement data can be downloaded directly from the database: <http://ebas.nilu.no/>

Component	2001	2002	2003	2004	2005	2006	2007	2008	2009	2010	2011	2012	2013	2014	2015	
Carbondioxide - Zeppelin												394.8	397.3	399.6	401.2	
Carbondioxide - Birkenes											393.5	396.5	397.8	400.7	402.8	405.1
Methane - Zeppelin	1843.4	1842.4	1855.3	1853.1	1852.2	1853.2	1863.6	1873.4	1888.1	1881.0	1879.5	1891.8	1897.9	1910.0	1920.2	
Methane - Birkenes											1885.0	1895.4	1900.5	1902.0	1917.4	1925.9
Carbon monoxide	124.6	126.0	140.3	131.2	128.3	126.5	120.1	119.8	117.7	127.3	115.2	120.5	113.0	113.4	113.6	
Nitrous oxide												324.2	325.0	326.1	327.1	328.1
Chlorofluorocarbons																
CFC-11*	258.9	257.2	255.3	253.6	251.4	249.4	246.6	244.6	242.7	240.7	238.3	236.8	235.2	234.1	233.2	
CFC-12*	547.1	547.7	548.0	546.0	547.2	546.4	542.4	541.5	537.6	534.4	531.5	528.6	525.9	523.4	521.4	
CFC-113*	81.5	80.8	80.1	79.4	78.8	77.9	77.4	76.8	76.2	75.4	74.6	74.1	73.5	72.9	72.3	
CFC-115*	8.22	8.19	8.25	8.28	8.41	8.39	8.38	8.40	8.43	8.42	8.42	8.44	8.43	8.45	8.47	
Hydrochlorofluorocarbons																
HCFC-22	158.9	164.3	170.1	175.3	181.1	188.8	196.1	204.5	212.5	219.9	225.9	231.5	236.5	241.3	244.7	

Component	2001	2002	2003	2004	2005	2006	2007	2008	2009	2010	2011	2012	2013	2014	2015
HCFC-141b	16.6	17.9	18.7	19.3	19.6	20.0	20.5	21.1	21.5	22.1	23.0	23.9	24.7	25.4	26.1
HCFC-142b*	14.5	15.1	15.7	16.5	17.1	18.2	19.3	20.3	21.3	22.1	22.7	23.1	23.3	23.3	23.2
Hydrofluorocarbons															
HFC-125	2.30	2.96	3.50	4.28	4.86	5.62	6.46	7.49	8.59	10.03	11.77	13.54	15.61	17.86	20.27
HFC-134a	20.8	26.0	30.8	35.6	40.0	44.2	48.6	53.4	57.8	63.5	68.5	73.4	78.8	84.4	89.9
HFC-152a	2.80	3.49	4.23	4.95	5.67	6.78	7.74	8.63	9.04	9.55	10.04	10.34	10.20	10.13	9.79
HFC-23											8.04	24.72	25.62	26.71	27.76
HFC-365mfc											0.79	0.87	0.92	1.02	1.09
HFC-227ea											0.79	0.88	1.00	1.10	1.10
HFC-236fa											0.10	0.11	0.13	0.14	0.14
HFC-245fa											1.80	1.99	2.20	2.39	2.54
Perfluorinated compounds															
PFC-14															80.06
PFC-116											4.20	4.27	4.37	4.44	4.54
PFC-218											0.57	0.59	0.59	0.61	0.56
PFC-318											1.33	1.38	1.43	1.47	1.52
Nitrogen trifluoride															

Component	2001	2002	2003	2004	2005	2006	2007	2008	2009	2010	2011	2012	2013	2014	2015
Sulphurhexafluoride*	4.96	5.15	5.36	5.58	5.82	6.07	6.34	6.61	6.90	7.19	7.49	7.80	8.11	8.42	8.74
Halons															
H-1211*	4.39	4.44	4.49	4.53	4.52	4.48	4.43	4.39	4.33	4.26	4.18	4.09	3.98	3.86	3.77
H-1301	2.99	3.06	3.12	3.17	3.21	3.24	3.26	3.28	3.29	3.31	3.32	3.34	3.36	3.38	3.42
Other halocarbons															
Methylchloride	504.5	521.1	527.5	523.9	520.6	521.5	523.8	525.0	526.4	521.8	509.8	513.6	519.0	514.1	512.8
Methylbromide	8.93	9.08	8.94	8.92	8.61	8.60	8.35	7.77	7.37	7.28	7.20	7.02	6.95	6.85	6.89
Dichloromethane	30.9	31.0	32.0	32.0	31.7	33.1	35.1	37.2	38.2	41.8	42.2	45.2	53.9	54.5	54.1
Chloroform	10.9	10.6	10.7	10.5	10.5	10.5	10.6	10.4	10.8	11.4	11.9	12.0	12.7	13.4	13.7
Carbon tetrachloride											85.1	84.2	83.4	82.6	81.0
Methylchloroform	38.2	32.1	27.2	22.8	19.1	15.9	13.3	11.1	9.2	7.8	6.5	5.4	4.5	3.8	3.2
Trichloroethylene	0.67	0.58	0.40	0.45	0.39	0.38	0.29	0.32	0.51	0.52	0.54	0.51	0.55	0.48	0.33
Perchloroethylene	4.57	4.08	3.69	3.68	3.11	2.81	3.01	2.63	2.92	3.04	2.80	2.72	2.55	2.56	2.43
Volatile Organic Compounds (VOC)															
Ethane											1466.8	1575.2	1565.7	1647.0	1651.4
Propane											170.9	520.6	548.9	574.9	566.0
Butane											182.8	187.2	202.4	190.0	184.4
Pentane											60.1	58.2	66.9	63.2	60.4

Component	2001	2002	2003	2004	2005	2006	2007	2008	2009	2010	2011	2012	2013	2014	2015
Benzene											72.29	70.31	68.75	71.07	69.76
Toluene											28.54	24.59	25.83	27.87	25.75

Table A 2: All calculated trends per year, standard error and regression coefficient for the fit. The trends are all in pptv per year, except for CH₄, N₂O, and CO which are in ppbv. The negative trends are in blue, and the positive trends are shown in red. Generally the period is from 2001-2015 but for the compounds marked in green, the measurements started after September 2010. For these compounds, the trends are highly uncertain.

Component	Formula	Trend /yr	Error	R ²
Carbon dioxide - Zeppelin	CO ₂	2.13	0.011	0.934
Carbon dioxide - Birkenes		-	-	-
Methane - Zeppelin	CH ₄	5.23	0.056	0.835
Methane - Birkenes		-	-	-
Carbon monoxide	CO	-1.29	0.063	0.794
Nitrous oxide	N ₂ O	-	-	-
Chlorofluorocarbons				
CFC-11*	CCl ₃ F	-1.96	0.005	0.988
CFC-12*	CF ₂ Cl ₂	-2.1	0.015	0.925
CFC-113*	CF ₂ ClCFCl ₂	0.02	0.000	0.834
CFC-115*	CF ₃ CF ₂ Cl	0.018	0.000	0.417
Hydrochlorofluorocarbons				
HCFC-22	CHClF ₂	6.536	0.007	0.998
HCFC-141b	C ₂ H ₃ FCl ₂	0.629	0.002	0.977
HCFC-142b*	CH ₃ CF ₂ Cl	0.721	0.001	0.996
Hydrofluorocarbons				
HFC-125	CHF ₂ CF ₃	1.225	0.001	0.998
HFC-134a	CH ₂ FCF ₃	4.844	0.003	0.999
HFC-152a	CH ₃ CHF ₂	0.567	0.001	0.986
CHF ₃		1.017	0.002	0.997
HFC-365mfc	CH ₃ CF ₂ CH ₂ CF ₃	0.072	0.000	0.981
HFC-227ea	CF ₃ CHFCF ₃	0.102	0.000	0.996
HFC-236fa	CF ₃ CH ₂ CF ₃	0.012	0.000	0.952
HFC-245fa	CHF ₂ CH ₂ CF ₃	0.196	0.001	0.992
Perfluorinated compounds				
PFC-14	CF ₄	-1008.106	853.623	0.748
PFC-116	C ₂ F ₆	0.082	0.000	0.982
PFC-218	C ₃ F ₈	0.012	0.000	0.912
PFC-318	c-C ₄ F ₈	-0.117	0.015	0.542
Sulphurhexafluoride*	SF ₆	0.273	0.000	0.998

Component	Formula	Trend /yr	Error	R ²
Nitrogen trifluoride	NF ₃	In 2016		
Halons				
H-1211*	CBrClF ₂	-0.049	0.000	0.983
H-1301	CBrF ₃	0.026	0.000	0.760
Halogenated compounds				
Methylchloride	CH ₃ Cl	-0.279	0.071	0.858
Methylbromide	CH ₃ Br	-0.184	0.002	0.866
Dichloromethane	CH ₂ Cl ₂	1.843	0.012	0.933
Chloroform	CHCl ₃	0.207	0.003	0.805
Carbon tetrachloride	CCl ₄	-0.912	0.019	0.645
Methylchloroform	CH ₃ CCl ₃	-2.342	0.002	0.999
Trichloroethylene	CHClCCl ₂	-0.002	0.002	0.393
Perchloroethylene	CCl ₂ CCl ₂	-0.114	0.004	0.350
Non-methane hydrocarbons (NMHC) and Volatile Organic Compounds (VOC)				
Ethane	C ₂ H ₆	38.7	4.835	0.908
Propane	C ₃ H ₈	7.72	4.252	0.847
Butane	C ₄ H ₁₀	0.97	2.080	0.761
Pentane	C ₅ H ₁₂	-0.38	0.763	0.693
Benzene	C ₆ H ₆	-3.7	0.400	0.879
Toluene	C ₆ H ₅ CH ₃	-2.3	0.334	0.680

Table A 3: Monthly means and standard deviation of aerosol optical depth (AOD) at 500 nm at Ny-Ålesund.'

Month/Year	Mar	Apr	May	Jun	Jul	Aug	Sep
Aerosol optical depth (AOD)							
2002		0.06±0.01	0.08±0.03	0.06±0.02	0.07±0.12	0.07±0.08	0.06±0.05
2003	0.15±0.12	0.11±0.05	0.15±0.06	0.10±0.03	0.04±0.01	0.05±0.02	0.06±0.03
2004	0.06±0.00	0.12±0.08	0.13±0.09	0.06±0.01	0.10±0.07	0.05±0.02	0.04±0.02
2005	0.08±0.03	0.12±0.07	0.10±0.03	0.05±0.02	0.05±0.02	0.04±0.03	0.03±0.01
2006	0.12±0.03	0.16±0.07		0.04±0.00	0.05±0.02	0.05±0.04	0.04±0.03
2007		0.10±0.05	0.10±0.12	0.07±0.03	0.05±0.01	0.05±0.02	0.04±0.03
2008	0.13±0.05	0.14±0.06	0.14±0.04	0.06±0.02	0.06±0.02	0.09±0.03	0.16±0.03
2009			0.11±0.03	0.08±0.02	0.11±0.04	0.10±0.02	0.09±0.01
2010	0.11±0.03	0.08±0.03	0.08±0.01	0.06±0.01	0.05±0.01	0.05±0.01	
2011			0.08±0.02	0.08±0.01	0.05±0.01	0.06±0.02	0.05±0.01
2012	0.10±0.03	0.10±0.02	0.10±0.03	0.06±0.02	0.06±0.02	0.07±0.03	0.07±0.03
2013	0.11±0.04	0.09±0.04	0.06±0.02	0.05±0.01	0.06±0.02	0.05±0.01	0.04±0.02
2014		0.07±0.01	0.10±0.02	0.06±0.02	0.06±0.03	0.08±0.01	0.11±0.05
2015	0.05±0.02	0.10±0.03	0.07±0.02	0.05±0.01	0.15±0.20	0.05±0.02	0.05±0.01
Mean (2002-2015)	0.10±0.04	0.10±0.04	0.10±0.04	0.06±0.02	0.07±0.04	0.06±0.03	0.06±0.03

Table A 4: Monthly means and standard deviation of the Ångström coefficient (Å) at Ny-Ålesund. There are no observations of this parameter during the winter months due to polar night.

Month/Year	Mar	Apr	May	Jun	Jul	Aug	Sep
Ångström coefficient (Å)							
2002		0.9±0.1	1.4±0.1	1.2±0.3	1.2±0.2	1.3±0.4	1.2±0.5
2003	0.9±0.5	1.3±0.3	1.3±0.2	1.5±0.1	1.5±0.3	1.4±0.5	1.4±0.3
2004	1.3±0.1	1.2±0.3	1.4±0.5	1.7±0.2	1.6±0.4	1.5±0.3	1.3±0.3
2005	1.1±0.3	1.4±0.4	1.0±0.2	1.6±0.3	1.7±0.2	1.4±0.7	1.5±0.4
2006	0.9±0.1	0.9±0.3		1.7±0.2	1.4±0.3	1.3±0.6	1.4±0.3
2007		1.4±0.4	1.4±0.6	1.7±0.2	1.6±0.2	1.7±0.3	1.5±0.4
2008	1.4±0.2	1.3±0.2	1.4±0.2	1.4±0.4	1.2±0.2	1.3±0.3	1.4±0.3
2009			1.3±0.4	1.4±0.2	1.3±0.3	1.2±0.1	1.1±0.1
2010	1.0±0.3	1.4±0.2	1.3±0.2	1.3±0.3	1.4±0.2	1.0±0.1	
2011			1.7±0.3	1.8±0.1	1.5±0.1	1.4 ±0.3	1.6±0.2
2012	1.1±0.2	1.3±0.2	1.2±0.2	1.1±0.1	1.3±0.2	1.4±0.2	1.5±0.2
2013	1.3±0.2	1.2±0.3	1.4±0.2	1.6±0.3	1.3±0.2	1.4±0.2	1.2±0.5
2014		1.4±0.1	1.4±0.1	1.3±0.3	1.5±0.1	1.5±0.1	1.5±0.2
2015	1.3±0.2	1.2±0.3	1.5±0.1	1.5±0.2	1.5±0.2	1.6±0.2	1.2±0.5
Mean (2002 -2015)	1.2±0.2	1.3±0.3	1.4±0.3	1.5±0.2	1.4±0.2	1.4±0.3	1.4±0.3

Table A 5: Number of days with AOD observations at Ny-Ålesund made within the months.

Month/Year	Mar	Apr	May	Jun	Jul	Aug	Sep
Number of days with cloud-free and quality assured observations							
2002		4	15	11	6	9	14
2003	3	12	16	8	15	17	12
2004	2	8	13	9	5	12	12
2005	12	17	24	15	10		11
2006	6	12		5	12	4	13
2007		16	9	12	17	10	9
2008	15	12	14	20	16	13	2
2009			7	10	17	8	8
2010	7	18	7	10	12	3	1
2011			2	2	7	4	6
2012	6	18	12	15	16	11	4
2013	5	13	10	10	8	7	9
2014		13	9	9	9	14	4
2015	5	17	15	9	17	13	6
Total (2002-2015)	61	160	153	145	167	125	111

Table A 6: Monthly means and standard deviation of aerosol optical depth (AOD) at 500 nm at Birkenes.

Month/Year	Jan	Feb	Mar	Apr	May	Jun	Jul	Aug	Sep	Oct	Nov
Aerosol optical depth (AOD)											
2009				0.29 ±0.00	0.09 ±0.05	0.09 ±0.05	0.18 ±0.06	0.17 ±0.07	0.10 ±0.04	0.08 ±0.03	
2010					0.10 ±0.04	0.09 ±0.04	0.10 ±0.07	0.10 ±0.05	0.05 ±0.02	0.07 ±0.03	0.04 ±0.01
2011	0.02 ±0.01	0.03 ±0.01	0.07 ±0.02	0.21 ±0.19	0.13 ±0.07	0.10 ±0.04	0.13 ±0.06	0.09 ±0.05			
2012			0.07 ±0.05	0.05 ±0.02	0.08 ±0.04	0.09 ±0.04	0.07 ±0.03	0.08 ±0.03	0.07 ±0.01	0.06 ±0.03	0.04 ±0.00
2013							0.17 ±0.17	0.12 ±0.09	0.05 ±0.03	0.05 ±0.03	
2014			0.15 ±0.14	0.11 ±0.06	0.10 ±0.03	0.08 ±0.03	0.13 ±0.06	0.15 ±0.07	0.14 ±0.06		
2015			0.04 ±0.02	0.07 ±0.02	0.07 ±0.03	0.06 ±0.02	0.10 ±0.07	0.09 ±0.06	0.04 ±0.02	0.03 ±0.03	0.04 ±0.01
Mean 09-15	0.02 0.01	0.03 ±0.01	0.08 ±0.06	0.11 ±0.07	0.10 ±0.04	0.08 ±0.04	0.13 ±0.07	0.11 ±0.06	0.08 ±0.03	0.06 ±0.03	0.04 ±0.01

Table A 7: Monthly means and standard deviation of the Ångström coefficient (Å) at Birkenes

Month/Year	Jan	Feb	Mar	Apr	May	Jun	Jul	Aug	Sep	Oct	Nov
Ångström coefficient (Å)											
2009				1.5 ±0.0	1.2 ±0.3	1.4 ±0.3	1.4 ±0.4	1.1 ±0.2	1.0 ±0.2	1.1 ±0.2	
2010					1.3 ±0.3	1.4 ±0.3	1.4 ±0.2	1.4 ±0.2	1.3 ±0.3	1.3 ±0.3	1.3 ±0.23
2011	1.0 ±0.2	1.0 ±0.1	1.0 ±0.3	1.2 ±0.5	1.3 ±0.3	1.5 ±0.3	1.6 ±0.3	1.6 ±0.1			
2012			1.1 ±0.4	1.6 ±0.3	1.4 ±0.4	1.7 ±0.1	1.6 ±0.3	1.5 ±0.3	1.1 ±0.3	1.4 ±0.4	0.8 ±0.3
2013							1.3 ±0.2	1.2 ±0.3	0.8 ±0.2	0.8 ±0.3	
2014			0.9 ±0.5	1.0 ±0.3	1.1 ±0.3	1.0 ±0.2	1.4 ±0.3	1.1 ±0.3	1.2 ±0.2		
2015			0.9 ±0.2	1.1 ±0.1	1.1 ±0.2	1.3 ±0.2	1.5 ±0.2	1.4 ±0.3	1.3 ±0.2	1.2 ±0.3	0.8 ±0.3
Mean 09-15	1.0 ±0.1	1.0 ±0.0	1.0 ±0.3	1.2 ±0.3	1.2 ±0.2	1.4 ±0.2	1.5 ±0.3	1.3 ±0.2	1.1 ±0.2	1.2 ±0.3	1.0 ±0.3

Table A 8: Number of days with AOD observations at Birkenes made within the months.

Month/Year	Jan	Feb	Mar	Apr	May	Jun	Jul	Aug	Sep	Oct	Nov
Number of days with cloud-free and quality assured observations (lev 2; lev 1.5 for 2013)											
2009				1	22	25	11	13	15	12	
2010					13	16	18	15	16	10	6
2011	7	2	20	23	18	20	15	13			
2012			11	12	10	7	16	18	9	12	2
2013							26	18	13	7	
2014			12	17	16	25	20	13	6		
2015			6	1	14	21	21	16	9	11	3
Total	7	2	49	54	93	114	127	107	68	52	11

APPENDIX II

Description of instruments and methodologies

In this appendix are the instrumental methods used for the measurements of the various greenhouse gases presented. Additionally we explain the theoretical methods used in the calculation of the trends.

Details about greenhouse gas measurements and recent improvement and extensions

Table A 9: Instrumental details for greenhouse gas measurements at Zeppelin and Birkenes.

Component		Instrument and method	Time res.	Calibration procedures	Start - End	Comment
Methane (Birkenes)	CH ₄	Picarro CRDS G1301 CO ₂ /CH ₄ /H ₂ O	5 s	Working std. calibrated against GAW stds at EMPA	19. May 2009 ->	Data coverage in 2015: 94%
Methane (Zeppelin)	CH ₄	GC-FID/	1h	NOAA reference standards	Aug 2001- Apr 2012	
Methane (Zeppelin)	CH ₄	Picarro CRDS	5 sec	NOAA reference standards	20.Apr. 2012 ->	Data coverage 2015: 92% (97%)
Nitrous oxide (Zeppelin)	N ₂ O	GC-ECD	30 min	Hourly, working std. calibrated vs. NOAA stds		Data coverage 2015 83% (86%)
Carbon monoxide (Zeppelin)	CO	GC-HgO/UV	20 min	Every 20 min, working std. calibrated vs. GAW std.	Sep. 2001 - 2012	Discontinued after 2012
Carbon monoxide (Zeppelin)	CO	Picarro CRDS	5 sec	NOAA reference standards.	20.Apr 2012 ->	Data coverage 2015: 84% (89%)
Carbon dioxide (Zeppelin)	CO ₂	Picarro CRDS from 20.4.2012	1 h 5 sec	NOAA reference standards	1989 - 2012 20.Apr. 2012 ->	CO ₂ measurements in cooperation with ITM Stockholm University (SU). Data coverage 2015: 91% (95%)
Carbon dioxide (Birkenes)	CO ₂	Picarro CRDS G1301 CO ₂ /CH ₄ /H ₂ O	5 s	Working std. calibrated against GAW stds at EMPA	Measurements started 19 May 2009.	Data coverage in 2015: 94%
CFC-11 CFC-12 CFC-113 CFC-115 HFC-125 HFC-134a HFC-152a HFC-365mfc HCFC-22 HCFC-141b HCFC-142b H-1301 H-1211	CFCl ₃ CF ₂ Cl ₂ CF ₂ ClCFCl ₂ CF ₃ CF ₂ Cl CHF ₂ CF ₃ CH ₂ FCF ₃ CH ₃ CHF ₂ CF ₃ CH ₂ CHF ₂ C H ₃ CHF ₂ Cl CH ₃ CFCl ₂ CH ₃ CF ₂ Cl CF ₃ Br CF ₂ ClBr	ADS-GCMS	4 h	Every 4 hours, working std. calibrated vs. AGAGE std.	4. Jan 2001- 2010	This instrument was in operation from 04.01.2001 to 31.12.2010. The measurements of the CFCs have higher uncertainty and are not within the required precision of AGAGE. See next section for details.

Table cont.:

Component		Instrument and method	Time res.	Calibration procedures	Start - End	Comment
Methyl Chloride	CH ₃ Cl					
Methyl Bromide	CH ₃ Br					
Methylenedichloride	CH ₂ Cl ₂					
Chloroform	CHCl ₃					
Methylchloroform	CH ₃ CCl ₃					
TriChloroethylene	CHClCCl ₂					
Perchloroethylene	CCl ₂ CCl ₂					
Sulphurhexafluoride	SF ₆					
Tetrafluormethane	CF ₄					
PFC-116	C ₂ F ₆					
PFC-218	C ₃ F ₈					
PFC-318	c-C ₄ F ₈					
	SF ₆					
	SO ₂ F ₂					
Sulphurhexafluoride	CHF ₃					
Sulfuryl fluoride	CH ₂ F ₂					
	CHF ₂ CF ₃					
	CH ₂ FCF ₃					
HFC-23	CH ₃ CF ₃					
HFC-32	CH ₃ CHF ₂					
	CF ₃ CHFCF ₃					
HFC-125	CF ₃ CH ₂ CF ₃					
	CF ₃ CH ₂ CHF ₂					
HFC-134a	CF ₃ CH ₂ CHF ₂ CH ₃					
	CHF ₂ Cl					
HFC-143a	CHClFCF ₃				01.09.2010- >	
HFC-152a	CH ₃ CF ₂ Cl					
	CFCl ₃					
HFC-227ea	CF ₂ Cl ₂					
	CF ₂ ClCFCl ₂					
HFC-236fa	CF ₂ ClCF ₂ Cl					
	CF ₃ CF ₂ Cl					
HFC-245fa	CF ₃ Br	Medusa- GCMS No. 19	2 h	Every 2 hours, working std. calibrated vs. AGAGE std		Data coverage 2015: 60% due to break down of crucial parts.
HFC-365mfc	CF ₂ BrCF ₂ Br					
HCFC-22	CH ₃ Cl					
HCFC-124	CH ₃ Br					
HCFC-141b	CH ₃ I					
HCFC-142b	CH ₂ Cl ₂					
CFC-11	CHCl ₃					
CFC-12	CH ₃ CCl ₃					
CFC-113	CH ₂ Br ₂					
CFC-114	CHBr ₃					
CFC-115	TCE					
H-1211	PCE					
H-1301	C ₂ H ₆					
H-2402	C ₃ H ₈					
Methyl Chloride	C ₄ H ₁₀					

Component		Instrument and method	Time res.	Calibration procedures	Start - End	Comment
Methyl Bromide	C ₅ H ₁₂ C ₆ H ₆ COS					
Methyl Iodide						
Methyldichloride						
Chloroform						
Methylchloroform						
Dibromomethane						
Bromoform						
TriChloroethylene						
Perchloroethylene						
Ethane						
Propane						
n-Butane						
n-Pentane						
Benzene						
Carbonyl Sulfide						
Ozone	O ₃		5 min			

DATA QUALITY AND UNCERTAINTIES

HALOCARBONS

In 2001 - 2010 measurements of a wide range of hydrochlorofluorocarbons, hydrofluorocarbons (HCFC-141b, HCFC-142b, HFC-134a etc.), methyl halides (CH₃Cl, CH₃Br, CH₃I) and the halons (e.g. H-1211, H-1301) were measured with good scientific quality by using ADS-GCMS. The system also measured other compounds like the chlorofluorocarbons, but the quality and the precision of these measurements was not at the same level. Table A 10 shows a list over those species measured with the ADS-GCMS at Zeppelin Observatory. The species that are in blue are of acceptable scientific quality and in accordance with recommendations and criteria of the AGAGE network for measurements of halogenated greenhouse gases in the atmosphere. Those listed in red have higher uncertainties and are not within the required precision of AGAGE. There are various reasons for this increased uncertainties; unsolved instrumental problems e.g. possible electron overload in detector (for the CFC's), influence from other species, detection limits (CH₃I, CHClCCl₂) and unsolved calibration problems (CHBr₃). Since 1. September 2010 the ADS-GCMS was replaced by a Medusa-GCMS system. The uncertainties improved for almost all species (Table A 911 for details), but there are periods where measurements of the CFC's were still not satisfactory. This is an unsolved problem within the AGAGE network.

Table A 10: ADS-GCMS measured species at Zeppelin from 4. January 2001 to 1. September 2010. Good scientific quality data in Blue; Data with reduced quality data in Red. The data are available through <http://ebas.nilu.no>. Please read and follow the stated data policy upon use.

Compound	Typical precision (%)	Compound	Typical precision (%)
SF ₆	1.5	H1301	1.5
HFC134a	0.4	H1211	0.4
HFC152a	0.6	CH ₃ Cl	0.6
HFC125	0.8	CH ₃ Br	0.8
HFC365mfc	1.7	CH ₃ I	5.1
HCFC22	0.2	CH ₂ Cl ₂	0.4
HCFC141b	0.5	CHCl ₃	0.3
HCFC142b	0.5	CHBr ₃	15
HCFC124	2.3	CCl ₄	0.5
CFC11	0.3	CH ₃ CCl ₃	0.6
CFC12	0.3	CHClCCl ₂	1.2
CFC113	0.2	CCl ₂ CCl ₂	0.7
CFC115	0.8		

Table below gives an overview over the species measured with the Medusa-GCMS systems at the AGAGE stations and the typical precision with the different instruments. The Medusa-GCMS instrument at the Zeppelin Observatory meet the same criteria as shown in the Table.

Table A 11: AGAGE measured species.

Compound	Typical precision (%)	Compound	Typical precision (%)
CF ₄	0.15	H1301	1.5
C ₂ F ₆	0.9	H1211	0.5
C ₃ F ₈	3	H2402	2
SF ₆	0.4	CH ₃ Cl	0.2
SO ₂ F ₂	1.6	CH ₃ Br	0.5
HFC23	0.7	CH ₃ I	2
HFC32	5	CH ₂ Cl ₂	0.8
HFC134a	0.4	CHCl ₃	0.6
HFC152a	1.2	CHBr ₃	0.6
HFC125	1	CCL ₄	1
HFC143a	1.2	CH ₃ CCl ₃	0.7
HFC365mfc	10	CHClCCl ₂	2.5
HCFC22	0.3	CCl ₂ CCl ₂	0.5
HCFC141b	0.4	C ₂ H ₂	0.5
HCFC142b	0.6	C ₂ H ₄	2
HCFC124	2	C ₂ H ₆	0.3
CFC11	0.15	C ₆ H ₆	0.3
CFC12	0.05	C ₇ H ₈	0.6
CFC13	2		
CFC113	0.2		
CFC114	0.3		
CFC115	0.8		

METHANE

Methane is measured using a Picarro CRDS (Cavity Ring-Down Spectrometer) monitor which is calibrated against NOAA reference standards. The instrument participates in yearly INGOS cucumber ring tests. The continuous data are also compared to weekly flask samples sent to NOAA CMDL, Boulder Colorado. All data will be available for download from the EBAS database <http://ebas.nilu.no>.

N₂O MEASUREMENTS

N₂O is measured using a gas chromatograph with an electron capture detector. The instrument is calibrated against NOAA reference standards. The instrument participates in yearly INGOS cucumber ring tests and measurements are compared to weekly flask samples sent to NOAA CMDL, Boulder Colorado. All data will be available for download from the EBAS database <http://ebas.nilu.no>. The instrument is getting rather old, with increasing needs for maintenance, but will soon be replaced by a new continuous measuring cavity ring-down spectrometer with enhanced precision and much higher sample frequency.

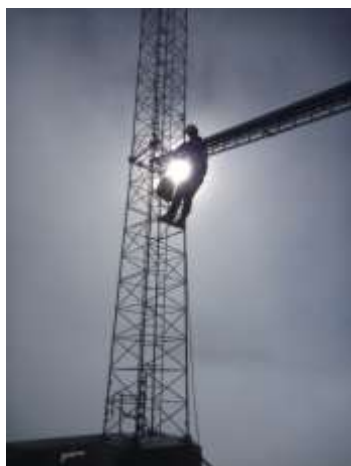
CO₂ MEASUREMENTS

At the Zeppelin station carbon dioxide (CO₂) is monitored in cooperation with Stockholm University (Institute of Applied Environmental Research, ITM). NILU is running the Picarro Cavity Ring-Down Spectrometer used for continuous measurements, calibrated against SU-ITM's set of NOAA reference standards as a cooperation between the two institutes. The instrument participates in yearly INGOS cucumber ring tests. The continuous data are also compared to weekly flask samples sent to NOAA CMDL, Boulder Colorado. All data will be available for download from the EBAS database <http://ebas.nilu.no>.

AIR INLET AT ZEPPELIN

In 2011 the air inlet for the GHG measurements at Zeppelin were improved to reduce possible influence from the station and visitors at the station. The inlet was moved away from the station and installed in a 15 m tower nearby for the following components:

- N₂O
- CH₄
- CO₂
- CO
- Halogenated compounds
- NOAA flaks sampling program
- Isotope flask sampling of CO₂ and CH₄



DETERMINATION OF BACKGROUND DATA

Based on the daily mean concentrations an algorithm is selected to find the values assumed as clean background air. If at least 75% of the trajectories within +/- 12 hours of the sampling day are arriving from a so-called clean sector, defined below, one can assume the air for that specific day to be non-polluted. The remaining 25% of the trajectories from European, Russian or North-American sector are removed before calculating the background.

CALCULATION OF TRENDS FOR GREENHOUSE GASES

To calculate the annual trends the observations have been fitted as described in Simmonds et al. (2006) by an empirical equation of Legendre polynomials and harmonic functions with linear, quadratic, and annual and semi-annual harmonic terms:

$$f(t) = a + b \left(\frac{N}{12} \right) \cdot P_1 \left(\frac{t}{N} - 1 \right) + \frac{1}{3} \cdot d \left(\frac{N}{12} \right)^2 \cdot P_2 \left(\frac{t}{N} - 1 \right) + c_1 \cdot \cos \left(\frac{2\pi t}{12} \right) + s_1 \sin \left(\frac{2\pi t}{12} \right) + c_2 \cos \left(\frac{4\pi t}{12} \right) + s_2 \sin \left(\frac{4\pi t}{12} \right)$$

The observed f can be expressed as functions of time measures from the 2N-months interval of interest. The coefficient a defines the average mole fraction, b defines the trend in the mole fraction and d defines the acceleration in the trend. The c and s define the annual and inter-annual cycles in mole fraction. N is the mid-point of the period of investigation. P_i are the Legendre polynomials of order i .

ON THE SURFACE IN SITU OBSERVATIONS OF AEROSOL MICROPHYSICAL AND OPTICAL PROPERTIES AT BIRKENES

With respect to microphysical aerosol properties, the particle number size distribution (PNSD) is observed at surface-level at Birkenes. The relevant and observed particle sizes cover a range of $0.01 \mu\text{m} - 10 \mu\text{m}$ in particle diameter. The diameter range of $1.0 \mu\text{m} - 10 \mu\text{m}$ is commonly referred to as coarse mode, the range $D_p < 1.0 \mu\text{m}$ as fine mode. The fine mode is separated further into Aitken-mode ($0.01 \mu\text{m} < D_p < 0.1 \mu\text{m}$) and accumulation mode ($0.1 \mu\text{m} < D_p < 1 \mu\text{m}$). The distinction of these modes is justified by different predominant physical processes as function of particle size. In the Aitken-mode, particles grow by condensation of precursor gases from the gas-phase, and coagulate among themselves or with accumulation mode particles. Accumulation mode particles grow by taking up Aitken-mode particles or by mass uptake while being activated as cloud droplets, and they are removed by precipitation. Coarse mode particles in turn are formed by break-up of biological or crustal material, including pollen, bacteria, and fungus spores, and removed by gravitational settling and wet removal. The PNSD of an aerosol is needed for quantifying any interaction or effect of the aerosol since all of them depend strongly on particle size.

To measure the PNSD at Birkenes, 2 measurement principles are combined. A Differential Mobility Particle Spectrometer (DMPS) measures the particle number size distribution, now in the range of $0.01 - 0.8 \mu\text{m}$ particle diameter after several improvements of the instrument. In a DMPS, the particles in the sample air stream are put into a defined state of charge by exposing them to an ionised atmosphere in thermal equilibrium. The DMPS uses a cylindrical capacitor to select a narrow size fraction of the particle phase. The particle size in the selected size fraction is determined by the voltage applied to the capacitor. The particle number concentration in the selected size fraction is then counted by a Condensation Particle Counter (CPC). A mathematical inversion that considers charge probability, diffusional losses of particles in the system, transfer function of the capacitor, and counting efficiency of the CPC is then used to calculate the particle number size distribution. The PNSD of particles with diameters $0.25 \mu\text{m} < D_p < 30 \mu\text{m}$ is measured with an Optical Particle Spectrometer (OPS). In the OPS, the particles in the sample stream are focussed through a laser beam. The instrument registers number and amplitude of the pulses of light scattered by the particles. The particle pulses are sorted into a histogram by their amplitude, where the pulse amplitude yields the particle diameter and the pulse number the particle concentration, i.e. together the PNSD. Both, the DMPS and the OPS, yield method specific measures of the particle diameter, the electrical mobility and the optical particle diameter, respectively. When related to the spherical equivalent geometric particle diameter commonly referred to, both particle size measures depend on particle shape (causing a 5% systematic uncertainty in particle diameter), the optical particle diameter in addition on particle refractive index (causing a 20% systematic uncertainty in particle diameter). In this report, the PNSDs provided by DMPS and OPS are joined into a common PNSD. To quality assure this process, PNSDs are accepted only if DMPS and OPS PNSD agree within 25% in particle diameter in their overlap size range. Together, both instruments provide a PNSD that spans over 3 orders of magnitude in particle diameter, and over 6 orders of magnitude in particle concentration.

Another microphysical property measured at Birkenes is the Cloud Condensation Nuclei (CCN) Concentration, i.e. the concentration of particles that could act as condensation nuclei for liquid-phase cloud droplets, which is a property depending on the water vapour supersaturation. The corresponding instrument, a Cloud Condensation Nucleus Counter (CCNC), exposes the aerosol sample to an “artificial cloud” of defined supersaturation, and

counts the cloud activated particles optically. Observations of the CCN concentration are essential for quantifying the indirect aerosol climate effect. The CCNC at Birkenes has been in operation since 2012, but is currently not included in the monitoring programme.

Optical aerosol parameters quantify the direct aerosol climate effect. The observation programme at Birkenes includes the spectral particle scattering coefficient $\sigma_{sp}(\lambda)$ and the spectral particle absorption coefficient $\sigma_{ap}(\lambda)$. The scattering coefficient quantifies the amount of light scattered by the aerosol particle population in a sample per distance a light beam travels through the sample. The absorption coefficient is the corresponding property quantifying the amount of light absorbed by the particle population in the sample. An integrating nephelometer is used for measuring $\sigma_{sp}(\lambda)$ at 450, 550, and 700 nm wavelength. In this instrument, the optical sensors look down a blackened tube that is filled with aerosol sample. The tube is illuminated by a light source with a perfect cosine intensity characteristic perpendicularly to the viewing direction. It can be shown mathematically that this setup integrates the scattered light seen by the optical sensors over all scattering angles. The particle absorption coefficient $\sigma_{ap}(\lambda)$ is measured by 2 Particle Soot Absorption Photometers (PSAPs). A PSAP infers $\sigma_{ap}(\lambda)$ by measuring the decrease in optical transmissivity of a filter while the filter is loaded with the aerosol sample. The transmissivity time series is subsequently translated into an absorption coefficient time series by using Lambert-Beer's law, the same law also used in optical spectroscopy. The PSAPs deployed at Birkenes are a home-built 1 wavelength version that has received quality assurance by intercomparisons within the EU network and infrastructure projects EUSAAR (European Supersites for Atmospheric Aerosol Research) and ACTRIS (Aerosols, Clouds, and Trace gases Research Infrastructure Network), and a 3-wavelength version. Both instruments are interpreted in combination to benefit from both, quality assurance in a research network and spectral capabilities. For comparison with the nephelometer, the PSAP data has been transferred to a wavelength of 550 nm assuming an absorption Ångström coefficient α_{ap} of -1, adding 2% systematic uncertainty to the data. The correction factor found for one Birkenes PSAP during the recent intercomparison workshop has been included in the analysis.

All in situ observations of aerosol properties representing the ground-level are conducted for the aerosol at dry-state (RH < 40%) for obtaining inter-comparability across the network.

DETAILS ABOUT AEROSOL OPTICAL DEPTH MEASUREMENTS

The amount of particles in the air during sunlit conditions is continuously monitored by means of a Precision-Filter-Radiometer (PFR) sun photometer, located at the Sverdrup station in Ny-Ålesund and a Cimel instrument at Birkenes. The observations in Ny-Ålesund are performed in collaboration with PMOD/WRC (C. Wehrli), Davos, Switzerland. The main instrument characteristics are given below.



AERONET - Cimel C-318

- Sun (9 channels) and sky radiances
- Wavelength range: 340-1640 nm
- 15 min sampling
- No temperature stabilization
- AOD uncertainty: 0.01-0.02



PFR-GAW- Precision Filter Radiometer

- Direct sun measurements (4 channels)
- Wavelength range: 368 - 862 nm
- 1 min averages
- Temperature stabilized
- AOD uncertainty: 0.01

Figure 48: Photos and typical features of the standard instrument of the AERONET (left panel) and GAW PFR network instruments (right panel)

The sun-photometer measurements in Ny-Ålesund are part of the global network of aerosol optical depth (AOD) observations, which started in 1999 on behalf of the WMO GAW program. The instrument is located on the roof of the Sverdrup station, Ny-Ålesund, close to the EMEP station on the Zeppelin Mountain (78.9°N, 11.9°E, 474 m a.s.l.). The Precision Filter Radiometer (PFR) has been in operation since May 2002. In Ny-Ålesund, the sun is below 5° of elevation from 10 October to 4 March, limiting the period with sufficient sunlight to the spring-early autumn season. However, during the summer months it is then possible to measure day and night if the weather conditions are satisfactory. The instrument measures direct solar radiation in four narrow spectral bands centered at 862 nm, 501 nm, 411 nm, and 368 nm. Data quality control includes instrumental control like detector temperature and solar pointing control as well as objective cloud screening. Measurements are made at full minutes are averages of 10 samples for each channel made over a total duration of 1.25 seconds. SCIAMACHY TOMSOMI and OMI ozone columns and meteorological data from Ny-Ålesund are used for the retrieval of aerosol optical depth (AOD).

Aerosol optical depth measurements started at the new Birkenes observatory in spring 2009, utilizing an automatic sun and sky radiometer (CIMEL type CE-318), with spectral interference filters centered at selected wavelengths: 340 nm, 380 nm, 440 nm, 500 nm, 675 nm, 870 nm, 1020 nm, and 1640 nm. The measurement frequency is approximately 15 minutes (this depends on the air-mass and time of day). Calibration was performed regularly about once per year in Spain (RIMA-AERONET sub-network). GOA manages the calibration for RIMA-AERONET sun photometers. In the context of ACTRIS (Aerosols, Clouds, and Trace gases Research Infra Structure Network, an EU (FP7) project) Transnational Access instrument

calibration has been completed 14 May 2013 and October/November 2014 at the GOA-UVA (Spain) installation of the AERONET-EUROPE Calibration Service Centre. Raw data are processed and quality assured centrally by AERONET. Data reported for 2009 - 2014 are quality assured AERONET level 2.0 data, which means they have been pre- and post-field calibrated, automatically cloud cleared and have been manually inspected by AERONET.

OUTLOOK ON OBSERVATIONS OF AEROSOL OPTICAL DEPTH IN NY-ÅLESUND BEYOND 2015

Two observational initiatives and collaborations should be mentioned here:

1. Collaborative observations between NILU and the Alfred Wegener Institute (AWI, Germany) using a sun-photometer on top of the Zeppelin Mountain, which is a unique opportunity to separate the boundary layer contribution from the total column, and thereby get new insights into the contribution of local versus long-range transport of aerosols. AWI financed the instruments, NILU had ordered the a solar-tracker in 2012, but due to long delivery times, only in spring 2013, measurements on a more routine bases started. The scientific evaluation of the data is ongoing and will be published potentially in 2016.
2. A major obstacle to obtaining a complete year around AOD climatology in the Arctic arises from the long polar night. To fill gaps in the aerosol climatology plans are ongoing to deploy and test a lunar photometer to Ny-Ålesund in autumn 2014. This is a collaborative initiative between PMOD/WRC, ISAC-CNR, NILU and others. Seed money for this activity was received from the Svalbard Science Forum for the SSF Strategic grant project Lunar Arctic project # 236774. The project aimed at coordinated remote sensing of Polar aerosol: LUNAR photometry was to be used to close the gap in the annual cycle of the ARCTIC aerosol climatology and to develop Svalbard as satellite validation site. The project started 1 March 2014. It was finalized at the end of June 2015, after a successful Lunar Photometry workshop 24 - 26 June 2015 at Valladolid University, Valladolid, Spain.



Figure 49: Moon PFR on the Kipp & Zonen tracker during the day (left, parking position) and during night-time measurements (right).

The PFR instrument modified by PMOD-WRC was installed on a tracker model Kipp & Zonen provided usually hosting a sun photometer. Figure 49 shows the instrument on the tracker during day-time and night-time. Six lunar cycles were monitored: the first during February 2014, while the other 5 during winter 2014-2015. We collected data on 66 measurement periods, from Moon-rise to Moon-set or from minimum-to-minimum elevation as in Polar Regions no set-rise events are possible. Among these, we obtained 17 distinct good measurement periods, due to the frequent occurrence of clouds. For further details see e.g. Mazzola at al., 2015.

APPENDIX III: Abbreviations

Abbreviation	Full name
ACSM-ToF	Aerosol Chemical Speciation Monitor
ACTRIS	Aerosols, Clouds, and Trace gases Research InfraStructure Network
ADS-GCMS	Adsorption-Desorption System - Gas Chromatograph Mass Spectrometer
AeroCom	Aerosol Comparisons between Observations and Models
AERONET	Aerosol Robotic Network
AGAGE	Advanced Global Atmospheric Gases Experiment
AIRS	Atmospheric Infrared Sounder
AMAP	Arctic Monitoring and Assessment
AOD	Aerosol optical depth
AWI	Alfred Wegener Institute
BC	Black carbon
CAMP	Comprehensive Atmospheric Monitoring Programme
CCN	Cloud Condensation Nuclei
CCNC	Cloud Condensation Nucleus Counter
CFC	Chlorofluorocarbons
CICERO	Center for International Climate and Environmental Research - Oslo
CIENS	Oslo Centre for Interdisciplinary Environmental and Social Research
CLTRAP	Convention on Long-range Transboundary Air Pollution
CO	Carbon monoxide
CPC	Condensation Particle Counter
DMPS	Differential Mobility Particle
EMEP	European Monitoring and Evaluation Programme
ENVR ^{plus}	Environmental Research Infrastructures Providing Shared Solutions for Science and Society
EOS	Earth Observing System
ERF	Effective radiative forcing ERF
ERFaci	ERF due to aerosol-cloud interaction
EU	European Union
EUSAAR	European Supersites for Atmospheric Aerosol Research
FLEXPART	FLEXible PARTicle dispersion model
GAW	Global Atmosphere Watch

Abbreviation	Full name
GB	Ground based
GHG	Greenhouse gas
GOA-UVA	Atmospheric Optics Group of Valladolid University
GOSAT	Greenhouse Gases Observing Satellite
GOSAT-IBUKI	Greenhouse Gases Observing Satellite "IBUKI"
GWP	Global Warming Potential
HCFC	Hydrochlorofluorocarbons
HFC	Hydrofluorocarbons
ICOS	Integrated Carbon Observation System
InGOS	Integrated non-CO2 Greenhouse gas Observing System
IPCC	Intergovernmental Panel on Climate Change
ISAC-CNR	Institute of Atmospheric Sciences and Climate (ISAC) of the Italian National Research Council
ITM	Stockholm University - Department of Applied Environmental Science
JAXA	Japan Aerospace Exploration Agency
LLGHG	Well-mixed greenhouse gases
MOCA	Methane Emissions from the Arctic Ocean to the Atmosphere: Present and Future Climate Effects
MOE	Ministry of the Environment
NARE	Norwegian Antarctic Research Expeditions
NASA	National Aeronautics and Space Administration
NEOS-ACCM	Norwegian Earth Observation Support for Atmospheric Composition and Climate Monitoring
NIES	National Institute for Environmental Studies
NOAA	<u>National Oceanic and Atmospheric Administration</u>
NRS	Norsk Romsenter
OC	Organic Carbon
ODS	Ozone-depleting substances
OH	Hydroxyl radical
OPS	Optical Particle Spectrometer
OSPAR	Convention for the Protection of the marine Environment of the North-East Atlantic
PFR	Precision filter radiometer
PMOD/WRC	Physikalisch-Meteorologisches Observatorium Davos/World Radiation Center

Abbreviation	Full name
PNSD	Particle number size distribution
ppb	Parts per billion
ppm	Parts per million
ppt	Parts per trillion
PSAP	Particle Soot Absorption Photometers
RF	Radiative forcing
RI	Research Infrastructure
RIMA	Red Ibérica de Medida fotométrica de Aerosoles
SACC	Strategic Aerosol Observation and Modelling Capacities for Northern and Polar Climate and Pollution
SCIAMACHY	SCanning Imaging Absorption spectroMeter for Atmospheric CHartographY
SIS	Strategisk instituttsatsing
SMPS	Scanning Mobility Particle
TES	Tropospheric Emission Spectrometer
TOA	Top Of Atmosphere
TOMS OMI	Total Ozone Mapping Spectrometer Ozone Monitoring instrument
UN	United Nations
UNFCCC	United Nations Framework Convention on Climate Change
VOC	Volatile organic compounds
WDCA	World Data Centre for Aerosol
WDCS	World Data Centre of Aerosols
WMGHG	Well-mixed greenhouse gases
WMO	World Meteorological Organization

Norwegian Environment Agency

Telephone: +47 73 58 05 00 | Fax: +47 73 58 05 01

E-mail: post@miljodir.no

Web: www.environmentagency.no

Postal address: Postboks 5672 Sluppen, N-7485 Trondheim

Visiting address Trondheim: Brattørkaia 15, 7010 Trondheim

Visiting address Oslo: Grensesvingen 7, 0661 Oslo

The Norwegian Environment Agency is working for a clean and diverse environment. Our primary tasks are to reduce greenhouse gas emissions, manage Norwegian nature, and prevent pollution.

We are a government agency under the Ministry of Climate and Environment and have 700 employees at our two offices in Trondheim and Oslo and at the Norwegian Nature Inspectorate's more than sixty local offices.

We implement and give advice on the development of climate and environmental policy. We are professionally independent. This means that we act independently in the individual cases that we decide and when we communicate knowledge and information or give advice.

Our principal functions include collating and communicating environmental information, exercising regulatory authority, supervising and guiding regional and local government level, giving professional and technical advice, and participating in international environmental activities.